Evapotranspiration and Microclimate at a Low-Level Radioactive-Waste Disposal Site in Northwestern Illinois

By R.W. HEALY, M.P. deVRIES, and A.M. STURROCK, JR.

U.S. GEOLOGICAL SURVEY WATER-SUPPLY PAPER 2327

DEPARTMENT OF THE INTERIOR
MANUEL LUJAN, JR., Secretary

U.S. GEOLOGICAL SURVEY
Dallas L. Peck, Director

Any use of trade, product, or firm names
in this publication is for descriptive purposes only
and does not imply endorsement by the U.S. Government

UNITED STATES GOVERNMENT PRINTING OFFICE, WASHINGTON : 1989

For sale by the
Books and Open-File Reports Section
U.S. Geological Survey
Federal Center, Box 25425
Denver, CO 80225

Library of Congress Cataloging-in-Publication Data

Healy, R.W.
Evapotranspiration and microclimate at a low-level radioactive-waste disposal site in northwestern Illinois.
(U.S. Geological Survey water-supply paper ; 2327)
Bibliography: p.
Supt. of Docs. no.: I 19.13:2327
1. Evapotranspiration—Illinois—Sheffield Region. 2. Microclimatology—Illinois—Sheffield Region. 3. Radioactive waste sites—Illinois—Sheffield Region. I. DeVries, M.P. II. Sturrock, Alex, M. III. Title. IV. Series.
QC915.7.U5H43 1988 551.6'6 87-600113

CONTENTS

Abstract **1**
Introduction **1**
- Background **1**
- Purpose and scope **2**

The Sheffield site **2**
- Location and history **2**
- Climate **2**
- Soils **3**
- Vegetation **5**

Techniques for estimating evapotranspiration **5**
- Aerodynamic profile **5**
- Energy budget **8**
- Water budget **9**
- Potential evapotranspiration **10**

Instrumentation **10**
- Precipitation **10**
- Radiation **10**
- Wind **11**
- Air temperature and water-vapor pressure **11**
- Soil-heat flux and temperature **11**
- Soil-water content and tension **12**
- Surface runoff **12**

Microclimate of the trench covers **12**
- Precipitation **12**
- Radiation **12**
- Wind **19**
- Air temperature and water-vapor pressure **20**
- Soil-heat flux and soil temperature **21**
- Soil-water content **23**

Evapotranspiration estimates **25**
- Energy-budget method **25**
- Aerodynamic-profile method **26**
- Water-budget method **27**
- Potential evapotranspiration **28**
- Error analysis **28**

Summary **29**
References cited **36**

FIGURES

1. Map showing location of Sheffield low-level radioactive-waste disposal site **3**
2. Map of Sheffield site showing waste-trench location, instrument location, topography, and line of section **4**

3–7. Graphs showing:
   3. Average monthly precipitation from National Weather Service stations near Sheffield site **5**
   4. Average monthly temperature from National Weather Service stations near Sheffield site **5**
   5. Frequency of occurrence, in percentage of time, of winds from various directions at Moline, Illinois, for June 1981 through December 1983 **6**

6. Mean monthly windspeeds at Moline, Illinois, for June 1981 through December 1983 **6**
7. Average monthly pan evaporation for April through October at Hennepin, Illinois, for 1963 through 1983 **7**
8. Schematic section *D–D′* of trench cover and location of moisture-probe access tubes and tensiometers **7**
9. Photograph showing vegetation at the Sheffield site in June 1983 **8**
10–37. Graphs showing:
10. Selected microclimatological parameters at the Sheffield site **13**
11. Monthly precipitation at the Sheffield site **19**
12. Monthly solar radiation at the Sheffield site **19**
13. Monthly ratios of solar radiation to clear-sky radiation at the Sheffield site **20**
14. Monthly surface albedo at the Sheffield site **20**
15. Monthly longwave radiation at the Sheffield site **21**
16. Monthly net radiation at the Sheffield site **21**
17. Frequency of occurrence, in percentage of time, of winds from various directions at the Sheffield site **22**
18. Mean monthly windspeed at the Sheffield site **22**
19. Vertical gradients in horizontal windspeed at the Sheffield site for 4 hours on June 2, 1984 **22**
20. Hourly variations in z/L' at the Sheffield site for June 2, 1984 **23**
21. Monthly air temperature at the Sheffield site **23**
22. Monthly water-vapor pressure at the Sheffield site **23**
23. Monthly soil-heat fluxes at the Sheffield site **23**
24. Soil temperatures at the Sheffield site **24**
25. Change in the amount of water stored within the upper 1.75 meters of soil at the Sheffield site **25**
26. Change in volumetric soil-moisture content with respect to depth for 4 days at the Sheffield site **26**
27. Monthly evapotranspiration at the Sheffield site **27**
28. Monthly energy budget for the Sheffield site with evapotranspiration estimated by the energy-budget method **28**
29. Monthly ratios of sensible- to latent-heat fluxes at the Sheffield site as estimated by the energy-budget, aerodynamic-profile, and water-budget methods **29**
30. Energy budget at the Sheffield site as estimated by the energy-budget method **30**
31. Monthly energy budget for the Sheffield site with evapotranspiration estimated by the aerodynamic-profile method **32**
32. Energy budget at the Sheffield site as estimated by the aerodynamic-profile method **33**
33. Monthly potential evapotranspiration at the Sheffield site **34**
34. Monthly ratios of actual evapotranspiration, as estimated by the energy-budget, aerodynamic-profile, and water-budget methods, to potential evapotranspiration at the Sheffield site **34**
35. Effect of temperature-gradient errors on hourly evapotranspiration estimates on May 31 through June 2, 1984 **35**
36. Effect of vapor-pressure gradient errors on hourly evapotranspiration estimates on May 31 through June 2, 1984, using the energy-budget method **35**
37. Effect of errors in horizontal windspeed gradient on hourly evapotranspiration estimates on May 31 through June 2, 1984, using the aerodynamic-profile method **36**

TABLES

1. Properties of surficial deposits **8**
2. Daily albedo for six days in January and February 1984 **20**
3. Hourly albedo for two days **20**
4. Hourly values of the ratio of sensible- to latent-heat flux **32**
5. Changes in computed daily evapotranspiration, when assuming systematic measurement errors **34**
6. Daily estimates of evapotranspiration **40**

METRIC CONVERSION FACTORS

The following factors may be used to convert the International System (SI) of units of measure used in this report to inch-pound units.

Multiply SI unit	By	To obtain inch-pound units
square centimeter (cm^2)	0.1550	square inch (in^2)
square meter (m^2)	10.76	square foot (ft^2)
joule (J)	0.0009478	British thermal units (mean) (Btu)
	0.2388	calorie (cal)
watt per square meter (W/m^2)	0.005290	British thermal unit per square foot per minute ($Btu/ft^2 \cdot min$)
	0.001424	calorie per square centimeter per minute ($cal/cm^2 \cdot min$)
watt per square meter per kelvin ($W/m^2 \cdot K$)	0.1761	British thermal unit per square foot per hour per degree Fahrenheit ($Btu/ft^2 \cdot h \cdot °F$)
nanometer (nm)	0.00003937	mil
micrometer (μm)	0.03937	mil
millimeter (mm)	0.03937	inch (in)
meter (m)	3.281	foot (ft)
kilometer (km)	0.6214	mile (mi)
kilogram (kg)	2.205	pound mass (lbm)
kilogram per cubic meter (kg/m^3)	0.06243	pound per cubic foot (lb/ft^3)
watt (W)	3.412	British thermal unit per hour (Btu/h)
	0.2388	calories per second (cal/s)
kilopascal (kPa)	0.2953	inch of mercury (in Hg)
	10.00	millibar (mbar)
degree Celsius (°C)	$F=1.8\ °C+32$	degree Fahrenheit (°F)
kelvin (K)	$(K-273.15)\ 1.8+32$	degree Fahrenheit (°F)
meter per second (m/s)	2.237	mile per hour (mi/h)
cubic meter (m^3)	0.0008107	acre-foot (acre-ft)

Evapotranspiration and Microclimate at a Low-Level Radioactive-Waste Disposal Site in Northwestern Illinois

By R.W. Healy, M.P. deVries, *and* A.M. Sturrock, Jr.

Abstract

From July 1982 through June 1984, a study was made of the evapotranspiration and microclimate at a low-level radioactive-waste disposal site near Sheffield, Bureau County, Illinois. Vegetation at the site consists of mixed pasture grasses, primarily awnless brome (*Bromus inermis*) and red clover (*Trifoleum pratense*). Three methods were used to estimate evapotranspiration: (1) an energy budget with the Bowen ratio, (2) an aerodynamic profile, and (3) a soil-based water budget. For the aerodynamic-profile method, sensible-heat flux was estimated by a profile equation and evapotranspiration was then calculated as the residual in the energy-balance equation. Estimates by the energy-budget and aerodynamic-profile methods were computed from hourly data and then summed by days and months. Yearly estimates (for March through November) by these methods were in close agreement: 648 and 626 millimeters, respectively. Daily estimates reach a maximum of about 6 millimeters. The water-budget method produced only monthly estimates based on weekly or biweekly soil-moisture content measurements. The yearly evapotranspiration estimated by this method (which actually included only the months of April through October) was 655 millimeters. The March-through-November average for the three methods of 657 millimeters was equivalent to 70 percent of total precipitation.

Continuous measurements were made of incoming and reflected shortwave radiation, incoming and emitted longwave radiation, net radiation, soil-heat flux, soil temperature, horizontal windspeed, and wet- and dry-bulb air temperature. Windspeed and air temperature were measured at heights of 0.5 and 2.0 meters (and also at 1.0 meter after September 1983). Soil-moisture content of the soil zone was measured with a gamma-attenuation gage.

Annual precipitation (938 millimeters) and average temperature (10.8 degrees Celsius) at the Sheffield site were virtually identical to long-term averages from nearby National Weather Service stations. Solar radiation averaged 65 percent of that normally expected under clear skies. Net radiation averaged 70.1 watts per square meter and was highest in July and negative during some winter months. Wind direction varied but was predominately south-southeasterly. Wind speed at the 2-meter height averaged 3.5 meters per second and was slightly higher in winter months than the rest of the year. The amount of water stored within the soil zone was greatest in early spring and least in late summer.

Seasonal and diurnal trends of evapotranspiration rates mirrored those of net radiation; July was usually the month with the highest evapotranspiration rate. The ratio of sensible- to latent-heat fluxes (commonly called the Bowen ratio) for the 2-year study period was 0.38, as averaged from the three methods. Monthly Bowen ratios fluctuated somewhat but averaged about 0.35 for late spring through summer. In fall, the ratio declined to zero or to slightly negative values. When the ratio was negative, the latent-heat flux was slightly greater than the net radiation because of additional energy supplied by the cooling soil and air.

Evapotranspiration calculated by the three methods averaged 75 percent of potential evapotranspiration, as estimated by the Penman equation. There was no apparent seasonal trend in the relation between actual and potential evapotranspiration rates.

INTRODUCTION

Background

The Low-Level Radioactive-Waste Policy Act, enacted by Congress in 1980, states that, by 1986, each State will be responsible for the disposal of low-level waste generated within its borders. To comply with the Act, most States are joining in compacts with neighbor States to develop regional disposal sites. According to the U.S. Nuclear Regulatory Commission, in 10 CFR (Code of Federal Regulations), Part 61, these new disposal sites must be designed to minimize contact of water and buried waste. Such designs will require detailed knowledge of the rate of water percolation through the geologic material in which the wastes are buried. This, in turn, will require knowledge of the entire hydrologic budget at proposed site locations.

Although a great deal of research has been conducted on phenomena related to water and radionuclide movement within porous media, a relatively small amount of this work has actually been performed at existing commercial disposal sites in the United States. The work that has been done at these sites has been directed primarily toward studying water and radionuclide movement within the saturated zones (see

Fischer, 1983, p. 52). In light of the above-mentioned requirements, surprisingly few studies have focused on the hydrologic cycle at or near existing sites. Gee and Kirkham (1984) investigated the water balance in the arid region close to Richland, Washington, and Schulz (1984) studied the water balance at Maxey Flats in Kentucky. Design of new sites, therefore, requires further research into quantification of the hydrologic budget in different parts of the country.

Next to precipitation, evapotranspiration is the largest component in the hydrologic budget in the midwestern part of the country. Most precipitation that infiltrates the soil remains in the soil zone and eventually returns to the atmosphere through the process of evapotranspiration. Jones (1966, p. 12) estimated that, in northern Illinois, annual evapotranspiration averages about 635 to 760 mm (millimeters). This is 71 to 85 percent of the long-term average annual precipitation of 890 mm for the Sheffield area. Hence, quantification of the entire hydrologic budget in this area requires an accurate estimate of evapotranspiration.

The U.S. Geological Survey, although not a regulatory agency, has been directed by Congress to conduct investigations and research aimed at establishing a technical basis upon which earth-science criteria for the selection and operation of low-level-waste disposal sites can be developed, tested, and enforced by other agencies (Robertson, 1981, p. 22). As a part of that effort, a comprehensive study of evapotranspiration and the microclimate of vegetated trench covers was conducted, from July 1982 through June 1984, at the disposal site near Sheffield, Bureau County, Illinois. Precipitation, incoming and reflected shortwave radiation, incoming and outgoing longwave radiation, and soil-surface temperature were continuously recorded, as were wet- and dry-bulb air temperature and windspeed at three heights, soil temperature at seven depths, and soil-heat flux at three depths. Soil-moisture content to a depth of 1.75 m (meters) was measured at 1- to 2-week intervals with a gamma-attenuation density gage.

This study was part of a larger U.S. Geological Survey study of water and radionuclide movement through the unsaturated zone at the Sheffield site. Other aspects of that study included studies of water movement through a waste-trench cover, water movement through the entire thickness of the unsaturated zone, and the hydrogeochemistry of the unsaturated zone. Concepts and techniques used in these studies can be found in Healy and others (1986). Other studies done by the U.S. Geological Survey at the site include hydrogeology (Foster and Erickson, 1980; Foster, Erickson, and Healy, 1984; Foster, Garklavs, and Mackey, 1984; and Garklavs and Healy, 1986), surface runoff and sediment transport (Gray, 1984), and transport of gaseous radionuclides within the unsaturated zone (Striegl, 1984).

Purpose and Scope

The purpose of this report is to present the theory, methods, and results of a 2-year study of evapotranspiration and microclimate conducted at the low-level radioactive-waste disposal site near Sheffield, Illinois. Included is a description of the microclimate and estimates of evapotranspiration at the site for the period of data collection. Details on the microclimate are provided so that assumptions inherent in each method used to estimate evapotranspiration may be fully understood. Three different methods were used to estimate evapotranspiration: energy budget/Bowen ratio, aerodynamic profile, and water budget. Evapotranspiration rates are given on a daily basis and, for a selected number of days, on an hourly basis.

THE SHEFFIELD SITE

Location and History

The study area is the low-level radioactive-waste disposal site located near Sheffield, Bureau County, Illinois (fig. 1). The 8-hectare site, situated on gently rolling terrain, was operated from 1967 through 1978. During that time, 21 trenches (fig. 2) were constructed and filled with approximately 83,000 m^3 (cubic meters) of waste (Foster, Erickson, and Healy, 1984). Total activity of the waste at the time of burial was estimated at 60,000 curies (K. Dragonette, U.S. Nuclear Regulatory Commission, written commun., 1979). More details on the history of the site, trench construction, and geology are given by Foster, Erickson, and Healy (1984).

Climate

Data concerning long-term annual, monthly, and daily variations in precipitation and temperature are available from the National Weather Service for the following stations: Kewanee, 16 km (kilometers) to the south; Walnut, 31 km to the north; and Tiskilwa, 23 km to the east (U.S. Department of Commerce, 1939–84). Pan-evaporation data may be obtained from the National Weather Service station at the Hennepin powerplant, located on the Illinois River near Hennepin, 39 km east of the site.

Annual precipitation at these weather stations ranged from a minimum of 646 mm to a maximum of 1,330 mm, and averaged 890 mm. Monthly distribution of precipitation is shown in figure 3. June is the wettest month, averaging 116 mm, whereas February is the dryest month, averaging 33 mm. Most precipitation occurs during the months of May through September, a period dominated by convective thunderstorms (Huff, 1979). Most storms move through the region from the southwest to the northeast (J.L. Vogel, Illinois State Water Survey, written commun., 1985). Much of the precipitation during the winter months (December through February) is in the form of snow. Average annual snowfall for the three weather stations is 850 mm. Snow is on the ground for an average of 53 days each year.

The mean annual temperature is 10.3 °C (Celsius). January is typically the coldest (−6.5 °C) month of the year, whereas July is the warmest (23.7 °C) (fig. 4).

Windspeed and direction were measured at the Moline airport, approximately 68 km west of the site. The percentage of time during which the wind was coming from each of 36 sectors for the period June 1, 1981, through December 31, 1983, is shown in figure 5. During that time, the direction was variable but predominantly out of the south-southwest and west-northwest. Daily windspeed at the airport averaged 4.7 m/s (meters per second). There was no apparent correlation between windspeed and direction. Mean monthly windspeeds are shown in figure 6. There appears to be a good correlation between windspeed and time of year, in that summer months have the lowest windspeeds.

The average relative humidity at Moline for the above-mentioned period was 70.6 percent. Average monthly relative humidity varied little throughout the year. The average station-barometric pressure was 99.49 kPa (kilopascals) (altitude of 181.0 m).

Average pan evaporation for April through October at Hennepin is shown in figure 7. Averages are based on data for 1963 through 1983. July has the highest average. The yearly average for the 7-month period is 1,140 mm.

Soils

The soil at the study site is a clayey-silt type that developed in the upper part of the Peoria Loess (a Wisconsinan eolian deposit). The soil has been reworked over much of the site as a result of trench construction. Figure 8 shows a schematic diagram of a typical trench cover. Four types

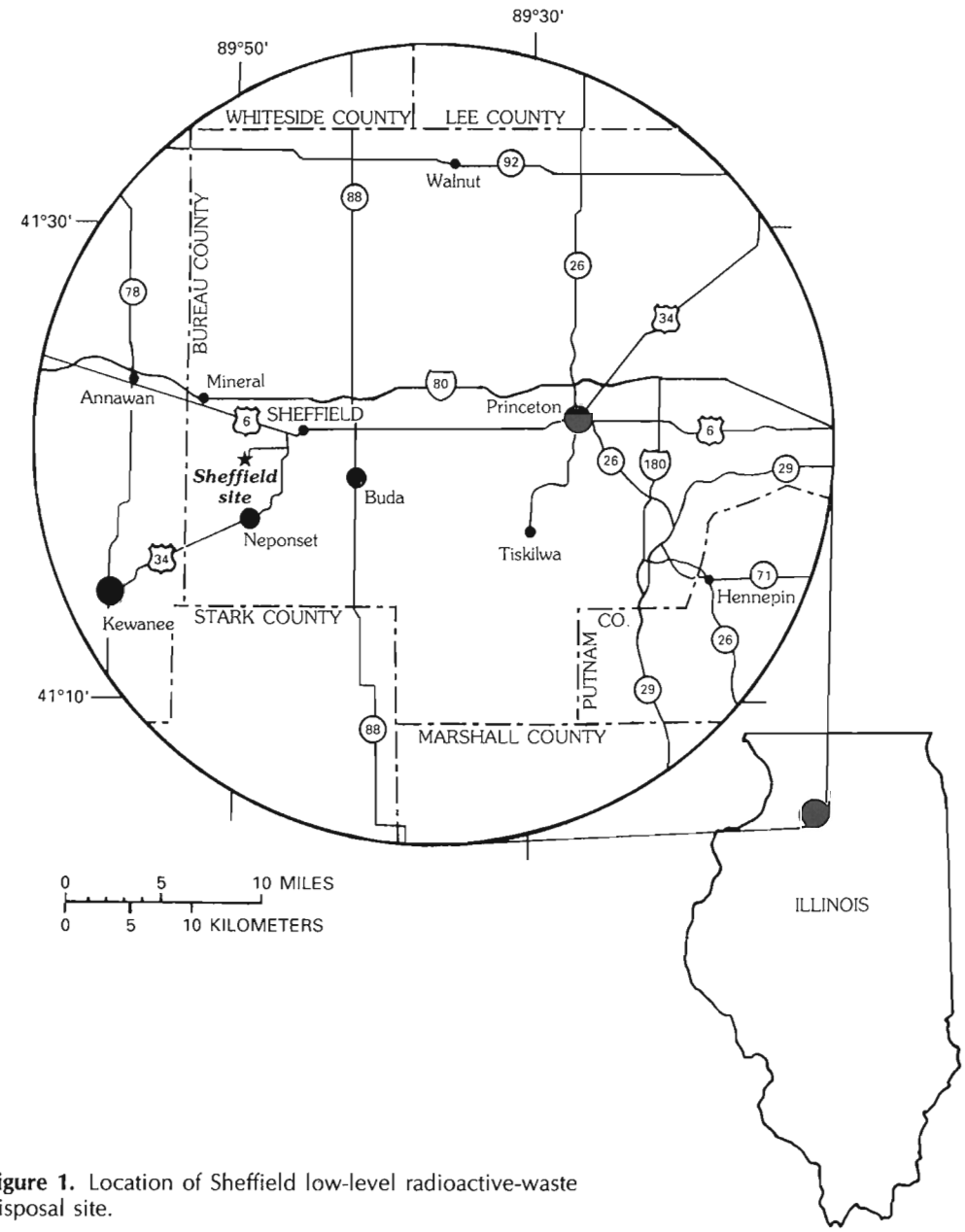

Figure 1. Location of Sheffield low-level radioactive-waste disposal site.

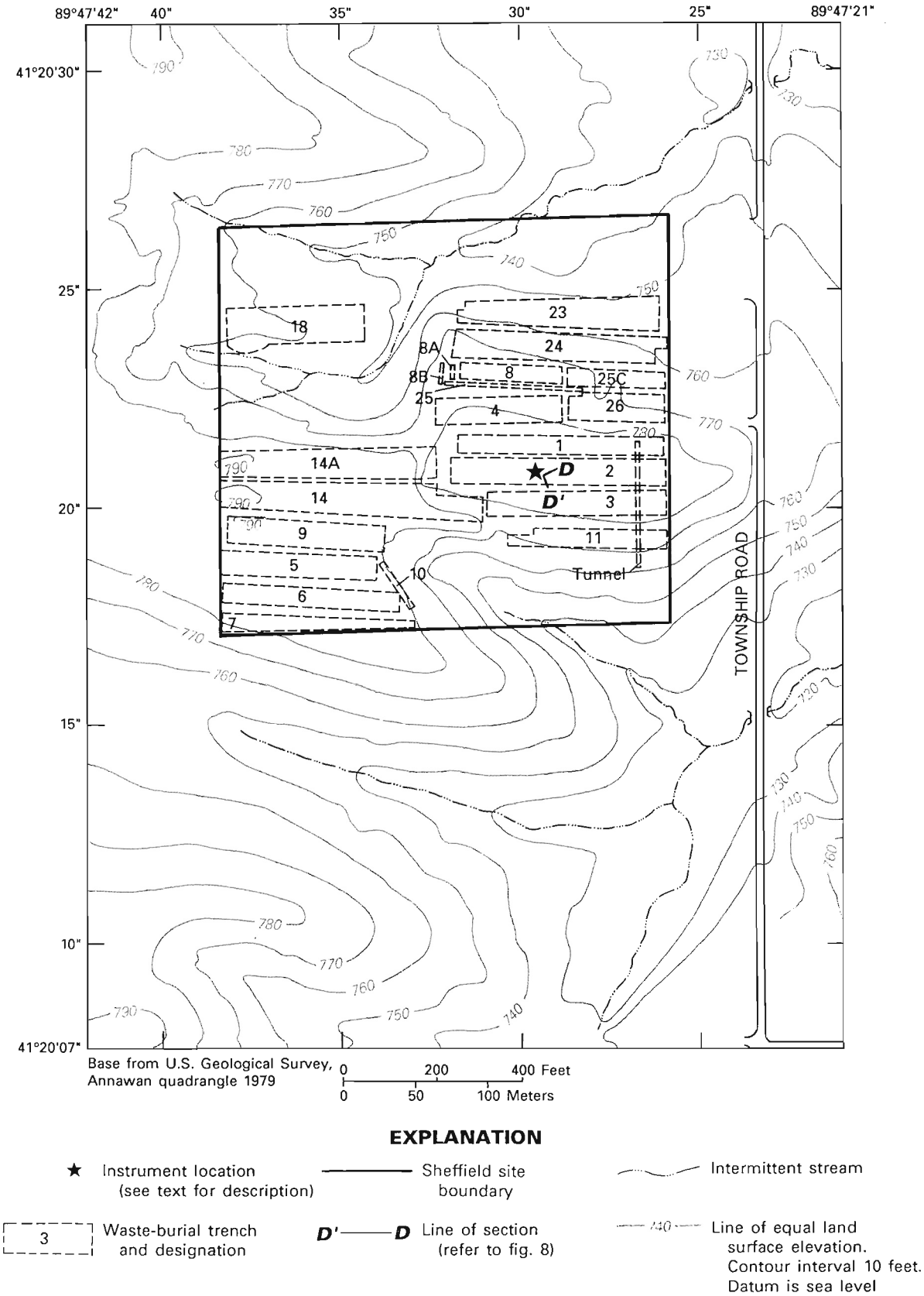

Figure 2. Sheffield site showing waste-trench location, instrument location, topography, and line of section.

of cover material are shown. These have been categorized on the basis of lithology and bulk density; table 1 gives a brief description of each type.

Vegetation

The entire study site is vegetated with pasture grass. Awnless brome grass (*Bromus inermis*) and red clover (*Trifoleum pratense*) are the most common species, with alfalfa (*Medicago sativa*) and timothy (*Phleum pratense*) present to a lesser degree. Figure 9 shows the vegetation in June 1983. The average height of the vegetation was about 0.2 m. It was mowed three or four times a year to a height of about 0.1 m. Roots have been found as deep as 1.5 m.

TECHNIQUES FOR ESTIMATING EVAPOTRANSPIRATION

There are many methods for estimating evapotranspiration. Details concerning the theory behind the most commonly used methods can be found in textbooks related to evapotranspiration and microclimatology (see Sellers, 1965; Monteith, 1973; and Brutsaert, 1982). Brutsaert (1982) presents an interesting sketch of the history of evaporation theory—even the ancient Greeks studied water movement from the earth to the atmosphere. Jensen (1973) presents a survey and comparison of several different estimation techniques.

Evapotranspiration rates obtained during this study were estimated using three techniques: aerodynamic profile, energy budget, and water budget. It is advantageous to use more than one technique because of the inaccuracies inherent in each.

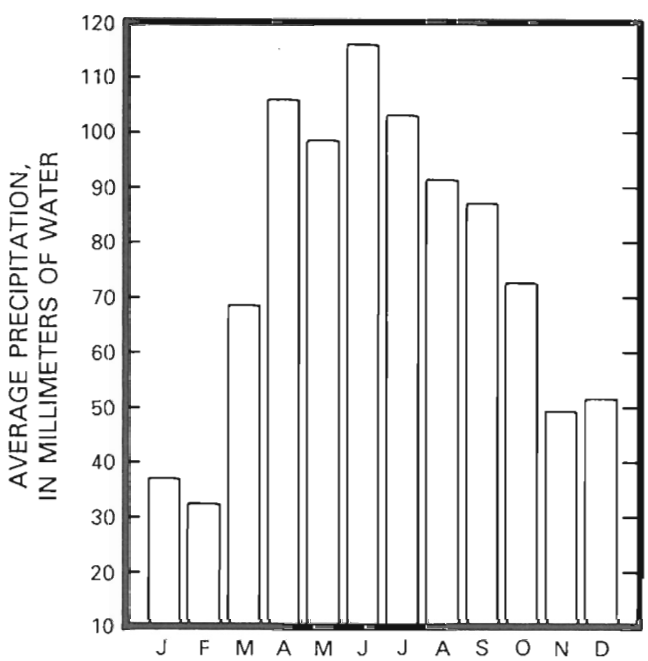

Figure 3. Average monthly precipitation from National Weather Service stations near Sheffield site.

Estimates of potential evapotranspiration are included in this study so that they may be compared with estimated evapotranspiration rates. The ratio of actual to potential evapotranspiration is an indication of to what extent the vegetation and soil moisture are filling the atmosphere's demand for water. This has several important ramifications. In agriculture, the ratio (sometimes referred to as the crop coefficient) is an important indicator of crop stress. If the ratio is too low, there may not be enough available soil moisture for growth. With respect to radioactive- or hazardous-waste disposal, it is desirable to maximize evapotranspiration to inhibit the downward movement of water into the waste trenches. The ratio of actual to potential evapotranspiration gives an indication of how well the vegetation and soil-water storage capability are meeting this goal. The effect of any future site modifications designed to increase evapotranspiration may be gaged by the resulting ratio of actual to potential evapotranspiration. It should be noted that there are several other important considerations in selection of site vegetation, such as rooting depth and control of erosion.

Aerodynamic Profile

Within the laminar boundary layer, heat, water vapor, and momentum are transferred vertically only by molecular processes. However, this layer is at most a few millimeters thick (Sellers, 1965, p. 141). Because the laminar boundary layer is so thin, it is virtually impossible to measure fluxes across it. Beyond this layer, transfer of heat, water vapor, and momentum is accomplished by turbulent processes. The aerodynamic-profile method is based on the assumption that turbulent transfer is described by the same equations that

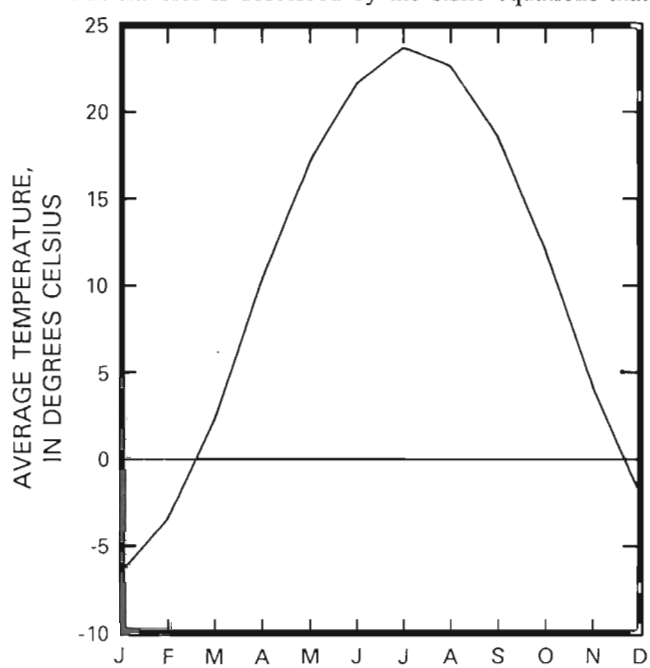

Figure 4. Average monthly temperature from National Weather Service stations near Sheffield site.

govern molecular transfer. Hence, the vertical fluxes of sensible heat (H), latent heat (LE), and momentum (τ) are described by the following equations (Sellers, 1965, p. 144):

$$H = -\rho_a C_p K_h \frac{\partial T}{\partial z}, \tag{1}$$

$$LE = -\rho_a L K_w \frac{\partial q}{\partial z}, \tag{2}$$

and

$$\tau = \rho_a K_m \frac{\partial u}{\partial z}, \tag{3}$$

where

ρ_a=density of air, in kilograms per cubic meter;
C_p=specific heat of dry air at constant pressure, in joules per kilogram per degree Celsius;
K_h=eddy diffusivity of heat, in square meters per second;
T=temperature, in degrees Celsius;
K_w=eddy diffusivity of water vapor, in square meters per second;
L=latent heat of vaporization for water, in joules per kilogram;
q=specific humidity, dimensionless;
K_m=eddy diffusivity of momentum, in square meters per second;
u=horizontal windspeed, in meters per second; and
z=height, in meters.

If $K_h = K_w = K_m$, usually a reasonable assumption (Dyer, 1974; Brutsaert, 1982, p. 61), then these equations can be rearranged to give

$$LE = -\tau L \frac{\partial q}{\partial u} \tag{4}$$

and

$$H = -\tau C_p \frac{\partial T}{\partial u}. \tag{5}$$

To make practical use of these formulas, more insight is needed on the variation of horizontal windspeed with height. If u increases linearly with the logarithm of height, then:

$$\frac{\partial u}{\partial \ln z} = C, \tag{6}$$

where C is a constant equal to the slope of the plot of windspeed versus the logarithm of height. According to Sellers (1965, p. 148)

$$C = \frac{1}{k} (\tau/\rho_a)^{1/2} = u^*/k, \tag{7}$$

where

u^*=friction velocity, in meters per second; and
k=von Karmann constant, usually taken to be about 0.40 (Brutsaert, 1982, p. 58), dimensionless.

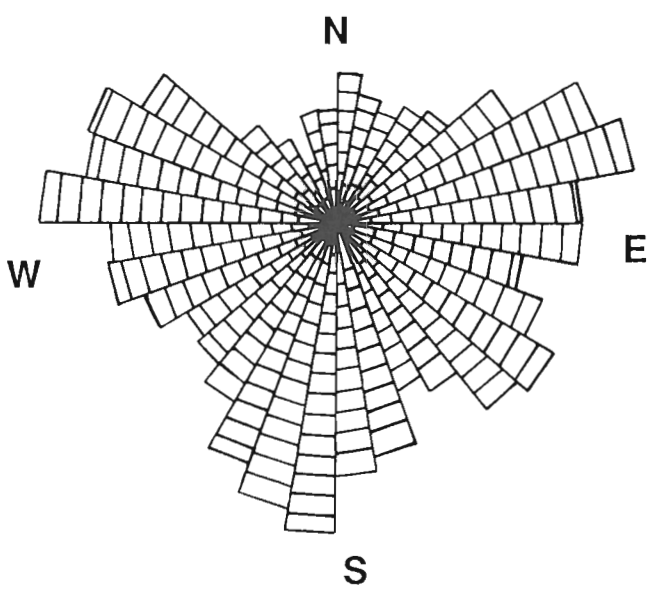

Figure 5. Frequency of occurrence, in percentage of time, of winds from various directions at Moline, Illinois, for June 1981 through December 1983. Radius of sector is proportional to frequency of occurrence.

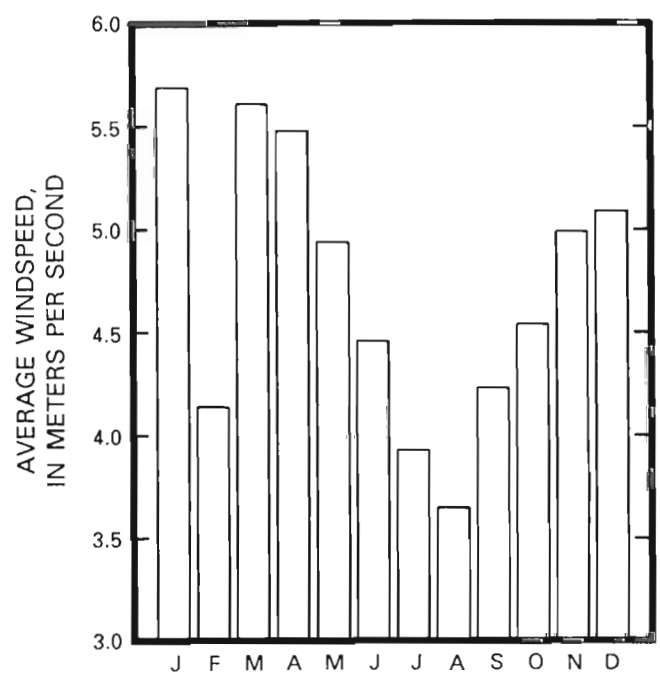

Figure 6. Mean monthly windspeeds at Moline, Illinois, for June 1981 through December 1983.

The windspeed at any height z can then be defined by

$$u=\frac{u^*}{k}\ \ln\ [(z-d)/z_o], \tag{8}$$

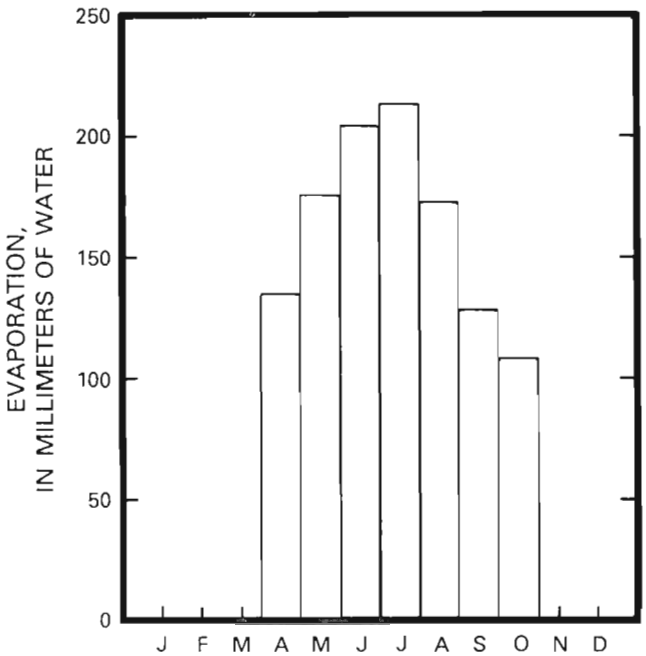

Figure 7. Average monthly pan evaporation for April through October at Hennepin, Illinois, for 1963 through 1983.

where

z_o=height at which u=0 (called the roughness length), in meters; and

d=zero-plane displacement, assumed to be equal to 0.6 times the height of the vegetation (Monteith, 1973), in meters.

The momentum flux can then be written as

$$\tau=\rho_a\ k^2\left(\frac{\partial u}{\partial \ln z}\right)^2=\rho_a\ u^{*2} \tag{9}$$

so that equations 4 and 5 become

$$E=-\rho_a\ k^2\ \frac{\partial q \partial u}{(\partial \ln z)^2}=-\rho_a\ \frac{\varepsilon}{P}\ u^{*2}\ \frac{\partial e}{\partial u} \tag{10}$$

and

$$H=\rho_a\ k^2\ C_p\ \frac{\partial T \partial u}{(\partial \ln z)^2}=-\rho_a\ C_p\ u^{*2}\ \frac{\partial T}{\partial u}, \tag{11}$$

where

e=water-vapor pressure, in kilopascals;

ε=ratio of molecular weights of water and air, dimensionless; and

P=barometric pressure, in kilopascals.

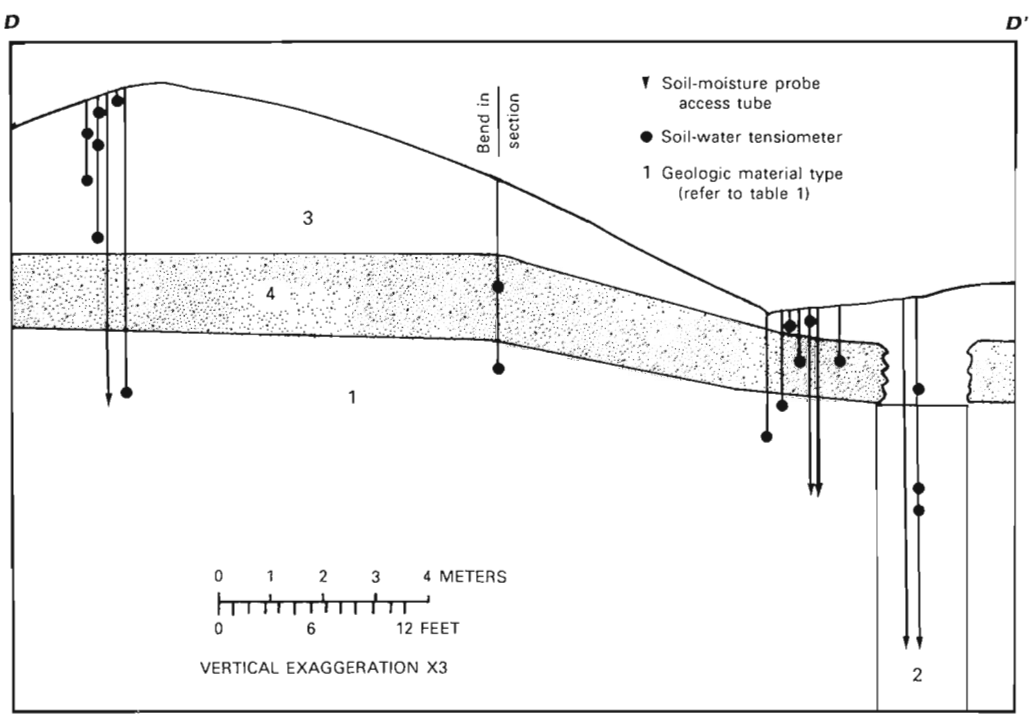

Figure 8. Section *D–D'* (see fig. 2) of trench cover and location of moisture-probe access tubes and tensiometers.

Table 1. Properties of surficial deposits
[Location of material types is shown in figure 8; g/cm^3, grams per cubic centimeter]

Type	Lithology	Bulk density (g/cm^3)	Description
1	Silt	1.25	Trench backfill similar to type 2, but waste containers are present in some locations
2	Silt	1.45	Undisturbed lower part of Peoria Loess
3	Clayey silt	1.65	Soil developed in upper part of Peoria Loess; other sediments may be mixed in
4	Clayey silt	1.85	Same as type 3, only more compacted

The forms of equations 10 and 11 to the right of the first equal signs were first proposed by Thornthwaite and Holzman (1942).

As mentioned earlier, the development of these equations requires that the wind profile be a logarithmic function of height. Under neutral conditions, this would usually be expected (Sellers, 1965, p. 148). However, under stable or unstable conditions, buoyancy effects can either inhibit or enhance the change in windspeed with height.

The term "stable" implies that there is an increase in temperature with height; hence, colder, heavier air has no tendency to rise. Unstable conditions occur when temperature decreases with height at a rate greater than the adiabatic lapse rate (about 0.01 °C/m) (Brutsaert, 1982, p. 44). Under these conditions, warmer, lighter air near land surface will tend to rise because of buoyancy. Neutral conditions imply that the temperature decreases with height at a rate less than or equal the adiabatic lapse rate. There are no buoyancy effects under neutral conditions.

Figure 9. Vegetation at the Sheffield site in June 1983.

To account for buoyancy effects in equations 10 and 11, several authors have proposed the use of the stability functions Q_h, Q_w, and Q_m, where the subscripts refer to heat, water vapor, and momentum, respectively. Sellers (1965, p. 153) cites eight different formulations of these functions in the literature. Most of these relate Q to either the Richardson number, R_i (Richardson, 1920), or the Monin-Obukov length, L' (Monin and Obukov, 1954), the two most common stability indexes. For this study, the formulations of Grant (1975) were used, where

$$Q_h = Q_w = Q_m^2 = \{1 - 15(z-d)/L'\}^{-0.5}$$

under unstable conditions; (12)

and

$$Q_h = Q_w = Q_m = 1 + 4.7(z-d)/L'$$

under stable conditions. (13)

The Monin-Obukov length was determined according to Campbell (1977, p. 41) as

$$L' = -u^{*3}\ \rho_a C_p T_k/(kgH), \tag{14}$$

where

g = acceleration due to gravity, in meters per square second; and

T_k = temperature, in kelvins.

The Monin-Obukov length is negative for unstable conditions and positive for stable conditions. Under neutral conditions, L' approaches infinity. Incorporating the stability functions into equations 10 and 11 gives

$$E = -\rho_a \frac{\varepsilon}{P} u^{*2} \frac{\partial e}{\partial u} Q_m Q_w^{-1} \tag{15}$$

and

$$H = -\rho_a C_p u^{*2} \frac{\partial T}{\partial u} Q_m Q_h^{-1}. \tag{16}$$

Equations 15 and 16 are the forms of the aerodynamic-profile equations that were used in this study. Note that equation 16 must be used with the energy-balance equation to estimate E. As will be discussed later, equation 16 gave much more satisfactory results than equation 15. Use of this method, then, requires determination of vertical profiles of horizontal windspeed, vapor pressure, and temperature.

Energy Budget

The energy-budget method for estimating evapotranspiration is based on the principle of conservation of energy. The primary source of available energy at the Earth's surface is solar radiation. This available energy is used to heat the soil surface, heat the air, and to evapotranspire available water. The energy budget can be written as

$$R_n-(H+L*E+G)=0, \tag{17}$$

where

R_n=net radiation, in watts per square meter;
H=sensible heat flux, in watts per square meter;
$L*E$=latent heat flux, in watts per square meter;
L=latent heat of vaporization, in joules per kilogram;
E=evapotranspiration rate, in kilograms per square meter per second (or millimeters per second); and
G=soil heat flux, in watts per square meter.

In applying equation 17 to an actual test site, energy absorbed by photosynthesis and energy stored within the plant canopy are ignored. Energy absorbed by snowmelt also is ignored. Only vertical fluxes are measured; horizontal fluxes are considered to be negligible. Measurements are made at only one location, so extrapolation of results over the entire study area requires that uniform conditions exist throughout. All fluxes appearing in equation 17 are assumed to occur at the soil or plant-canopy surfaces. However, in practice, these fluxes can only be measured at some finite distance from these surfaces.

In the energy-budget equation, R_n and G can be measured relatively easily. On the other hand, measurements of H and LE are not as straightforward, because estimating eddy diffusivities for heat and water vapor is difficult.

Bowen (1926) proposed solving the energy-balance equation by using the ratio of sensible- to latent-heat fluxes as follows:

$$\beta=\frac{H}{LE}=\frac{\rho_a\ C_p\ K_h\ \partial T/\partial z}{\rho_a\ L\ \varepsilon/P\ K_w\ \partial e/\partial z}, \tag{18}$$

where

β=Bowen ratio, dimensionless;
ρ_a=density of air, in kilograms per cubic meter;
C_p=specific heat of dry air at constant pressure, in joules per kilogram per degree Celsius;
$\frac{\partial T}{\partial z}$= vertical gradient of air temperature, in degrees Celsius per meter;
$\frac{\partial e}{\partial z}$= vertical gradient of water-vapor pressure, in kilopascals per meter;
ε=ratio of mole weights of water vapor and dry air, dimensionless, assumed to be 0.622;
K_h=eddy diffusivity for heat, in square meters per second;
K_w=eddy diffusivity for water vapor, in square meters per second; and
P=absolute barometric pressure, in kilopascals.

In computing β, it is again usually assumed that $K_h=K_w$ (Denmead and McIlroy, 1970; Swinbank and Dyer, 1967). Campbell (1973) showed that only under very stable conditions (such as at night) or extremely unstable conditions (such as during the day in an arid region) does K_h differ from K_w by more than 10 percent.

Substituting equation 18 into 17 gives

$$E=\frac{R_n-G}{(1+\beta)L}. \tag{19}$$

Use of this method, therefore, requires measurement of net radiation, soil-heat flux, barometric pressure, and vertical gradients of air temperature and water-vapor pressure.

Water Budget

The water-budget method for estimating evapotranspiration is based on the principle of conservation of water. For a soil column of thickness D and unit horizontal area, the water-budget equation can be written as

$$E=-\int_0^D \frac{\partial\theta}{\partial t}\,dz+PR-R-q_D, \tag{20}$$

where

E=evapotranspiration rate, in millimeters per day;
$\frac{\partial\theta}{\partial t}$= change in volumetric soil-moisture content with respect to time, per day;
z=depth, in millimeters;
PR=precipitation, in millimeters per day;
R=runoff, in millimeters per day; and
q_D=rate of drainage downward from the soil column at $z=D$, in millimeters per day.

Derivation of equation 20 assumes that all terms are averaged over the length of the sampling period. Lateral flow into the soil column is assumed to be negligible.

Soil-moisture content can be measured either in place or by soil sampling and gravimetric determination. The latter method generally is limited to studies of bare-soil evaporation because of the difficulty in sampling the entire depth of rooting for a vegetated cover. The most common in-place methods are the use of a weighing lysimeter and a soil-moisture probe or soil-water tensiometers. Of these, the weighing lysimeter is the most accurate; readings can be recorded automatically to provide detailed information on changes in evapotranspiration rates over time. Construction and operation of weighing lysimeters, though, is costly and time consuming (van Hylckama, 1974). The moisture-probe method was used for this study. This method is most useful when q_D is negligible (Brutsaert, 1982, p. 232). Although not negligible, the term is small when compared to evapotranspiration rates at the Sheffield site. Foster, Erickson, and Healy (1984) estimated that q_D ranges from 25 to 50 mm per year. In addition, virtually all of the drainage from the soil zone occurs in late winter or early spring (Healy and others, 1984)—times of low rates of evapotranspiration. Values for q_D can be estimated using Darcy's equations, if pressure heads are known at different depths within the soil zone. These pressure heads were measured with soil-water tensiometers.

The water-budget method has limited accuracy over short time periods; however, reliable estimates can be obtained over periods of several days (van Hylckama, 1980, p. 4). Several investigators have used this method with success (Jensen, 1967; van Bavel and Ehrler, 1968; and Wallace and others, 1981).

Potential Evapotranspiration

According to Penman (1956), potential evapotranspiration (PET) is "the amount of water transpired in a unit time by a short green crop, completely shading the ground, of uniform height, and never short of water." It is a measure of the capacity of the atmosphere to absorb water from a vegetated surface. There are many different techniques for estimating PET. A good review of the standard methods can be found in Deacon and others (1958). McGuinness and Bordine (1972) compared 14 different methods with lysimeter-derived data and showed that, although there were substantial differences in the magnitudes of the different estimates, there were high correlations among all methods. All methods showed similar trends throughout the year. Probably the most widely used methods are those of Penman (1948), Thornthwaite (1948), and Blaney and Criddle (1962).

The Penman (1948) method for estimating PET was used in this study because of its sound physical basis. It is also one of the more popular methods and, as such, may serve as a good index for comparisons with other locations. The Penman equation can be stated as

$$\mathrm{PET}=\frac{1}{L}\left[\frac{(R_n-G)\Delta}{\Delta+\gamma}+\frac{\gamma L E_a}{\Delta+\gamma}\right], \tag{21}$$

where

PET = potential evapotranspiration, in millimeters of water per second;
R_n = net radiation, in watts per square meter;
G = soil-heat flux, in watts per square meter;
Δ = slope of vapor saturation curve, in kilopascals per degree Celsius;
γ = psychrometric constant, in kilopascals per degree Celsius;
E_a = a measure of the drying power of the wind, in millimeters of water per second;
= f(u)* (e_s-e); f(u) is an empirical wind function; e and e_s are actual and saturated vapor pressures, respectively, in kilopascals.

Penman (1948) used the wind function

$$\mathrm{f(u)}=3.01\times10^{-5}\,(0.5+0.54\,u_{2m}), \tag{22}$$

where

u_{2m} = windspeed at 2 m height, in meters per second.

Penman (1948) originally derived equation 21 for estimating potential evaporation of open water. Penman and Schofield (1951) modified it to account for the difference between evaporation and evapotranspiration by adding correction factors to account for stomatal resistance to vapor flow and the opening and closing of the stomata during the diurnal cycle. Tanner and Pelton (1960), however, found little basis for general application of these factors. They suggested that the wind function be modified to account for surface roughness. Several authors, including Monteith (1973) and Thom and Oliver (1977), have proposed alternative formulations for f(u). van Bavel (1966) proposed use of the wind function

$$\mathrm{f(u)}=\frac{\rho_a\,\varepsilon\,k^2}{P}\,\frac{u}{[\ln\,(z-d)/z_o]^2}, \tag{23}$$

where

ρ_a = density of air, in grams per cubic meter;
ε = ratio of molecular weight of water to air, dimensionless;
k = van Karmann constant, dimensionless;
P = barometric pressure, in kilopascals;
u = windspeed at height z, in meters per second;
z = height of windspeed measurement, in meters;
z_o = roughness length, in meters; and
d = zero-plane displacement, in meters.

Equation 23 is the formulation of f(u) that was used in this study. Daily PET values were computed for the entire period of record. In calculating these values, a daytime-nighttime weighting scheme was employed (Tanner and Pelton, 1960).

INSTRUMENTATION

Instruments used in this study were monitored with microprocessor-based data loggers (Campbell Scientific models CR-21 and CR-7), which are capable of accepting analog, electrical-resistance, and electric pulses. Most sensors were read at 10-second intervals. Readings were then averaged or totaled for each hour and day. The hourly and daily values were then stored on magnetic-tape cassettes and routinely transferred to computer storage. Sensors were located close to the center of the site (fig. 2), which provided a wind fetch of at least 100 m in all directions.

Precipitation

Precipitation was measured with tipping-bucket and weighing rain gages. The tipping-bucket gage measured precipitation in increments of 0.25 mm. The data logger then accumulated precipitation in both 1-minute and 1-hour intervals. The weighing rain gage was used to obtain daily precipitation totals during the winter.

Radiation

Net radiation was measured directly using a Fritschen-type (Fritschen and Gay, 1979) net radiometer. It was also computed as the sum of its individual components (incom-

ing and outgoing shortwave-solar and longwave-terrestrial radiation). Each of these individual components was measured by a radiometer consisting of a temperature-compensated thermopile located between an exposed and shielded surface. The exposed surface is coated with a nonwavelength-selective, radiation-absorbing black lacquer, whereas the other surface is shielded from external radiation. Wavelength specificity is achieved with hemispherical filters of known optical transmission (0.3 to 3.0 micrometers for shortwave radiation and 4.0 to 50.0 micrometers for longwave radiation). Radiant energy is converted to heat at the lacquer surface. The amount of heat—and, therefore, radiant energy—is determined from the difference in temperature between the two surfaces. Longwave radiometers require an additional temperature-dependent correction to compensate for radiation emitted by the detector. The net radiometer operates on the same principle as individual-component types; however, it differs in its broadened width of wavelength receptance and simultaneous acceptance of incoming and outgoing radiation. Calibration is factory-determined using International Pyrheliometric Scale standards for shortwave and a low-temperature blackbody for longwave radiometers. Incoming radiometers were mounted at a height of 2 m, whereas outgoing and net radiometers were mounted at a height of 1 m.

Wind

Horizontal windspeed was measured at two heights (0.5 and 2.0 m) prior to October 1983; after that time, it was measured at three heights (0.5, 1.0, and 2.0 m). Three-cup electro-optical anemometers were used. These instruments contain a small infrared light source that is separated from a photo-Darlington sensor by an opaque disk containing a single window. For each rotation of the cup wheel, the window passes between the light source and detector causing a short electric pulse to be sent to the data logger. The logger calculates windspeed by counting these pulses over a 10-second interval.

A potentiometric wind vane, mounted at a height of 2 m, was used to determine wind direction. This device transforms direction into electrical resistance. The data logger measures the amount of resistance and computes a vectorized wind direction and speed.

Air Temperature and Water-Vapor Pressure

Dry- and wet-bulb air temperatures were measured with linearized thermistors installed at heights of 0.5 and 2.0 m (and also at 1.0 m after September 1983). The wet-bulb thermistors were kept wet with cotton wicks that drew from water reservoirs. The thermistors were contained in a shelter consisting of a radiation shield and tetraskelion-design air-passage systems to allow natural wind (as opposed to forced draft) to ventilate the thermistors. The design of these psychrometers is more fully explained by Bellaire and Anderson (1951). Those authors found that accurate water-vapor pressures could be obtained if the windspeed was at least 0.44 m/s. The design has been used in previous studies (see Anderson, 1954, p. 71; and van Hylckama, 1980).

The Rankin-Dupré formula (Sutton, 1953, p. 5) and the psychrometric equation (Chemical Rubber Co., 1972, p. e–39) were used to compute the saturated and actual vapor pressures:

$$e_s = 0.1 \exp\left[54.721 - 6788/(T_w + 273.16) - 5.0016 \cdot \ln(T_w + 273.16)\right] \quad (24)$$

and

$$e = e_s - \left[P \cdot 0.00066 \cdot (T_a - T_w) \cdot (1 + 0.00115 T_w)\right], \quad (25)$$

where

e_s = saturation vapor pressure, in kilopascals;
e = vapor pressure of overlying atmosphere, in kilopascals;
T_a = dry-bulb temperature, in degrees Celsius;
T_w = wet-bulb temperature, in degrees Celsius; and
P = barometric pressure, in kilopascals.

The thermistors used (Yellow Springs Instruments Model 44212) were listed by the manufacturer to have an accuracy of ±0.15 °C. This accuracy was improved to at least ±0.10 °C by calibration in a stirred alcohol bath for the range of possible temperatures encountered at the site. New thermistors were placed in the psychrometers at approximately 60-day intervals. In addition, the individual psychrometers were periodically rotated to stations with different heights to reduce instrument bias.

Soil-Heat Flux and Temperature

Conductive soil-heat flux was measured with heat-flux disks, which are thin ceramic plates that contain a thermopile. The thermopile determines the difference in temperature between the top and the bottom of the plates. If the thermal conductivity of the plates is known, soil-heat flux can be determined using Fourier's first law of heat conduction:

$$Q = -K \frac{\partial T}{\partial z}, \quad (26)$$

where

Q = the soil-heat flow, in watts per square meter;
K = the thermal conductivity, in watts per meter per degree Celsius; and
$\frac{\partial T}{\partial z}$ = the change in temperature with respect to depth, in degrees Celsius per meter.

The heat-flux disks used in this study were 3 mm thick and 28 mm in diameter. They were factory calibrated and had a thermal conductivity of approximately 0.33 W/m °C (watts per meter per degree Celsius). They were installed at three different depths (20, 50, and 100 mm) to define the soil-heat flux gradient.

Soil temperatures were measured at seven depths, ranging from 0.02 to 1.00 m, using copper-constantan thermocouples that were used as a backup for the heat-flux disks in computing conductive heat transfer.

Surface temperature was measured with an infrared thermometer. This device actually measures infrared radiation being emitted by the object at which it is aimed. The temperature of that object is then determined internally within the thermometer according to the Stefan-Boltzmann Law:

$$Q' = \varepsilon' \sigma T_k^4, \tag{27}$$

where

Q' = flux of infrared radiation, in watts per square meter;
ε' = emissivity, dimensionless;
σ = Stefan-Boltzmann constant, in watts per square meter per Kelvin to the fourth power (5.66×10^{-8} W/m^2 °K^4); and
T_k = temperature, in Kelvins.

Equation 27 does not account for any radiation reflected by the object. This should have little effect upon surface-temperature measurements because of the high emissivity of both bare soil and vegetated surfaces.

The thermometer was mounted at a height of 1.5 m and was aimed directly downward. Emissivity, which can be adjusted by a dial on the thermometer, was usually set at 0.98, which according to Brutsaert (1982, p. 137) should be typical for grassy vegetation.

Soil-Water Content and Tension

A gamma-attenuation soil-density gage was used to determine soil-water content. Use of this device requires two parallel access tubes. A gamma-emitting radioactive source (cesium-137) is lowered down one tube, while a detector is maintained at the same depth as the source in the other tube. The number of gamma photons arriving at the detector is a function of the total density of the material between the tubes. Therefore, the dry bulk density of the soil must be known in order to obtain the water content. Additional details of the operation of this type of gage appear in Healy and others (1986). Weekly or biweekly measurements were made during the study period at three locations (figs. 2 and 8) in depth increments of 51 mm below land surface to the bottom of the access tubes. Depths to the bottom of the tubes ranged from 1.5 to 2.5 m.

A series of 32 soil-water tensiometers were installed adjacent to the moisture-probe measurement sites (figs. 2 and 8) at depths ranging from 0.05 to 2.20 m. Readings from the tensiometers were automatically recorded using pressure transducers and data loggers.

Surface Runoff

Three stations were used to gage runoff from the site. The average drainage area of these stations was about 1.79 hectares. Although each station was located on an ephemeral streambed, they were all equipped with a continuous stage recorder to insure that runoff occurring immediately following precipitation was measured.

More detail on the measurement of surface runoff at the site can be found in Gray (1984). In addition, small runoff-collection plots, which are described in Gray and deVries (1984), were located near the moisture-probe access tubes. The average drainage area of these plots was 11 m^2 (square meters).

MICROCLIMATE OF THE TRENCH COVERS

Discussion of certain aspects of the microclimate of the trench-cover vegetation is warranted in order to illustrate the effects of assumptions made when estimating evapotranspiration. Weather patterns are examined for both seasonal and diurnal trends. To aid in this discussion, figure 10 shows hourly values of several microclimatological parameters for six 3-day periods. All times shown in figure 10, and all subsequent figures and tables, refer to local time (either central standard or central daylight).

Precipitation

Monthly precipitation totals for the 2-year period of study are shown in figure 11. Although the temporal distribution of precipitation varied during the 2-year study period, annual totals were very similar. From July 1, 1982, through June 30, 1983, a total of 927 mm of precipitation fell, whereas from July 1, 1983, through June 30, 1984, the total was 949 mm. As mentioned previously, the long-term average for the area is about 890 mm. Precipitation was recorded on 112 days during the 2-year period. Much of the precipitation was in the form of heavy thunderstorms. A storm is defined as a period of precipitation separated from preceding and succeeding precipitation by 6 or more hours (Huff, 1979, p. 6). Of the 1,876-mm total precipitation, 889 mm fell during 20 storms, each of which produced more than 25 mm. This is slightly different from long-term trends. Changnon and Huff (1980, p. 35) indicate that, on the average, 60 percent of the annual precipitation in this part of Illinois falls in storms totaling 3 to 25 mm.

During the winter of 1982–83, 406 mm of snowfall (equivalent to 40 mm of water) was measured at the nearby National Weather Service stations, and snow was on the ground for a total of 18 days. The winter of 1983–84 was much more severe: a total of 726 mm of snow (equivalent to 69 mm of water) fell, and snow was on the ground for 65 days.

Radiation

Figure 12 shows mean monthly incoming and reflected solar radiation for the 2-year study period. On the average, incoming solar radiation was 156 W/m^2 (watts per square meter). This is approximately 65 percent of clear-sky solar radiation, as computed by a formula given by the U.S. Department of Energy (1978). There were a total of 117

clear-sky days (measured solar radiation was 90 percent or more of clear-sky solar radiation). For the same time period, Moline airport reported 160 clear-sky days. Monthly ratios of actual to clear-sky solar radiation are shown in figure 13. These give a good indication of the amount of daytime cloud cover during the year.

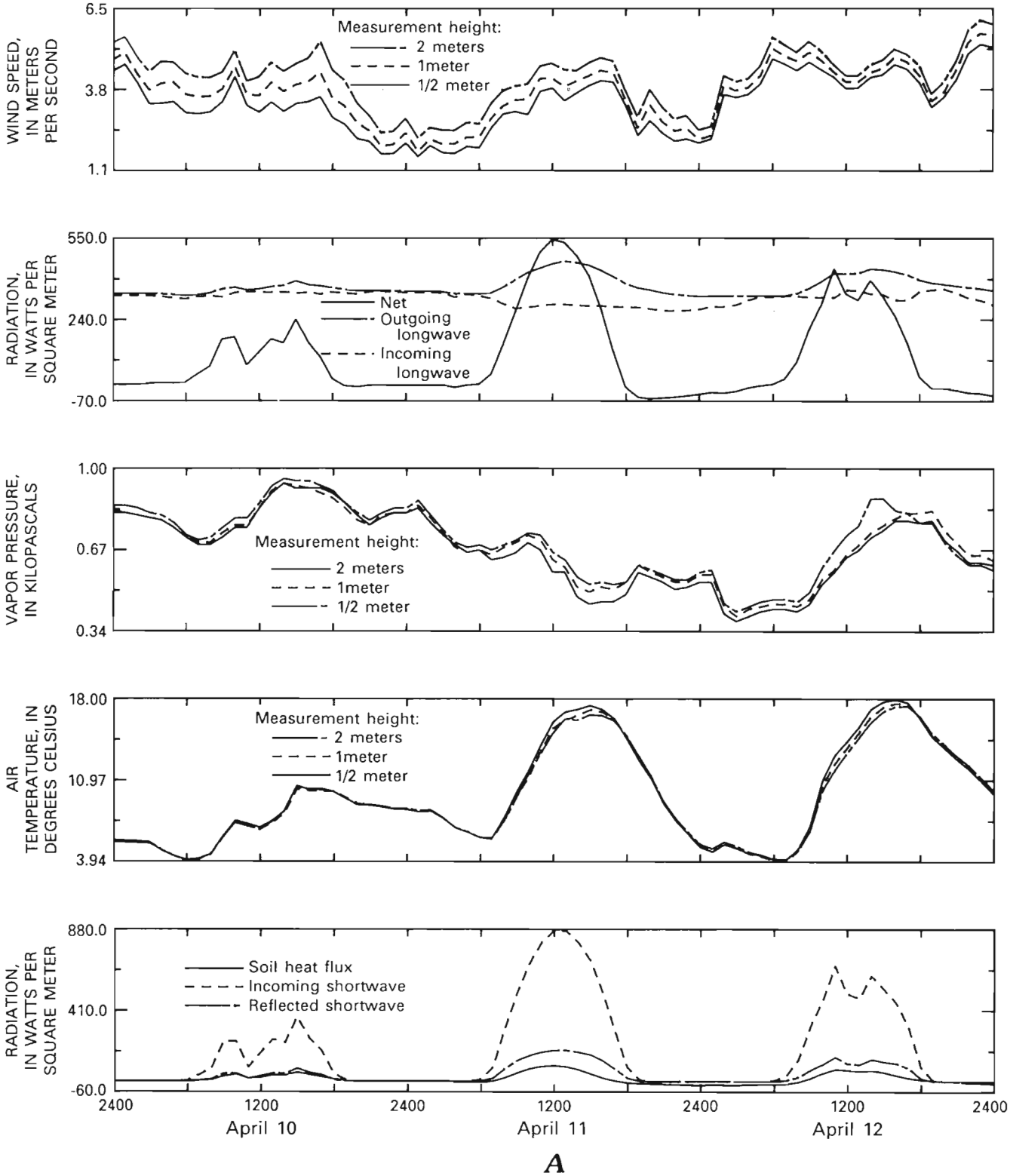

Figure 10. Selected microclimotological parameters at the Sheffield site. *A*, April 10–12, 1984. *B*, May 31 through June 2, 1984. *C*, July 1–3, 1982. *D*, August 15–17, 1983. *E*, September 13–15, 1982. *F*, October 30 through November 1, 1983.

The ratio of reflected to incoming solar radiation is termed the surface albedo. Albedo values at the site ranged from about 0.20 during summer to about 0.95 following a fresh snow in winter. Figure 14 shows monthly albedo values obtained during the study period. While viewing figure 14, keep in mind that albedo can change drastically from day to day in cold weather depending on whether snow is falling or melting. For example, table 2 shows daily albedo values for

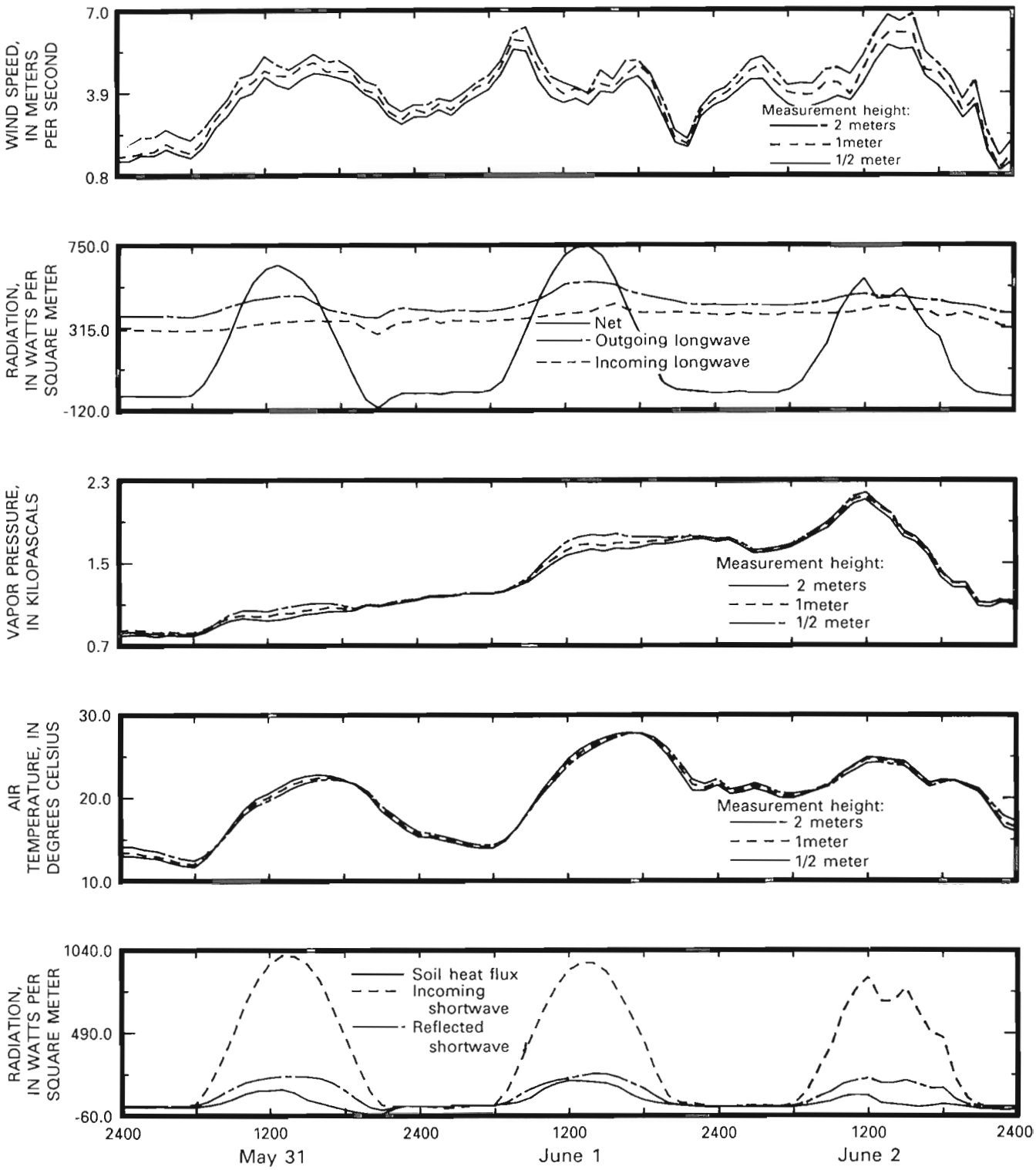

Figure 10. Continued.

January 29 through February 3, 1984. Snow fell on January 30 and 31 and melted on February 1–3. On days when there was no change in surface conditions, there was a diurnal trend in albedo values. Table 3 shows hourly albedo values for 2 days. June 2, 1984, was a day of 83 percent clear-sky radiation, whereas November 1, 1983, was a day of 57 percent clear-sky radiation. A similar trend in albedo is apparent for both days; the lowest values occurred around solar noon and

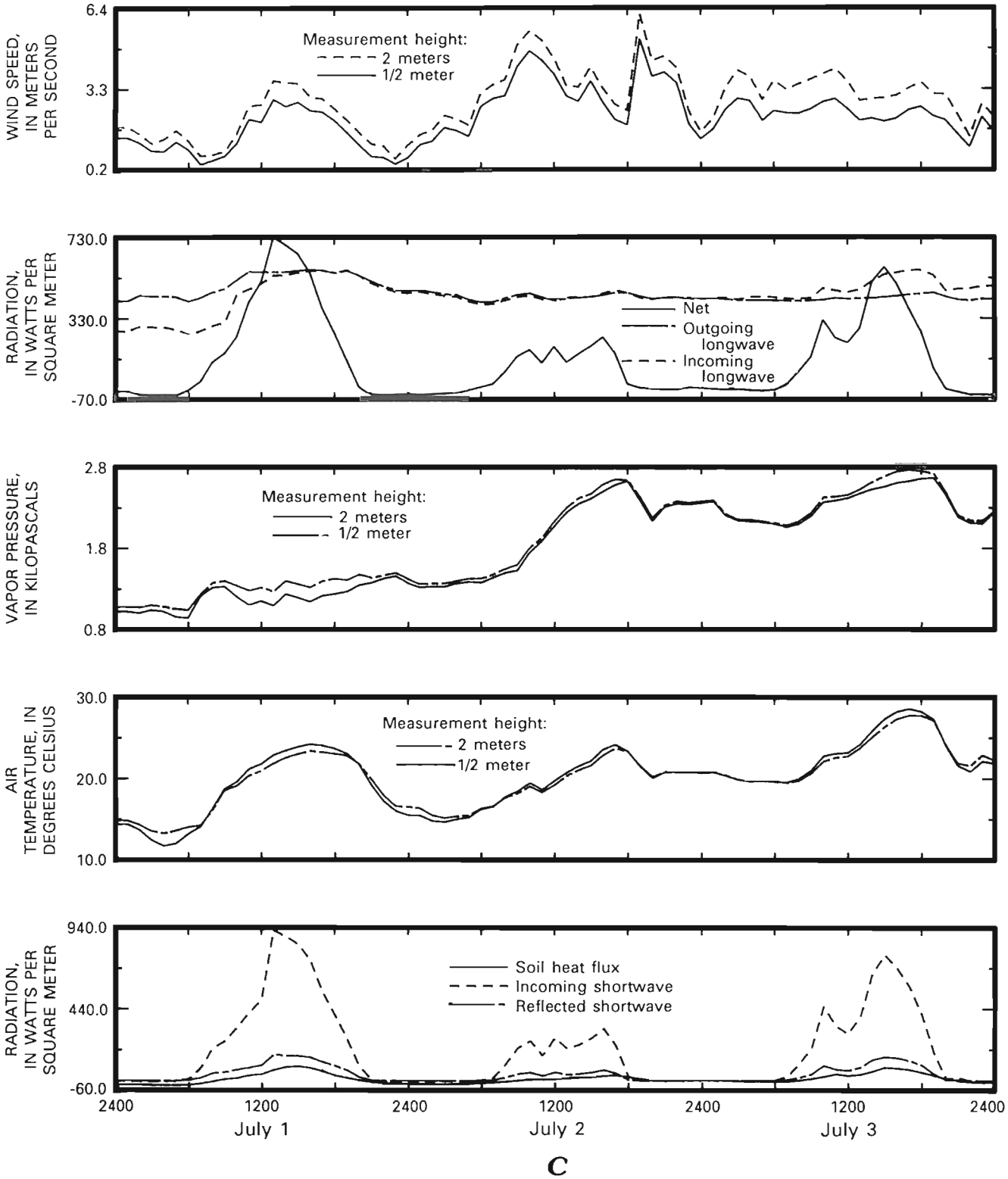

Figure 10. Continued.

values increased toward dawn and dusk. Similar trends have been measured elsewhere (Geiger, 1961; Rouse, 1984). Budyko (1956) cites the high zenith angle of the sun near dusk and dawn as the primary reason for this trend.

Monthly values of longwave radiation outgoing from the Earth and incoming from the atmosphere are shown in figure 15. Because longwave radiation is directly proportional to the fourth power of the absolute temperature (from the

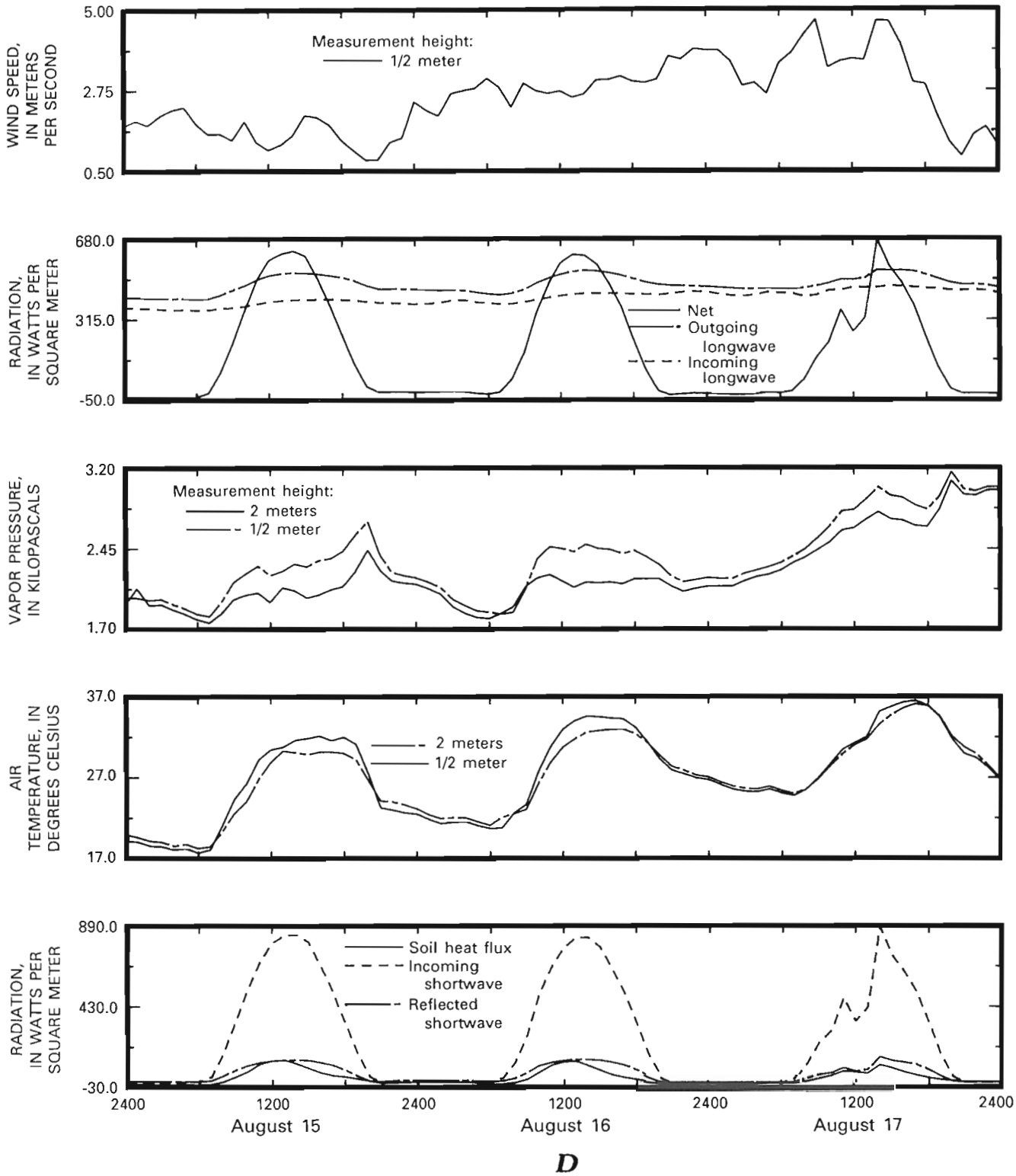

Figure 10. Continued.

Stefan-Boltzmann law—equation 27), seasonal trends in both outgoing and incoming radiation should parallel those of air and soil-surface temperatures. This trend is indeed apparent. The highest longwave-radiation values were obtained during the warmest months and the lowest values during the coldest months. The ratio of incoming to outgoing longwave radiation is dependent primarily upon cloud cover. Clouds absorb most longwave radiation and then re-emit it back to

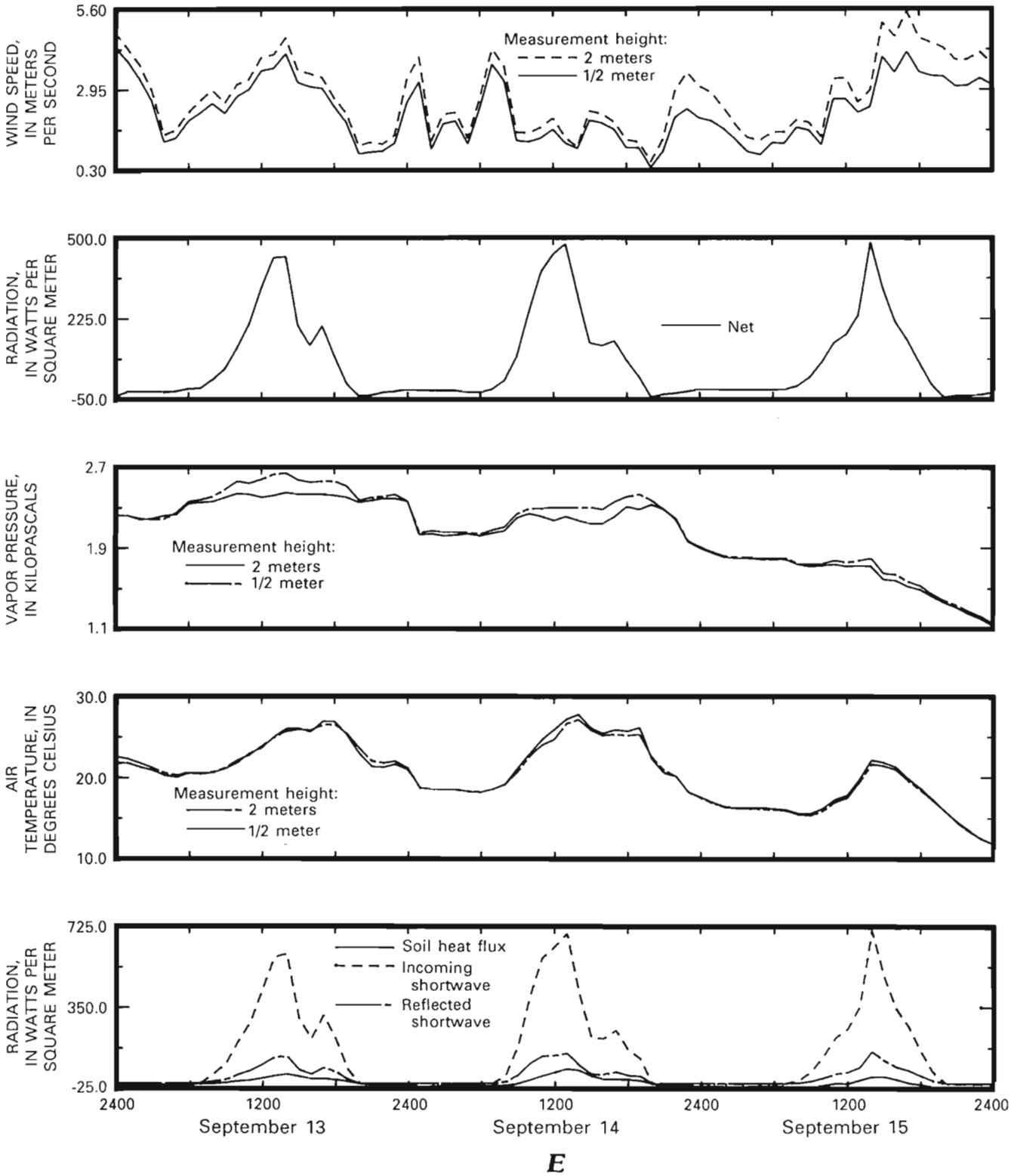

Figure 10. Continued.

Earth, and so the ratio increases with increased cloud-cover density. The ratio is lowest on clear-sky days.

Net radiation is the total of incoming solar and longwave radiation minus reflected solar and outgoing longwave radiation. Its magnitude is usually larger than all other elements in the energy-balance equation. Figure 16 shows monthly values for the study period. The average for the entire study period was 70.1 W/m^2, while daily averages

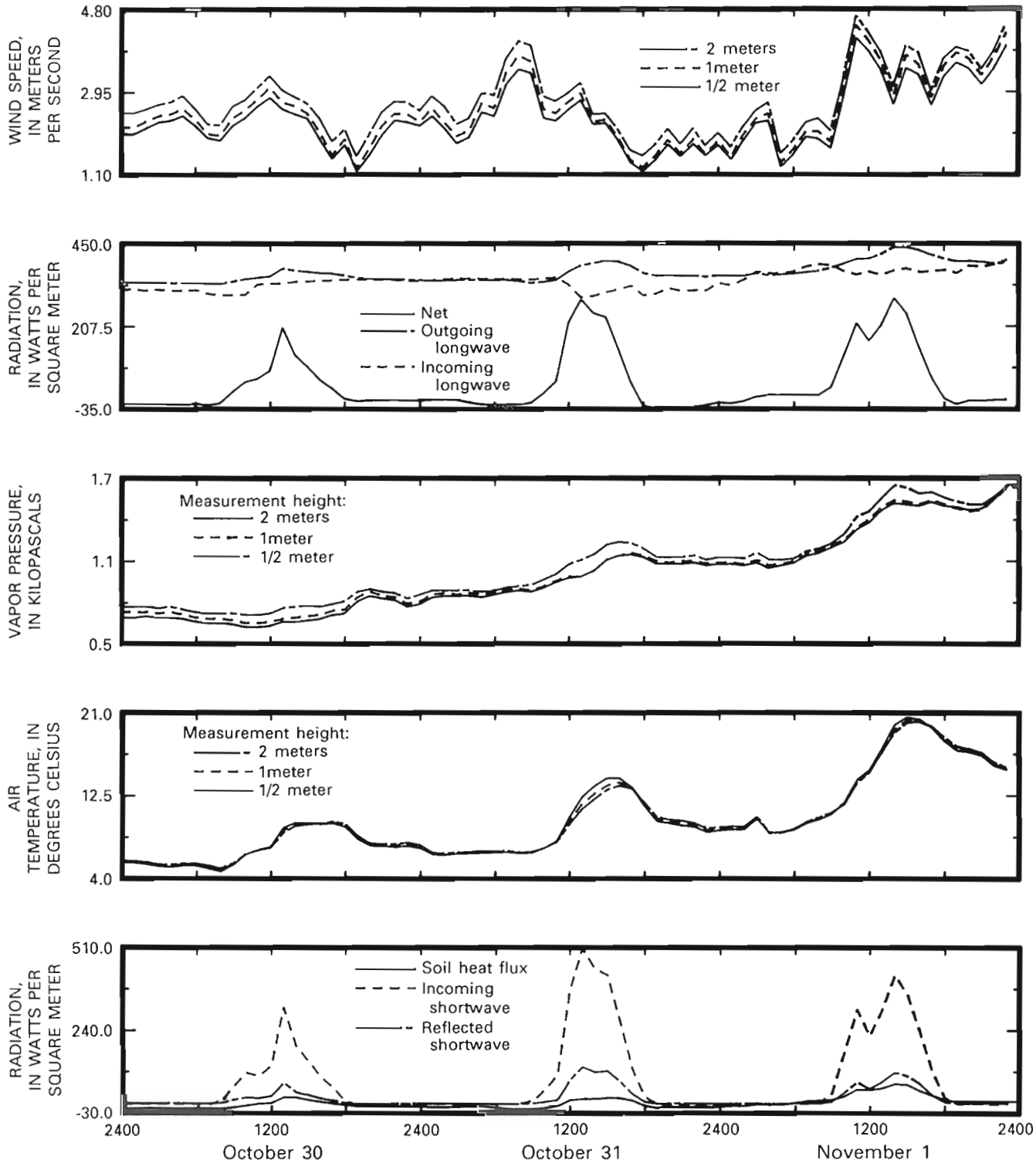

F

Figure 10. Continued.

ranged from −90 to 350 W/m^2. Diurnal trends are illustrated in figure 10. During daylight hours, net radiation is usually positive and follows the same trend as incoming solar radiation; values increase after dawn, reaching a maximum around solar noon, after which they decrease until dusk. After sunset, net radiation is equal to the difference in incoming and outgoing longwave radiation. Because the amount of outgoing radiation is greater than that of incoming, net radiation is negative at night. The magnitude of nighttime net radiation is generally much less than daytime net radiation.

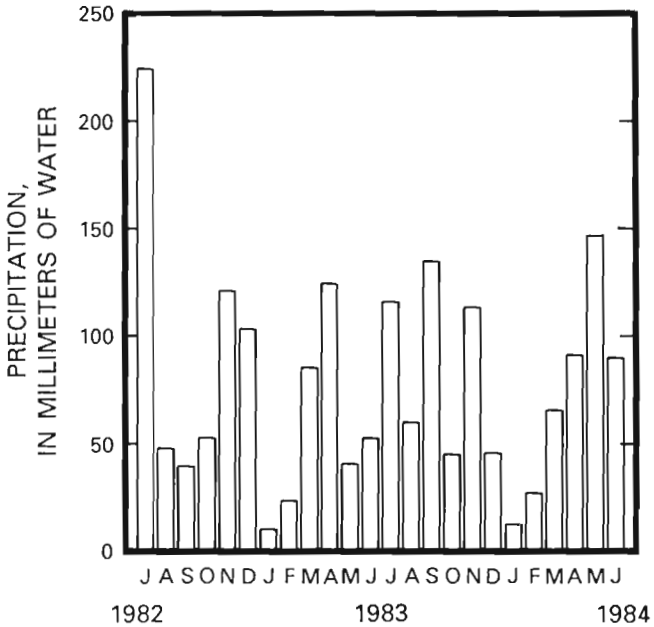

Figure 11. Monthly precipitation at the Sheffield site.

Wind

As shown in figure 17, the surface winds at the Sheffield site were predominantly out of the south-southeast for the 2-year study period. This direction is slightly different from the prevailing winds from the south-southwest and west-northwest at the Moline Airport. The difference may be due to the fact that the weather vane at the Sheffield site was mounted at a much lower height (2 m) than at Moline. At the lower height, wind direction is more influenced by small, localized wind eddies. Also, the wind direction at Moline was based on a reading taken each hour (1-minute duration), whereas readings at the Sheffield site were taken every 10 seconds.

Figure 18 illustrates mean monthly windspeeds. Some months are missing because of instrument downtime due to malfunction. The average windspeed for the 2-year study period at the 2-m height was 3.5 m/s. Daily average windspeed ranged from less than 1 m/s to as much as 10.2 m/s, whereas hourly averages were as much as 15.0 m/s. Windspeeds were slightly higher during winter months (fig. 18).

As discussed earlier, strict use of the aerodynamic-profile equations requires that the plot of windspeed as a function of the logarithm of height be a straight line. Typical variations of windspeed with height and time of day are shown in figure 19. The data for 0600 and 1800 hours appear to lie on a straight line. However, there is a significant change in slope on the curves at 1500 and 2400 hours. The shapes of these curves are related to the stability of the overly-

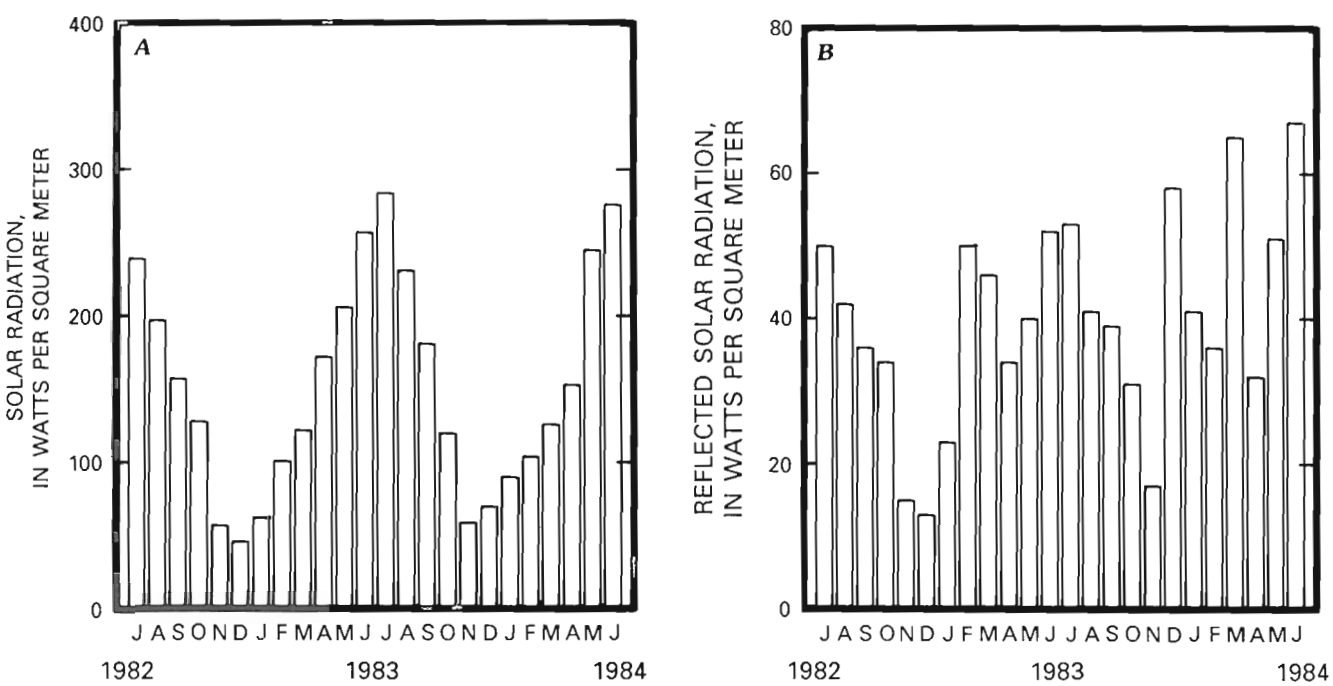

Figure 12. Monthly solar radiation at the Sheffield site. *A*, Incoming radiation. *B*, Reflected radiation.

ing atmosphere. The degree of stability is indicated by figure 20, which shows hourly values of z/L' (where z is the measurement height and L' is the Monin-Obukov length) for the same day. Values of z/L' at about 0700 and 1900 hours were very close to zero, indicating nearly neutral conditions. Between these hours, unstable conditions prevailed (z/L' was less than zero). Before dawn and after dusk, z/L' was greater than zero, indicating that stable conditions prevailed. These changing stability conditions necessitated the use of stability functions (eqs. 12 and 13) to modify the aerodynamic-profile equations for estimating evapotranspiration.

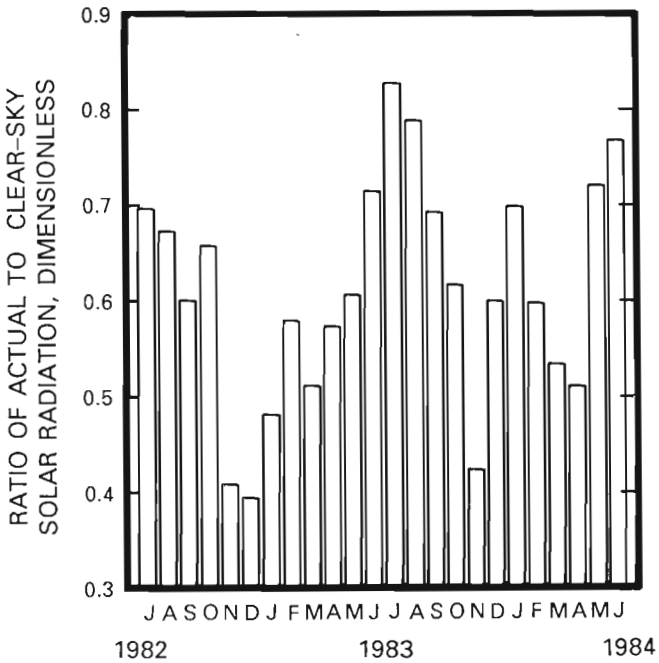

Figure 13. Monthly ratios of solar radiation to clear-sky radiation at the Sheffield site.

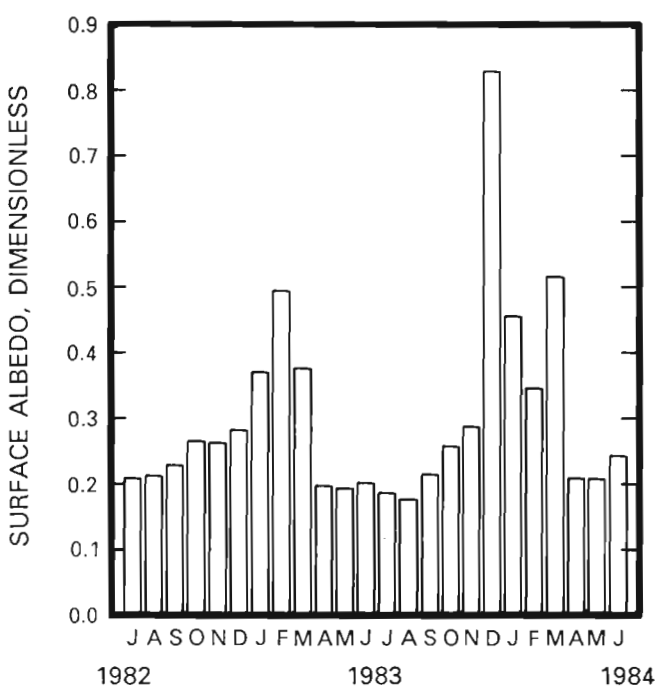

Figure 14. Monthly surface albedo at the Sheffield site.

Table 2. Daily albedo for six days in January and February 1984

Day	Albedo
Jan. 29	0.25
Jan. 30	.95
Jan. 31	.91
Feb. 1	.87
Feb. 2	.50
Feb. 3	.37

Table 3. Hourly albedo for two days
[Dashes indicate an hour of no solar radiation]

Time[1]	Albedo	
	June 2, 1984 (average solar radiation = 293 W/m^2)	November 1, 1983 (average solar radiation = 32 W/m^2)
7:00	0.28	--
8:00	.27	0.19
9:00	.26	.18
10:00	.24	.18
11:00	.23	.18
12:00	.22	.18
13:00	.22	.19
14:00	.22	.19
15:00	.22	.19
16:00	.22	.22
17:00	.24	--
18:00	.25	--
19:00	.27	--
20:00	.27	--
21:00	.29	--

[1] Central standard or Central daylight.

Air Temperature and Water-Vapor Pressure

The average recorded temperature at the Sheffield site over the 2-year study period was about 10.8 °C. Daily averages ranged from a low of −26 °C on December 25, 1983, to a high of 32 °C on July 22, 1983. Figure 21 shows average monthly temperatures for the study period. July was the warmest month and December and January were the coldest.

The daily trend for the vertical gradient in air temperature is shown in figure 10. From early morning (usually about 2 hours after dawn) until late afternoon (usually about 4 hours before dusk), the gradient was negative; temperatures decreased with height. This pattern represents a positive sensible-heat flux. The magnitude of the gradient was greatest during hours of peak solar radiation. In late afternoon, the gradient reversed, producing a temperature inversion. This

condition usually lasted throughout the night. On infrequent occasions, temperature inversions occurred during daylight hours. Such an inversion represents a negative sensible-heat flux, implying that energy is being advected into the area in the form of a warm wind. This generally occurred only during days of low solar radiation.

Average monthly water-vapor pressures at the 0.5 m height for March through November are shown in figure 22. Values for some months are not presented because of freezing of the wet-bulb thermistors. Vapor pressure followed the same monthly pattern as air temperature, reaching maximum values in July and August.

Water-vapor pressure also followed a diurnal trend similar to that of air temperature. During daylight hours, a negative gradient prevailed, indicating that water vapor was moving away from the land surface; evapotranspiration was occurring. Again, the magnitude of the gradient corresponded to the magnitude of the net radiation. Either positive or negative gradients could occur during nighttime hours. Condensation occurred when air temperature suddenly dropped below the ambient dew point. Whether the gradient was positive or negative at night, its magnitude was much less than it was during daylight hours.

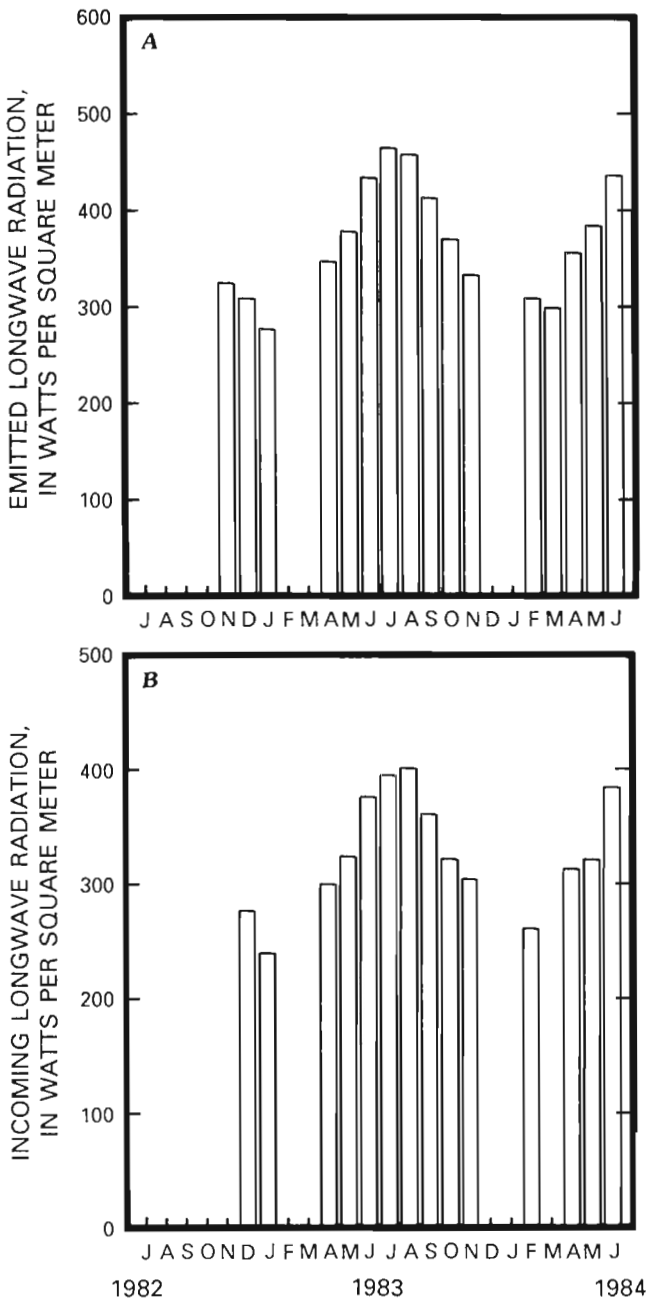

Figure 15. Monthly longwave radiation at the Sheffield site. *A*, Outgoing radiation (from Earth). *B*, Incoming radiation (from atmosphere).

Soil-Heat Flux and Soil Temperature

Monthly soil-heat fluxes are presented in figure 23. Monthly values reached a maximum in June and July and a minimum in November and December. During the 2-year study period, the maximum monthly heat flux was 23.4 W/m^2 in July 1983, and the minimum monthly flux was -13.0 W/m^2 in November 1982. From February through August, values were positive, indicating that the soil was gaining heat. Soil-heat flux was negative from September through January, indicating the release of heat.

Annual averages of soil-heat flux indicate a net gain of 0.5 and 5.7 W/m^2 for the first and second years of the study period, respectively. Soil temperatures did increase slightly during the second year but not enough to account for that rather large gain. Apparently, summertime fluxes were overestimated or negative fluxes were underestimated; the latter seems to be more likely. Because the thermal conductivity of the soil increases with increasing moisture

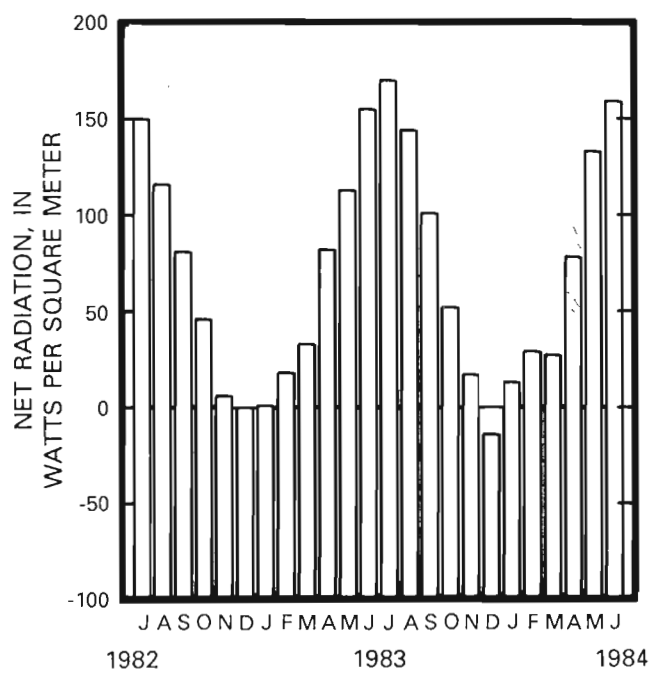

Figure 16. Monthly net radiation at the Sheffield site.

content (as well as when the soil freezes), it is less in summer than it is in fall through early spring. The thermal conductivity of the heat-flux disks is closer to that of the drier soil; hence, the disks are more likely to underestimate the magnitude of the heat flux in wet or frozen soil.

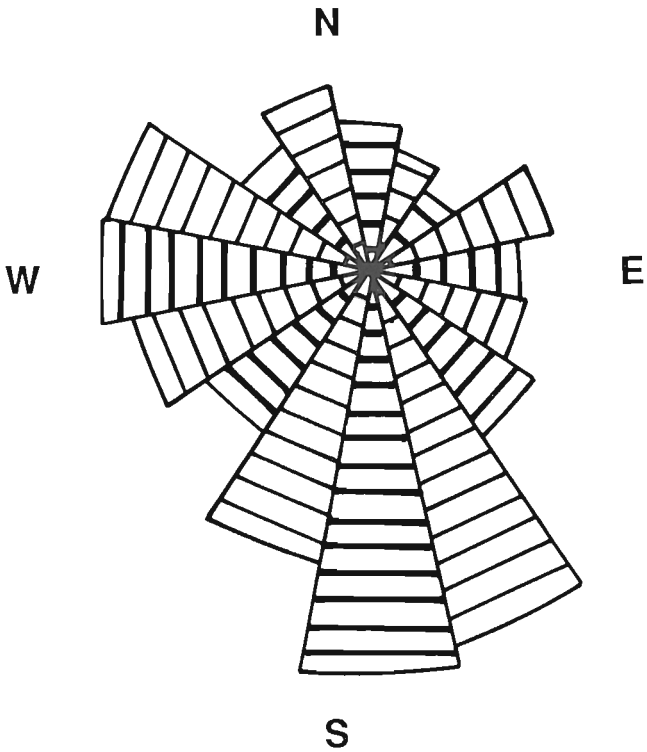

Figure 17. Frequency of occurrence, in percentage of time, of winds from various directions at the Sheffield site. Radius of sector is proportional to frequency of occurrence.

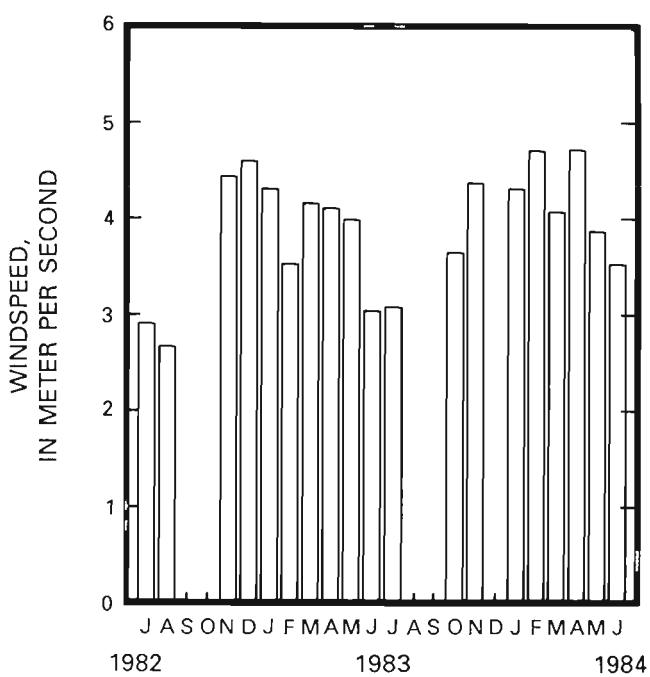

Figure 18. Mean monthly windspeed at the Sheffield site.

Diurnal trends of soil-heat flux are shown in figure 10. Shortly after sunrise, on clear days, the flux becomes positive, increasing to a maximum value just after the peak daily value of net radiation. The flux then decreases, becoming negative after sunset. During the night, the soil-heat flux slowly becomes more negative, with a minimum value usually occurring just before dawn. During warm, dry periods of the year, recorded values for soil-heat flux show an almost immediate and parallel response to changes in net radiation caused by variations in cloud cover.

Annual and diurnal trends in soil-heat flux were supported by the soil-temperature profiles. Figure 24 shows the daily trend of the vertical soil-temperature gradient for periods during the summer and fall of 1983. In general, the magnitude of the temperature gradient was greatest during the summer months.

Daily average temperatures over the 2-year study period at a depth of 100 mm ranged from a low of −5 °C on February 6, 1984, to a high of 28 °C on July 22, 1983. Because temperature fluctuations are increasingly damped and delayed with depth, daily averages at the 1.0-m depth ranged from a low of 1.7 °C on February 22, 1984, to a high of 21.9 °C on August 30, 1983. During the 1982–83

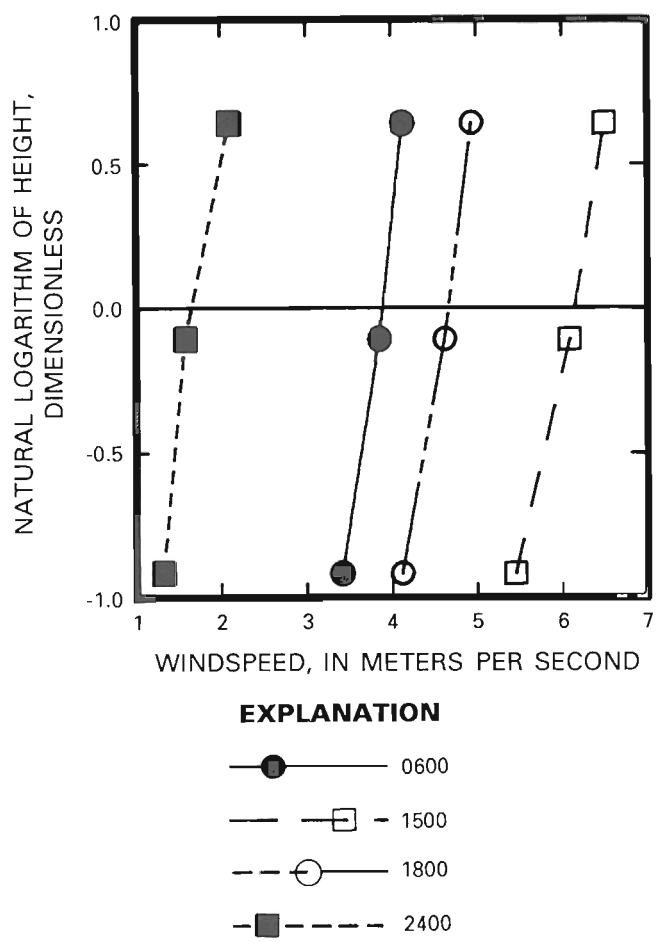

Figure 19. Vertical gradients in horizontal windspeed at the Sheffield site for 4 hours on June 2, 1984.

winter, the ground did not freeze to the 300-mm depth. In contrast, during the winter of 1983–84, the ground was frozen to a depth of 300 mm from January 14 through March 23.

Soil-Water Content

The soils that comprise the trench cap can store substantial amounts of water. The actual amount that is stored varies seasonally. Precipitation, evapotranspiration rates, and temperature are the factors that most affect changes in soil-moisture content. Figure 25 shows the amount of water stored within the upper 1.75 m of the trench cap for the period November 1982 through June 1984. The amount of water within the trench cap was greatest in early spring, when evapotranspiration rates were low and the ground had thawed. The driest time was in September. Figure 26 shows

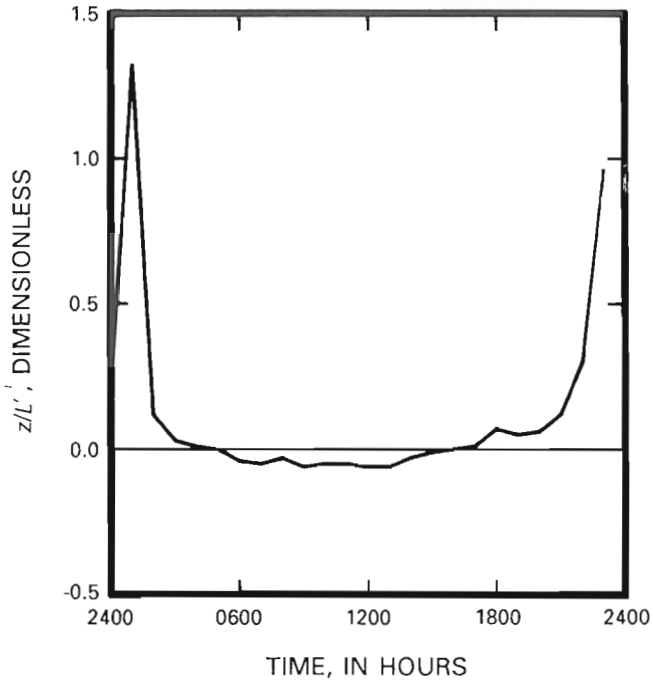

Figure 20. Hourly variations in z/L' at the Sheffield site for June 2, 1984.

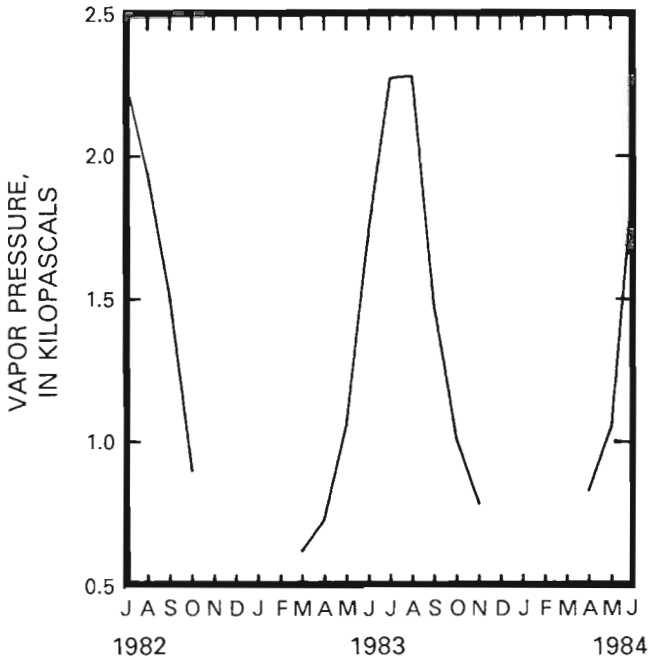

Figure 22. Monthly water-vapor pressure at the Sheffield site.

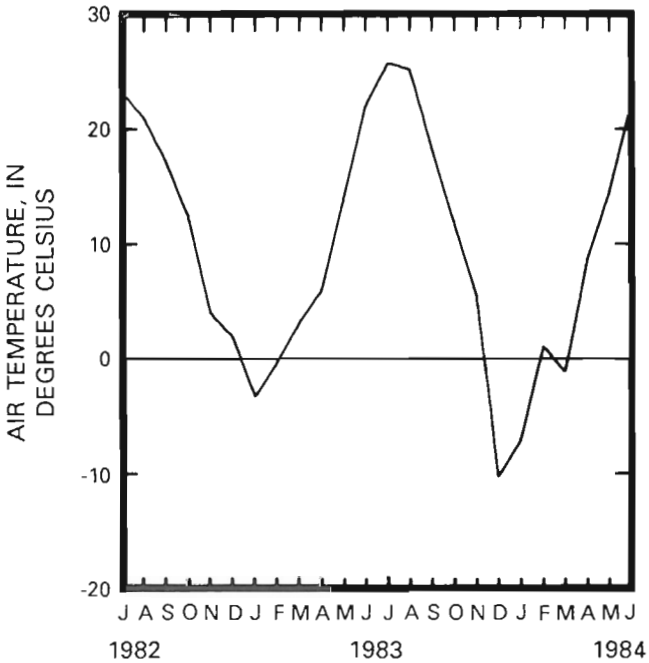

Figure 21. Monthly air temperature at the Sheffield site.

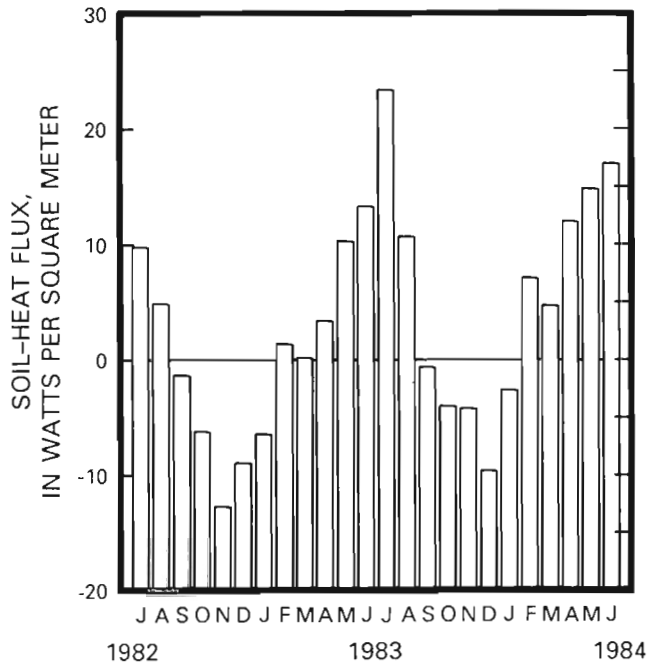

Figure 23. Monthly soil-heat fluxes at the Sheffield site.

the change in volumetric soil-moisture content with respect to depth for several days throughout the year. When evapotranspiration was beginning in midspring, water was readily drawn close to the surface. As the season progressed, more water was drawn from deeper depths. This trend was reversed in the fall when the rate of evapotranspiration was decreasing; then, the moisture content of the soils increased from the surface downward. The range of moisture-content fluctuation was greatest near the surface and decreased with depth. At a depth of 50 mm, moisture content ranged from 0.03 to 0.42 (full saturation). At a depth of 1.5 m, the range was much smaller—about 0.30 to 0.42.

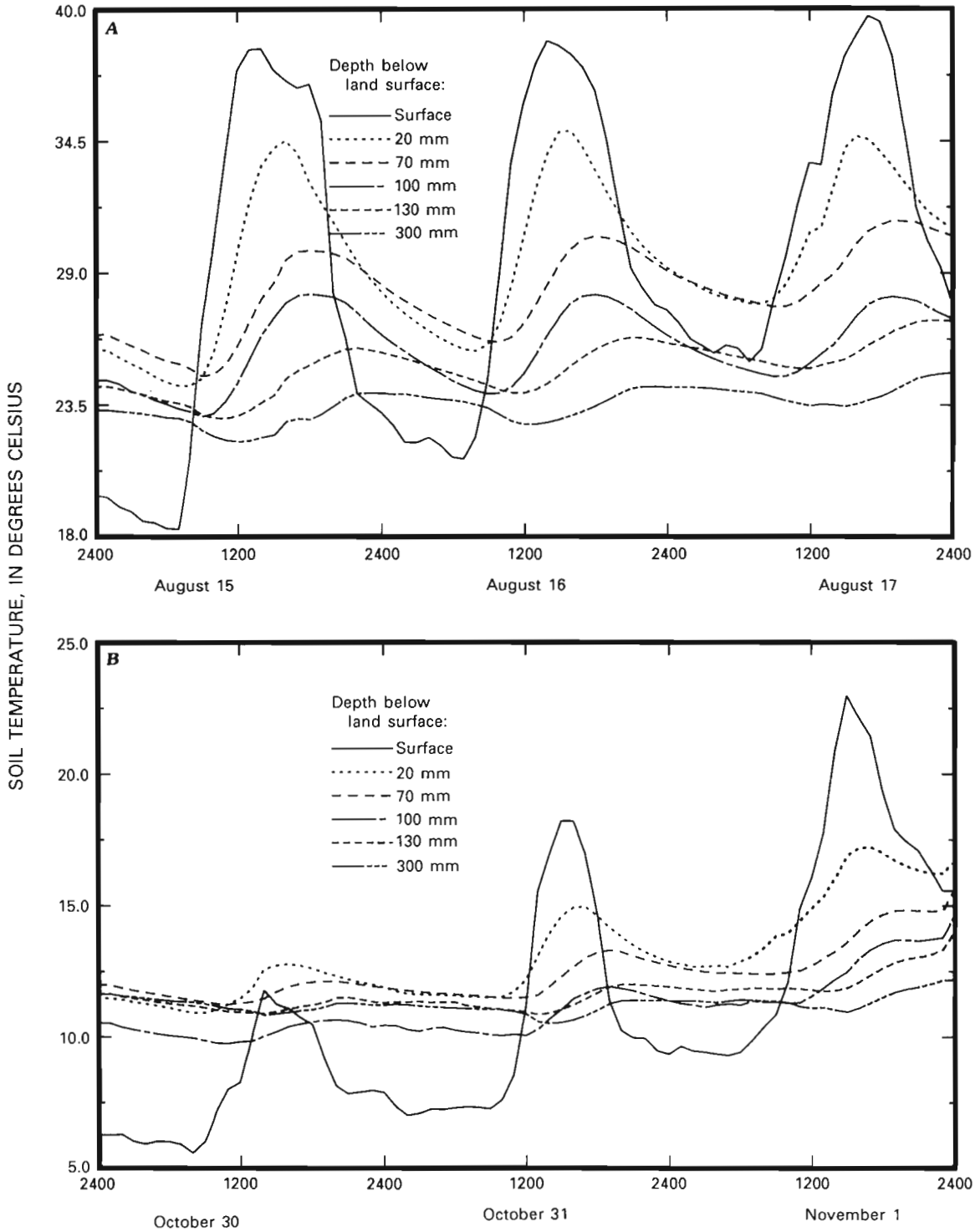

Figure 24. Soil temperatures at the Sheffield site. *A*, August 15–17, 1983. *B*, October 30 through November 1, 1983.

EVAPOTRANSPIRATION ESTIMATES

Daily estimates of evapotranspiration, as calculated by the energy-budget and aerodynamic-profile methods, are presented in table 6 along with estimates of potential evapotranspiration as calculated by the Penman equation (eq. 21). All estimates were computed using averaged hourly data. Vertical gradients in temperature, vapor pressure, and horizontal windspeed were determined using two heights (0.5 and 2.0 m). After September 1983, when three heights (0.5, 1.0, and 2.0 m) were monitored, evapotranspiration estimates were made with gradients computed from the three possible height combinations and then averaged. The months of December, January, and February are not included, as evapotranspiration during these months was essentially zero and the wet-bulb thermistors often froze. Monthly evapotranspiration estimates obtained with the methods discussed above and the water-budget method are included below.

Energy-Budget Method

The evapotranspiration cycle, as depicted in figure 27, began with low rates in early March and increased to maximum rates in July. Rates then declined steadily, dropping to approximately zero by late November. Although the magnitude of the monthly fluxes changed between years, the same monthly pattern is apparent. From July 1982 through June 1983, 622 mm of water are estimated to have evapotranspired; a total of 674 mm was estimated for the period July 1983 through June 1984. Therefore, the annual average evapotranspiration for the 2-year study period was 648 mm. Figure 28 shows the complete energy balance for the study period, using the latent-heat flux as estimated by the energy-budget method, and indicates that the trend in evapotranspiration is very similar to the trend in net radiation. The relatively high rate of latent-heat flux in late fall is noteworthy. In November, the latent-heat flux was greater than the net radiation. It is clear that the additional energy required for this was released by the cooling air and soil.

As discussed earlier, the ratio of sensible- to latent-heat fluxes (H/LE), referred to as the Bowen ratio, indicates how much of the available energy is being used to evaporate water and how much is being used to warm the air. A Bowen ratio of zero implies that all available energy is being used to evaporate water. A ratio of 1 implies that H is equal to LE. Campbell (1977, p. 136) states that a ratio of 0.2 is typical for well-watered short grass. A negative value indicates the occurrence of advection (horizontal heat transport from surrounding areas) and a temperature inversion.

Monthly Bowen ratios are presented in figure 29. The ratio was variable in the late spring and summer months; there was a noticeable downward trend in fall. The average ratio for the study period was 0.38.

Daily estimates of evapotranspiration calculated by the energy-budget method ranged from a low of essentially zero during winter months to a maximum of approximately 6.0 mm for a few summer days. Daily Bowen ratios showed more scatter than monthly values. Negative values occurred on a few days, usually as a result of low net radiation and high winds. However, seasonal trends that were noted for monthly values were also apparent for daily estimates.

Figure 30 shows hourly estimates of the energy budget for six well-defined periods of study. There is a clear diurnal pattern in all values. This pattern is very similar to that of the annual energy budget.

The trend of evapotranspiration was very similar to that of net radiation—both increase from near zero at dawn, reach a peak at solar noon, and decrease during late afternoon and evening to a value near zero at nighttime. Nighttime rates were all very close to zero, but could be either negative or positive. Negative rates correspond to condensation (dew). A significant amount of nighttime evaporation would be expected only with a wet surface, such as following precipitation or condensation.

Ratios of sensible- to latent-heat fluxes varied markedly throughout the day but did follow a pattern (table 4). Ratios obtained immediately after dawn were generally slightly greater than zero. As the day progressed, the ratio increased quickly (in 2 or 3 hours) and remained relatively constant until the late afternoon, when it began to decline. By early evening, the ratio became negative (usually very small in magnitude). This change in sign occurred simultaneously with a temperature inversion and is related to the decrease in net radiation. There was no longer enough incoming radiation to raise the soil-surface temperature above that of the

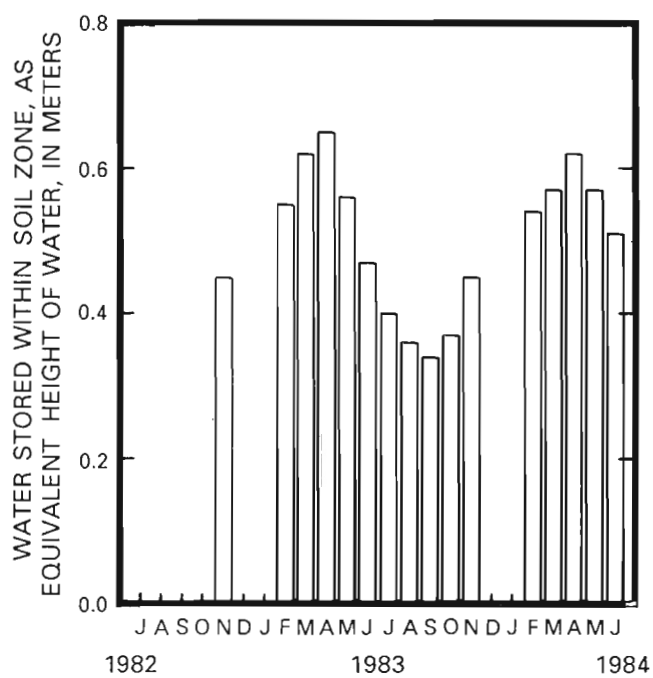

Figure 25. Change in the amount of water stored within the upper 1.75 meters of soil at the Sheffield site.

overlying air. The surface was cooling and, therefore, drawing heat from the warmer air. The warmer air provided additional energy for evapotranspiration to occur. Immediately after sunset, the ratio could vary considerably in both sign and magnitude.

There are numerical instabilities inherent in using the energy-budget method at night. Bowen ratios may be close to -1.0, implying that the latent-heat flux is equal in magnitude, but opposite in sign, to the sensible-heat flux. Because the term $(1+\beta)$ appears in the denominator of equation 19, the computed evapotranspiration rate approaches positive or negative infinity as β approaches -1. To circumvent this problem, hourly energy-budget evapotranspiration estimates were rejected if the Bowen ratio was within the range of -0.3 to -1.7. For these rejected hours, evapotranspiration was assumed to be equal to potential evapotranspiration (eq. 21). This should have little effect on overall results because nighttime fluxes are relatively unimportant under most conditions (Fritschen, 1965).

Aerodynamic-Profile Method

The estimates of evapotranspiration by the aerodynamic-profile method (table 6) were determined by estimating the sensible-heat flux using equation 16, then using the energy-balance equation (eq. 17) to determine the latent-heat flux. Use of equation 15—the more common aerodynamic-profile equation—presented several problems, so results obtained from it are not included. The method using equation 15 was more susceptible to problems with missing data (the method required both wet- and dry-bulb temperature and wind-speeds). Using equation 15, only 5 months out of the 2-year study period had acceptable evapotranspiration values for at least 50 percent of the days. In general, estimates obtained using equation 15 were much greater than estimates made using all other methods (including the Penman equation—equation 21). In fact, hourly estimates were sometimes as much as 100 percent higher than net radiation! The reason for this discrepancy is not clear. The remainder of this section discusses only estimates made using equation 16.

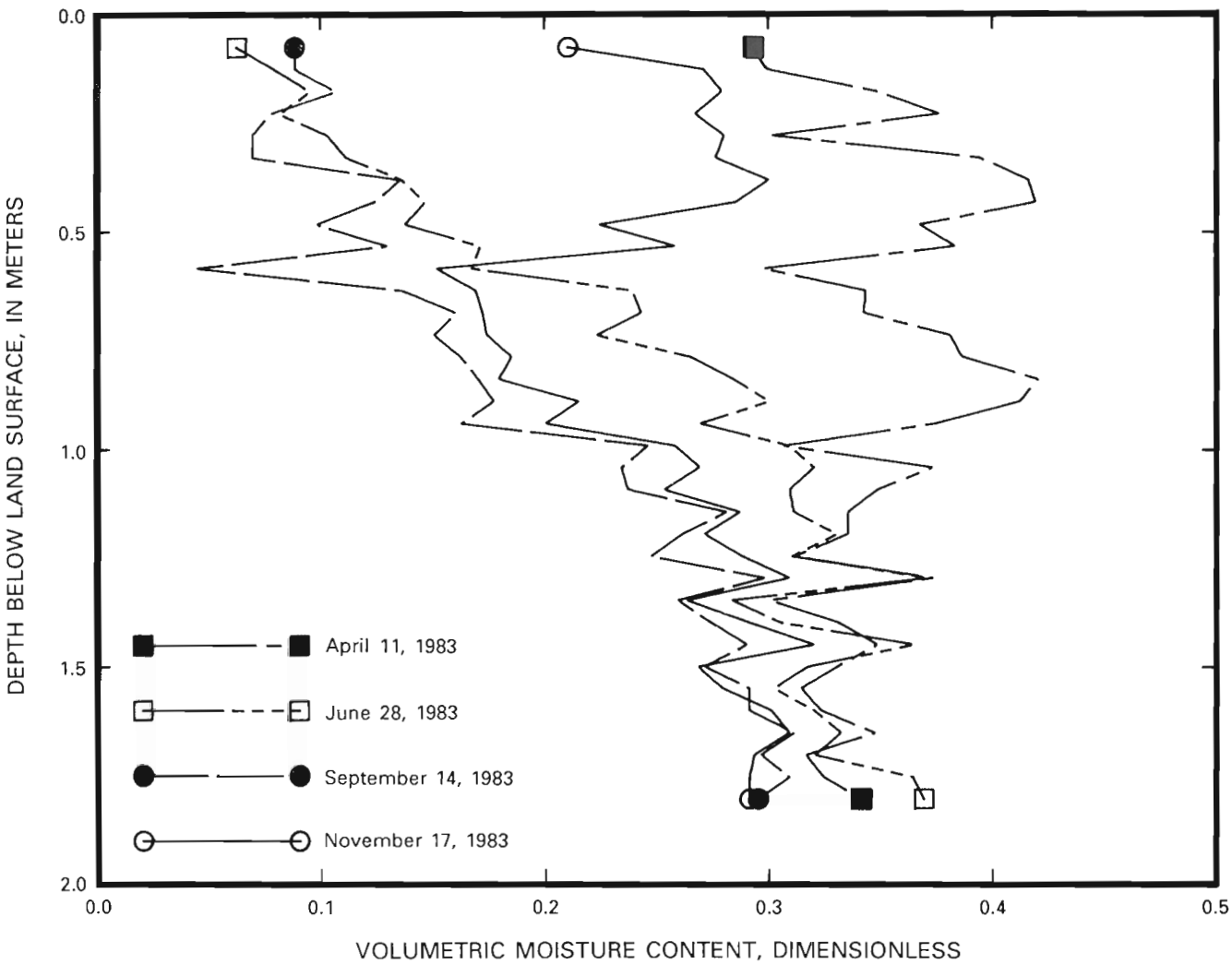

Figure 26. Change in volumetric soil-moisture content with respect to depth for 4 days at the Sheffield site.

For July 1982 through June 1983, evapotranspiration was estimated to be 591 mm. Because of instrument malfunction, evapotranspiration for October and November 1982 and August 1983 was assumed to be equal to that estimated by the energy-balance method. For July 1983 through June 1984, 660 mm of water was estimated to have evapotranspired. The estimated annual average for the 2-year study period was 626 mm; this is about 3 percent lower than that estimated by the energy-budget method. There was good qualitative agreement between the two methods, on a monthly basis, as shown in figures 27 and 29. Seasonal trends discussed previously were clearly apparent with this method. Figures 31 and 32 show that monthly and hourly energy budgets using the aerodynamic-profile method also were quite similar to those of the energy-budget method (figs. 28 and 30). Because of the similarities, detailed discussions of trends are not repeated here.

Water-Budget Method

Figure 27 shows monthly evapotranspiration totals for April 1983 through June 1984. Because of instrument problems, the moisture probe was not operated in 1982. Because of the limited accuracy of each measurement and the limited number of measurements that were made, it is not possible to estimate evapotranspiration on a daily basis.

A total of 688 mm of water is estimated to have been evapotranspired during the period of July 1983 through June 1984. The months of November through March are not included in this total because the rates of evapotranspiration for these months were too low to estimate accurately. By including estimates for March and November, as averaged from the energy-budget and aerodynamic-profile methods, the yearly total was 728 mm. This total is only 7 and 9 percent higher than the totals estimated by the energy-budget and aerodynamic-profile methods for the same period, respectively; however, some monthly totals were significantly different. Estimates of evapotranspiration rates for June, July, and August were, on the average, 20 percent higher when the water-budget method was used, but all methods matched well for the other months. When average values for

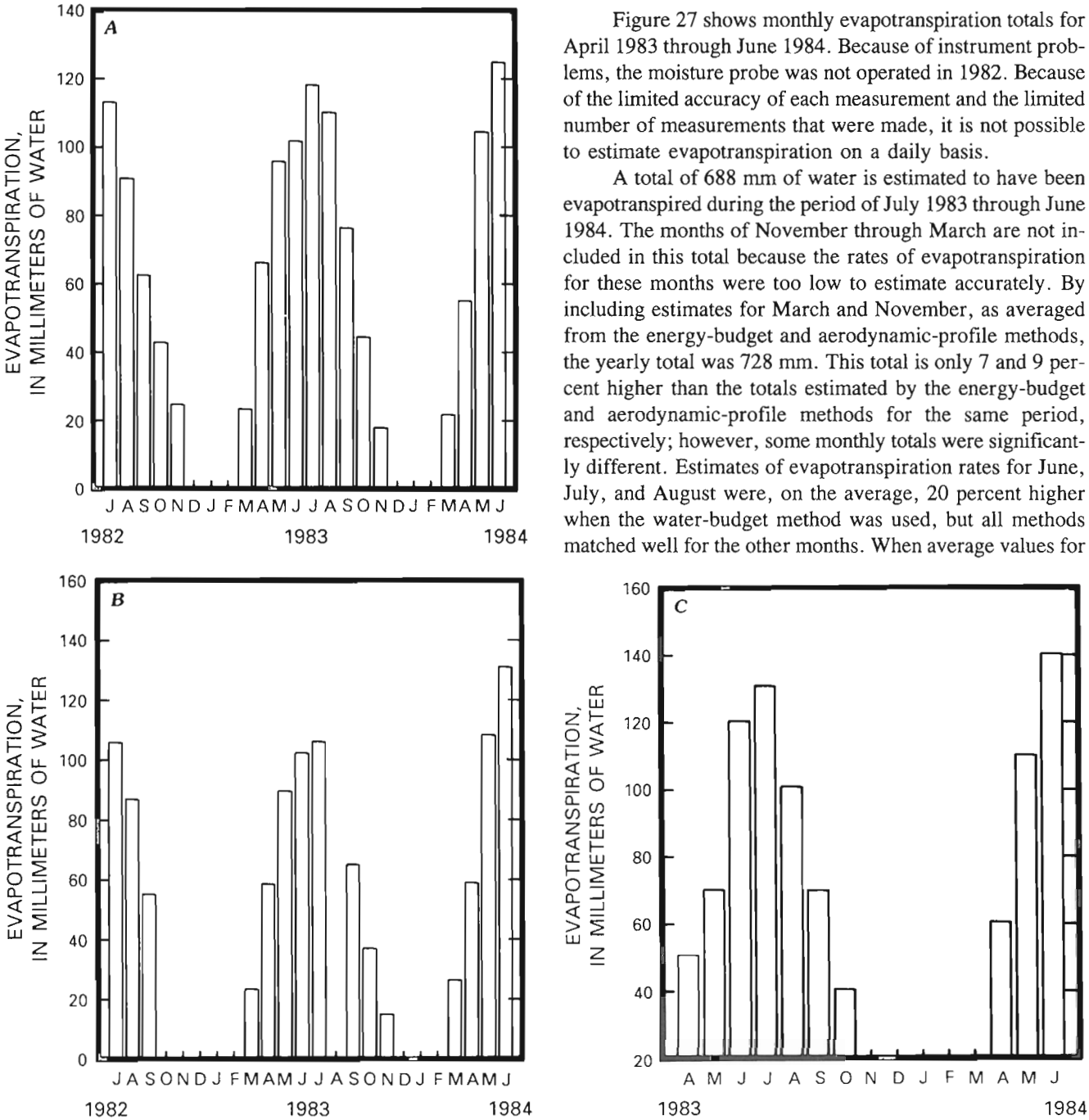

Figure 27. Monthly evapotranspiration at the Sheffield site. *A*, Energy-budget method. *B*, Aerodynamic-profile method. *C*, Water-budget method.

April, May, and June 1983 and 1984 are used, the annual total is 655 mm for April through October.

Potential Evapotranspiration

Estimates of daily potential evapotranspiration calculated by using equation 21 are included in table 6. The total potential evapotranspiration for July 1982 through June 1983 was 864 mm. For July 1983 through June 1984, the total was 888 mm. The annual average of 876 mm is equivalent to 97 percent of the net radiation and 93 percent of the precipitation. Figure 33 shows monthly averages of potential evapotranspiration for the study period. Actual evapotranspiration, as estimated by all three methods, was always less than potential evapotranspiration on a monthly basis. However, on any one day, estimates of actual evapotranspiration could be greater than potential evapotranspiration. There appears to be a seasonal trend in the monthly ratios of actual to potential evapotranspiration (fig. 34): With the exception of March 1984, the ratios are highest in the summer months. Analysis of daily values, however, indicates that this relationship does not always hold. Correlation coefficients determined for the ratios of actual to potential evapotranspiration as a function of potential evapotranspiration were 0.03 for the energy-budget method and 0.10 for the aerodynamic-profile method, indicating that the ratios are independent of the magnitude of the potential evapotranspiration. The energy-budget estimates averaged 74 percent of potential evapotranspiration. The aerodynamic-profile and water-budget estimates averaged 72 and 79 percent of potential evapotranspiration, respectively.

Error Analysis

Errors in estimating evapotranspiration by any method fall into two categories: errors inherent in assumptions upon which the methods are based, and errors inherent in measuring the data required for each method. The former errors were discussed briefly in the section "Techniques for Estimating Evapotranspiration" and will not be addressed further; the latter errors have been analyzed frequently in the literature (see Fuchs and Tanner, 1970; Revfeim and Jordan, 1976; and Grant, 1975), perhaps because these errors are quantified more easily. Rather than presenting a formal analysis, as those authors did, the analyses given in this report use an approach similar to that of Stricker and Brutsaert (1978) and will examine typical measurement errors and show how they affect the estimates already presented here.

It should first be noted that all hourly data collected for this study were manually inspected for gross errors. There are many reasons why invalid data might be recorded, such as faulty instruments, calibration drift, and inclement

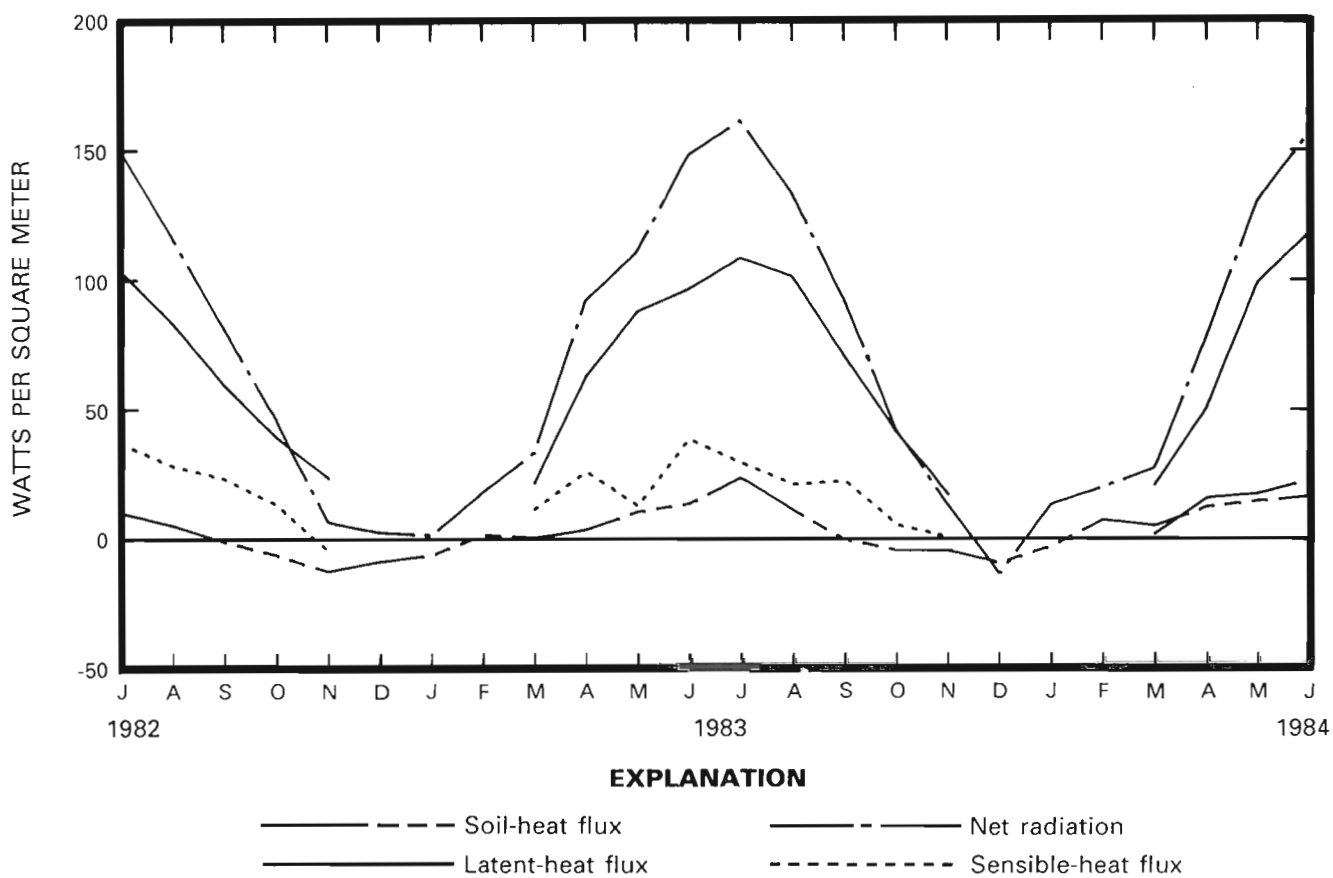

Figure 28. Monthly energy budget for the Sheffield site with evapotranspiration estimated by the energy-budget method.

weather. Regardless of the cause, some spurious data were recorded. These values were omitted from any computations only if a physical reason could be identified for their spurious nature. An example can be seen in figure 10*A* on April 12, 1984. The vapor pressures at the 0.5-m height for that day were obviously in error. This was attributed to the wet-bulb wick drying out. Thus, only the vapor pressures at the 1.0- and 2.0-m heights were used in evapotranspiration calculations for that day.

Figure 35 illustrates the effects produced by an error of ± 0.15 °C in the measured temperature gradient on hourly evapotranspiration estimates calculated by the energy-budget and aerodynamic-profile methods. Table 5 shows the cumulative effect of these errors on the daily totals. During daylight hours, a similar trend was apparent for the two methods: The hours of largest absolute errors corresponded to the hours of greatest evapotranspiration. The energy-budget method was slightly more sensitive to the temperature perturbation than the aerodynamic-profile method. The largest relative errors for the energy budget occurred at times when the magnitude of the Bowen ratio was largest (at night). According to Fuchs and Tanner (1970), this trend should be apparent for this method. It was not apparent for the aerodynamic-profile method.

Figure 36 and table 5 show the effect of assuming an error of ± 0.02 kPa in the vapor-pressure gradient on energy-budget method estimates. The difference in the estimates was

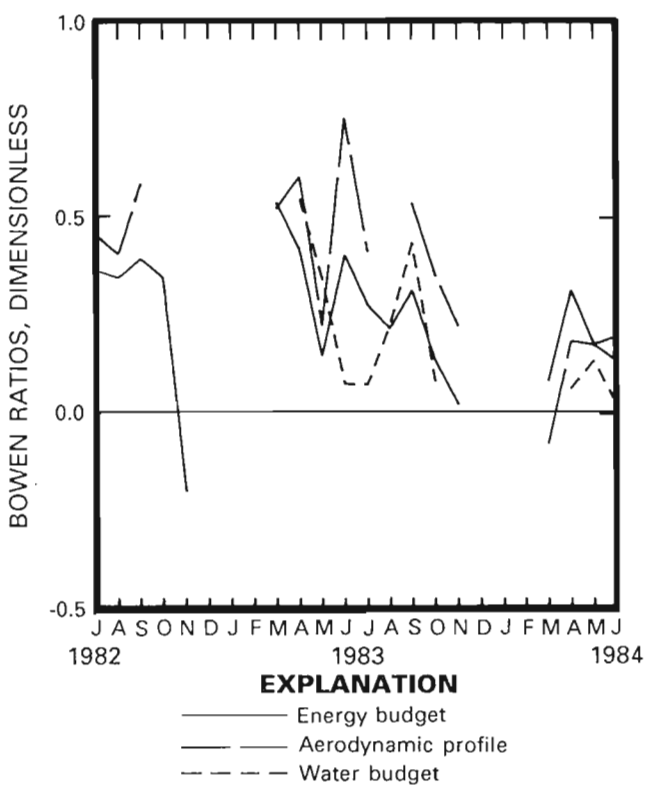

Figure 29. Monthly ratios of sensible- to latent-heat fluxes at the Sheffield site as estimated by the energy-budget, aerodynamic-profile, and water-budget methods.

significant during some hours, especially when the measured gradient was less than 0.02 kPa; then, subtraction of 0.02 kPa produced a vapor-pressure inversion. It should be kept in mind that for any error in temperature measurement there is a corresponding error in vapor pressure because of the manner in which vapor pressure was computed.

The effect on the aerodynamic-profile estimates of varying the vertical gradient in horizontal windspeed by ± 15 percent is shown in figure 37 and table 5. The effect was negligible.

The effects of errors in net radiation (R_n) and soil-heat flux (G) are more easily assessed. If $(R_n - G)$ is in error by a certain percentage, then the energy-budget estimate of evapotranspiration would be in error by that same percentage multiplied by $(R_n - G)/L(1+\beta)$. The aerodynamic-profile estimates would be in error by that same percentage multiplied by $(R_n - G)/L$.

An additional error in the aerodynamic-profile method is possible when estimating the value of d, the zero-plane displacement. However, modifying d by as much as 20 percent had virtually no effect on computed results. Furthermore, Sellers (1965, p. 151) states that, in most cases, d can be ignored.

The accuracy of the water-budget method is entirely related to the accuracy with which precipitation, runoff, and soil-moisture content can be measured. Precipitation measurements should be the least error prone of the three parameters. Runoff measurements were estimated to be accurate within 5 percent (J.R. Gray, U.S. Geological Survey, oral commun., 1985). If soil-moisture measurements are assumed to be correct to ± 1 percent of volumetric-moisture content, then the total error for the 1.75-m thick soil zone would be ± 17.5 mm of water per measurement. Total error ranges from about 13 percent to more than 40 percent of monthly evapotranspiration.

These results were all obtained by assuming a systematic error in computation. Actually, the measurement errors were probably much more random; hence, their effect on the results should be much less than those presented in this simple analysis. Nevertheless, it is apparent that there may be significant errors in the evapotranspiration estimates presented in table 6 and discussed herein. The good agreement among the three methods, in terms of annual averages, is quite surprising in light of the possible errors in each method. It would be unrealistic, however, to assume that, because the estimates are within 6 percent of each other, all of the estimates are accurate to within 6 percent of actual evapotranspiration. The desirability of estimating evapotranspiration by more than one method is obvious from this analysis.

SUMMARY

Evapotranspiration at the low-level radioactive-waste disposal site near Sheffield, Bureau County, Illinois, was

studied from July 1982 through June 1984. The site is vegetated with mixed pasture grass, primarily awnless brome (*Bromus inermis*) and red clover (*Trifolium pratense*). Energy-budget, aerodynamic-profile, and water-budget methods were used to estimate evapotranspiration. For the aerodynamic-profile method, sensible-heat flux was estimated by a profile equation, and evapotranspiration was then calculated as the residual in the energy-balance equation. Continual measurements were made of incoming and reflected shortwave radiation, incoming and emitted longwave radiation, net radiation, soil-heat flux, soil temperature, horizontal windspeed, and wet- and dry-bulb air temperatures. Windspeed and air temperature were measured at heights of 0.5 and 2.0 m (and also at 1.0 m after September 1983). Soil-moisture content was measured weekly or biweekly with a gamma-attenuation type density probe.

Average annual precipitation for the study period was 938 mm, which is quite close to the long-term average of 890 mm computed from three nearby National Weather Service stations. Most precipitation fell in heavy storms.

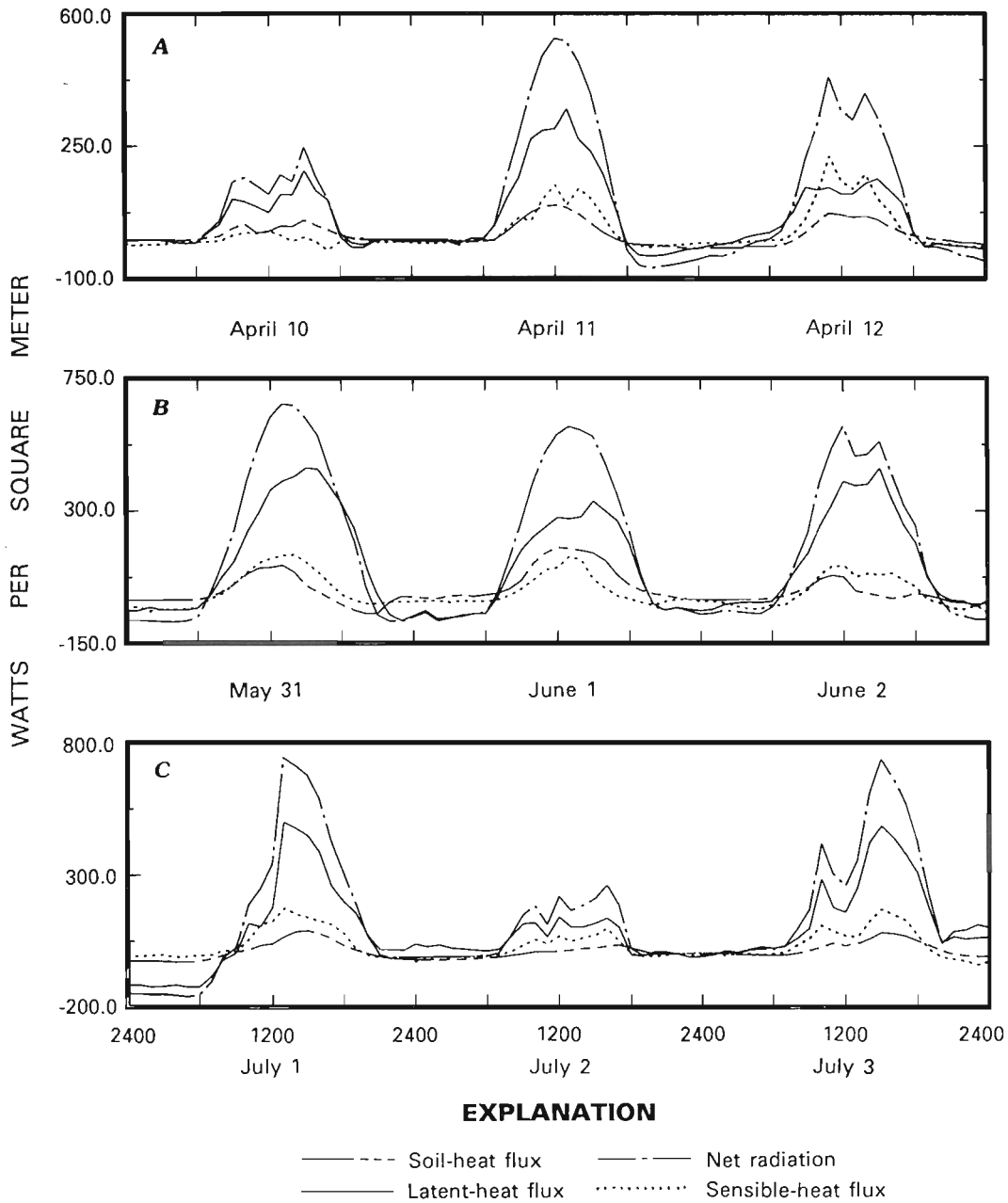

Figure 30. Energy budget at the Sheffield site as estimated by the energy-budget method. *A*, April 10–12, 1984. *B*, May 31 through June 2, 1984. *C*, July 1–3, 1982. *D*, August 15–17, 1983. *E*, September 13–15, 1982. *F*, October 30 through November 1, 1983.

Annual shortwave radiation for the study period averaged 156 W/m^2, which is 65 percent of clear-sky solar radiation. For 117 days during the study period, measured shortwave radiation was greater than or equal to 90 percent of clear-sky solar radiation. The surface albedo averaged about 20 percent in late spring to early fall; in the winter, the albedo was highly variable, depending on snow cover. Trends in incoming and outgoing longwave radiation were very similar to trends in air temperature. Net radiation averaged 70.1 W/m^2 annually and followed the same pattern as solar radiation.

Surface winds at the site during the study period were primarily out of the south-southeast and highly variable. The average windspeed was 3.5 m/s. Windspeeds in winter months tended to be slightly higher than in summer months. The plot of windspeed as a function of the logarithm of height was usually linear only near dawn and dusk because of atmospheric instability.

Air temperatures averaged 10.8 °C, with monthly averages ranging from a high of about 26 °C in July 1983, to a low of −10 °C in December 1983. The annual average is close to the long-term average of 10.3 °C as computed from nearby National Weather Service stations. Water-vapor pressure varied with temperature.

The amount of water stored in the soil zone was greatest in early spring at the start of the evapotranspiration cycle. Soil-water content decreased through the growing season and reached a minimum in mid- to late September. The annual variation in volumetric moisture content of the soil was found to be closely related to depth. At a depth of 50 mm, moisture

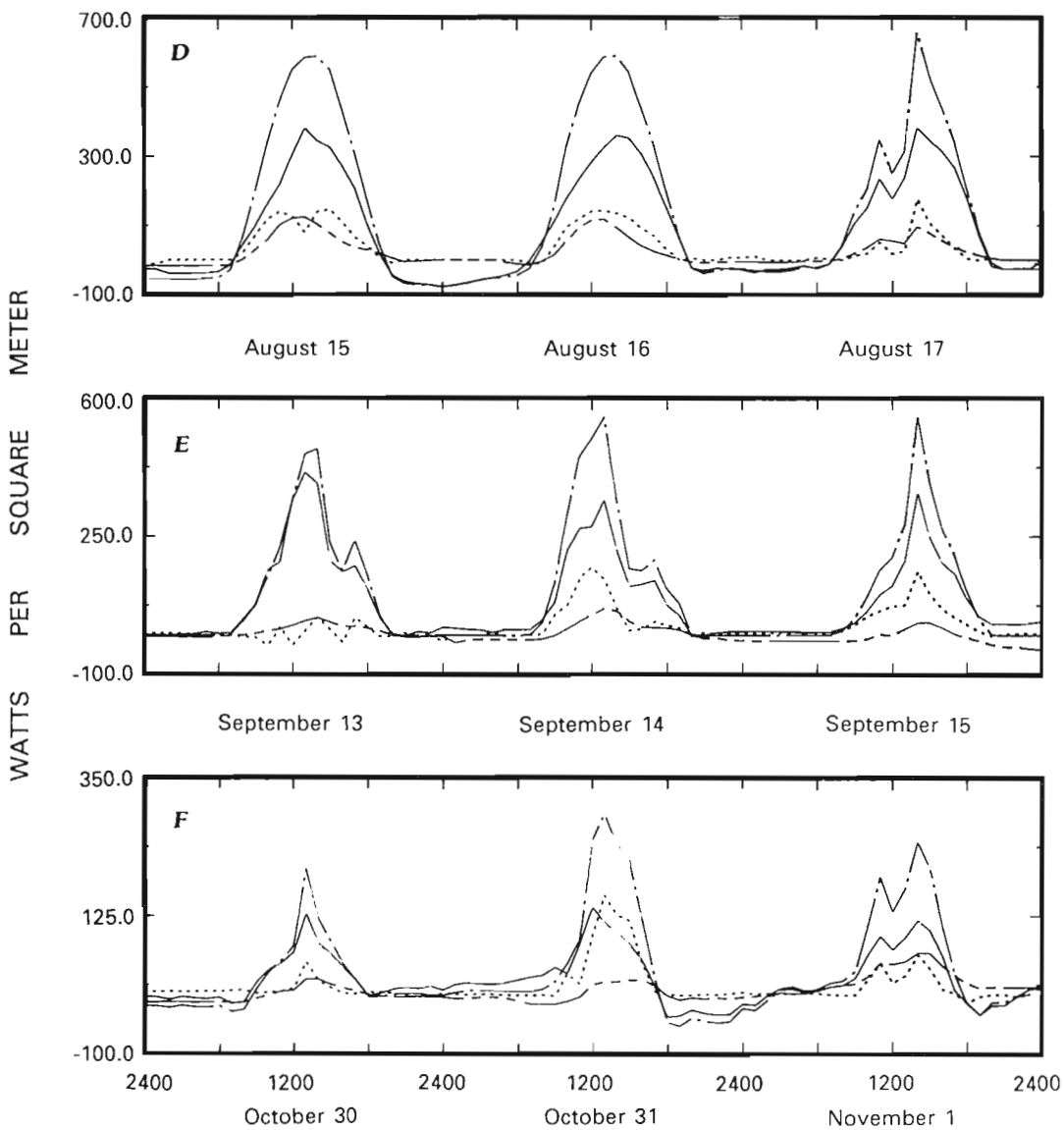

Figure 30. Continued.

Table 4. Hourly values of the ratio of sensible- to latent-heat flux

Hour[1]	Ratio of sensible- to latent-heat flux		
	July 2, 1982	Oct. 31, 1983	June 1, 1984
0100	0.25	-0.16	-14.42
0200	.53	-.16	12.45
0300	.87	-.18	8.10
0400	.85	-.17	18.17
0500	-6.10	-.19	-2.41
0600	-.14	-.15	-1.79
0700	-.08	-.24	1.44
0800	.12	-.10	.40
0900	.28	.00	.41
1000	.49	.04	.45
1100	.54	.10	.47
1200	.60	.39	.43
1300	.55	.23	.41
1400	.47	.12	.40
1500	.57	-.04	.25
1600	.53	-.11	.19
1700	.42	-.22	.06
1800	.06	-.15	-.10
1900	-.17	-.25	-.17
2000	-.24	-.36	1.21
2100	-.21	-.31	2.61
2200	.03	-.74	4.09
2300	.09	-.27	-4.26
2400	.26	-.40	-3.67

[1] Central daylight time.

content, as a percentage of total unit volume, ranged from 3 to 42 percent (full saturation). At a depth of 1.5 m, moisture content showed a much smaller change—ranging from 30 to 42 percent.

Estimates of evapotranspiration calculated by the energy-budget and aerodynamic-profile methods were calculated with data averaged on an hourly basis. Vertical gradients in temperature, vapor pressure, and horizontal windspeed were computed using data obtained at two sampling heights (0.5 and 2.0 m). After September 1983, when three heights (0.5, 1.0, and 2.0 m) were monitored, evapotranspiration estimates were made with gradients computed from the three possible height combinations and were then averaged.

Estimates of annual evapotranspiration (excluding the months of December, January, and February; March and November were also excluded when using the water-budget method) are as follows: the energy-budget method, 648 mm; the aerodynamic-profile method, 626 mm; and the water-budget method, 655 mm. The average for the three methods is 657 mm (assuming that the water-budget estimates for March and November were equal to the averages of the other two methods), which is approximately 70 percent of the total annual precipitation. Approximately 73 percent of net radiation was converted into heat and used as energy to evapotranspire water; the annual Bowen ratio was 0.38.

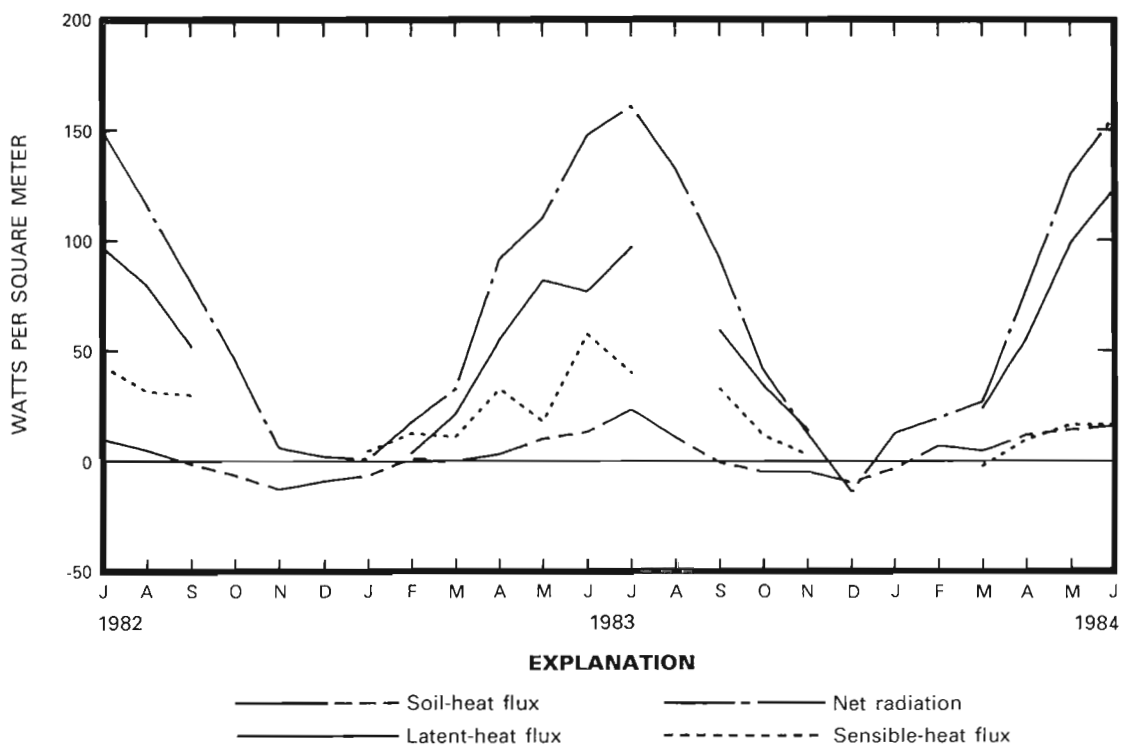

Figure 31. Monthly energy budget for the Sheffield site with evapotranspiration estimated by the aerodynamic-profile method.

Seasonal trends in evapotranspiration estimates were similar for all three methods and matched the trends in net radiation. June and July were the months with the highest evapotranspiration rates. Monthly Bowen ratios for late spring through summer were variable, averaging about 0.35. The ratios declined during fall, and some reached negative values in late fall. During November 1982 and 1983, the latent-heat flux was greater than the net radiation.

Daily evapotranspiration ranged from essentially zero during winter months to a maximum of approximately 6.0 mm in midsummer. Rates could vary substantially from day to day, depending upon the net radiation.

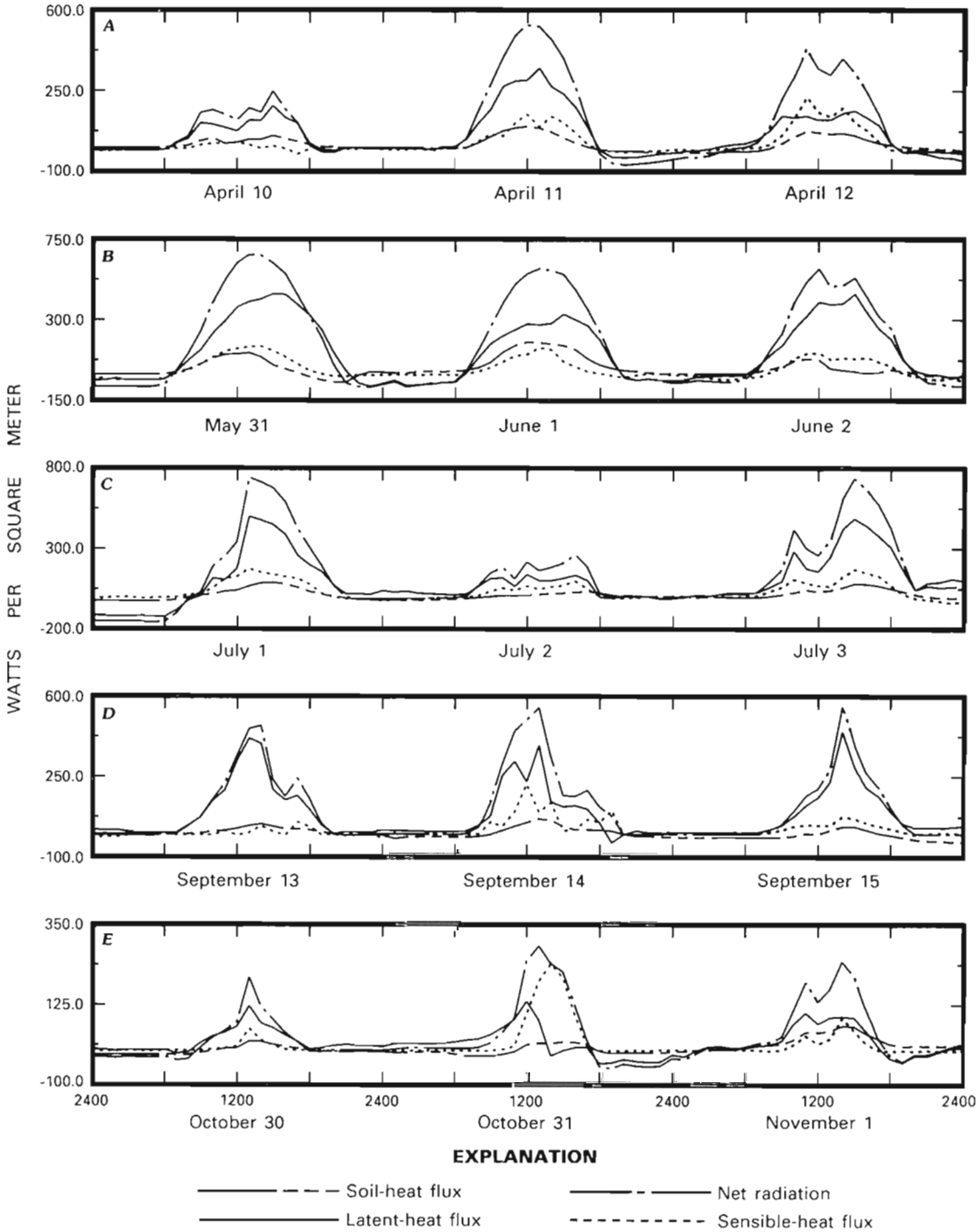

Figure 32. Energy budget at the Sheffield site as estimated by the aerodynamic-profile method. *A*, April 10–12, 1984. *B*, May 31 through June 2, 1984. *C*, July 1–3, 1982. *D*, September 13–15, 1982. *E*, October 30 through November 1, 1983.

Diurnal trends in evapotranspiration were similar to those of net radiation; the highest rates occurred around solar noon. The Bowen ratio also followed a diurnal pattern—that is, it was only slightly positive at dawn, rising to a low positive number in the morning, remaining fairly constant until late afternoon when it dropped to slightly below zero. At night the ratio could be either positive or negative and its magnitude could vary greatly.

Potential evapotranspiration was estimated using the Penman equation with the van Bavel wind function. The average annual estimate for the study period was 876 mm. Estimates calculated by the energy-budget method averaged

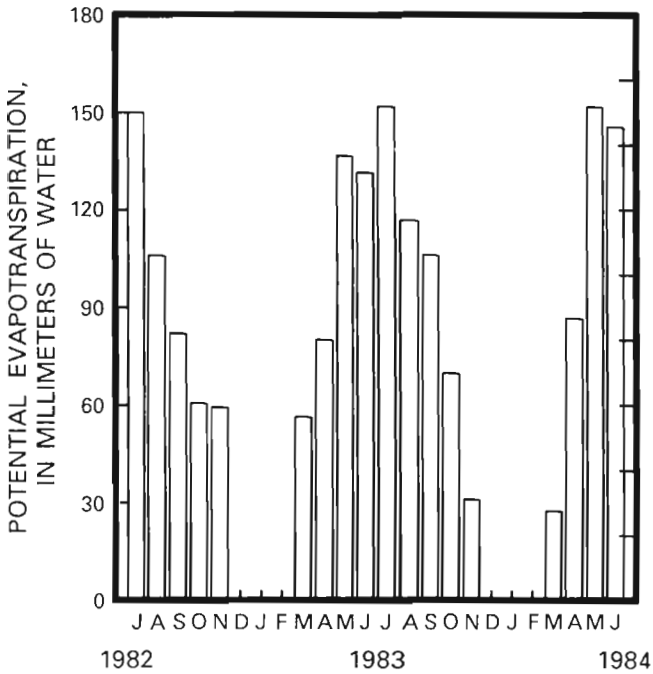

Figure 33. Monthly potential evapotranspiration at the Sheffield site.

Table 5. Changes in computed daily evapotranspiration, when assuming systematic measurement errors

[ΔT indicates change in air-temperature gradient; Δe indicates change in vapor-pressure gradient; Δu indicates change in horizontal wind-speed gradient]

	Evapotranspiration, in millimeters of water		
	May 31, 1984	June 1, 1984	June 2, 1984
Energy-budget method			
Original estimate	4.80	3.98	3.97
ΔT increased by 0.15 °C	5.84	4.35	5.14
ΔT decreased by 0.15 °C	3.71	4.52	2.54
Δe increased by 0.02 kPa	5.06	3.37	4.30
Δe decreased by 0.02 kPa	3.86	3.19	2.59
Aerodynamic-profile method			
Original estimate	5.07	3.24	4.69
ΔT increased by 0.15 °C	5.79	3.76	5.40
ΔT decreased by 0.15 °C	4.26	2.51	3.81
Δu increased by 15 percent	5.28	3.37	4.74
Δu decreased by 15 percent	4.91	3.12	4.57

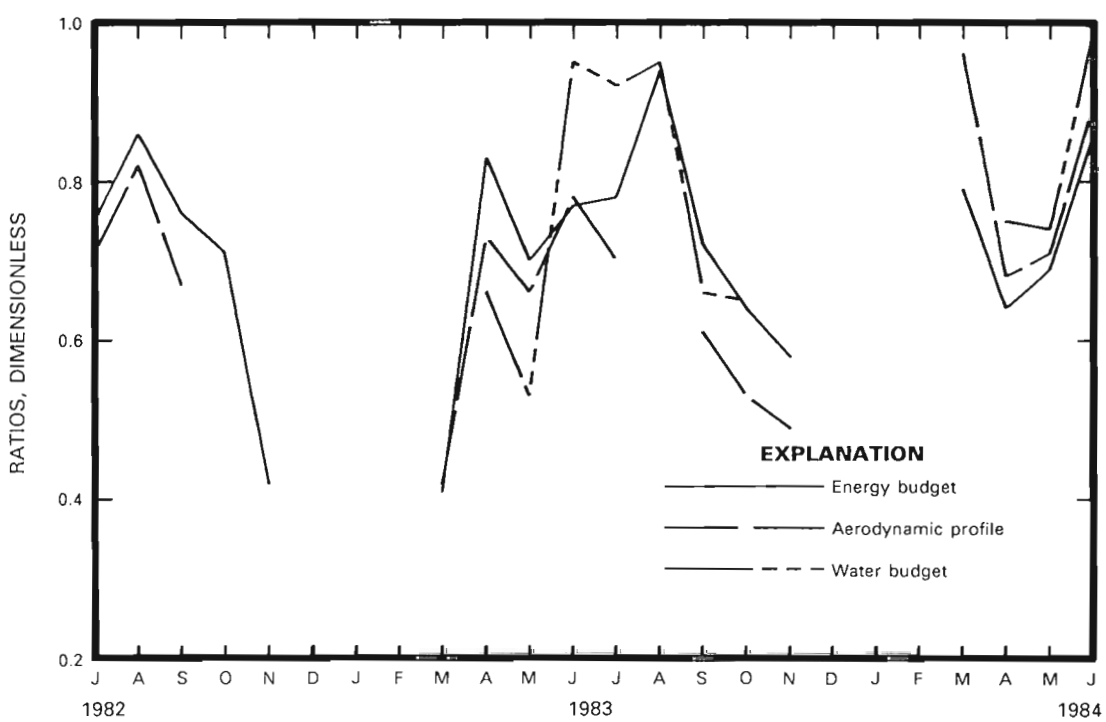

Figure 34. Monthly ratios of actual evapotranspiration, as estimated by the energy-budget, aerodynamic-profile, and water-budget methods, to potential evapotranspiration at the Sheffield site.

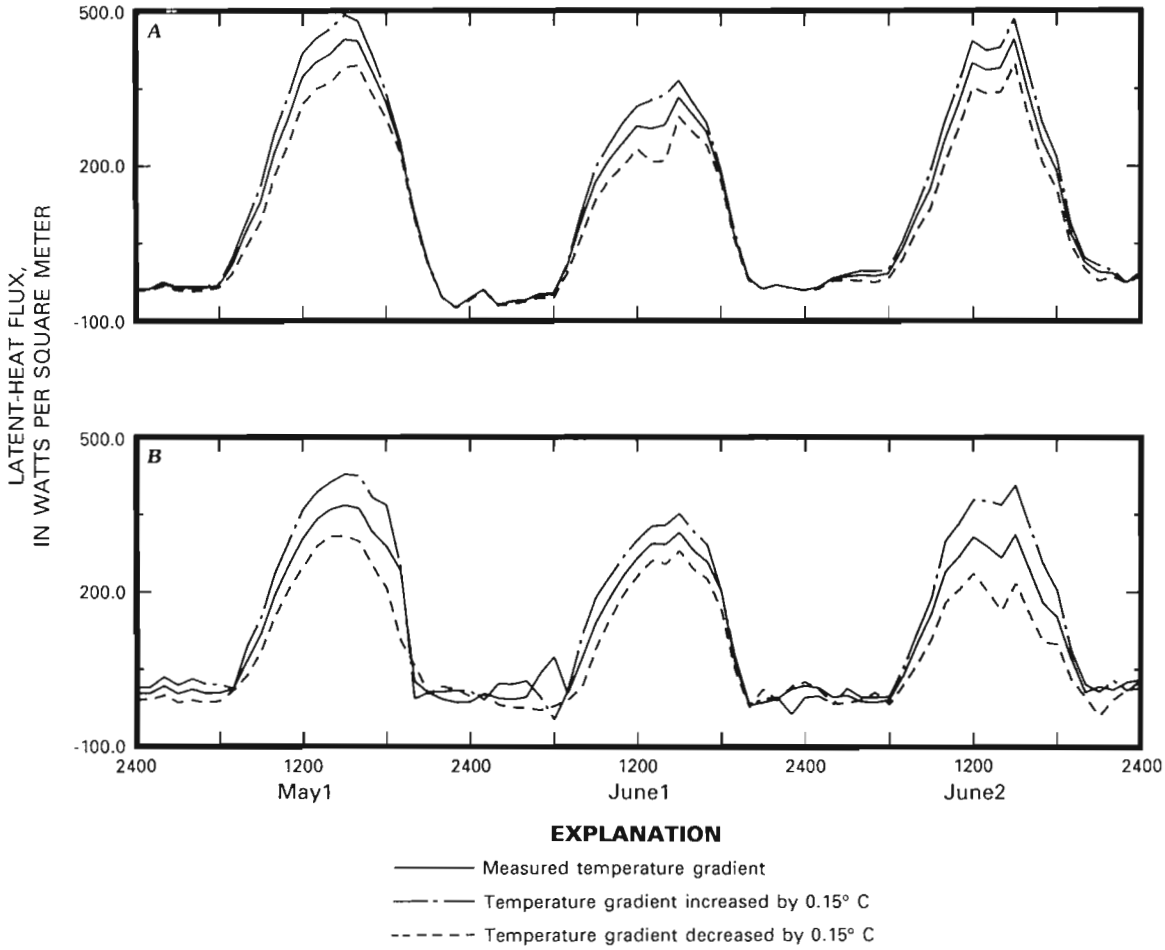

Figure 35. Effect of temperature-gradient errors on hourly evapotranspiration estimates on May 31 through June 2, 1984, using (*A*) the aerodynamic-profile method and (*B*) the energy-budget method.

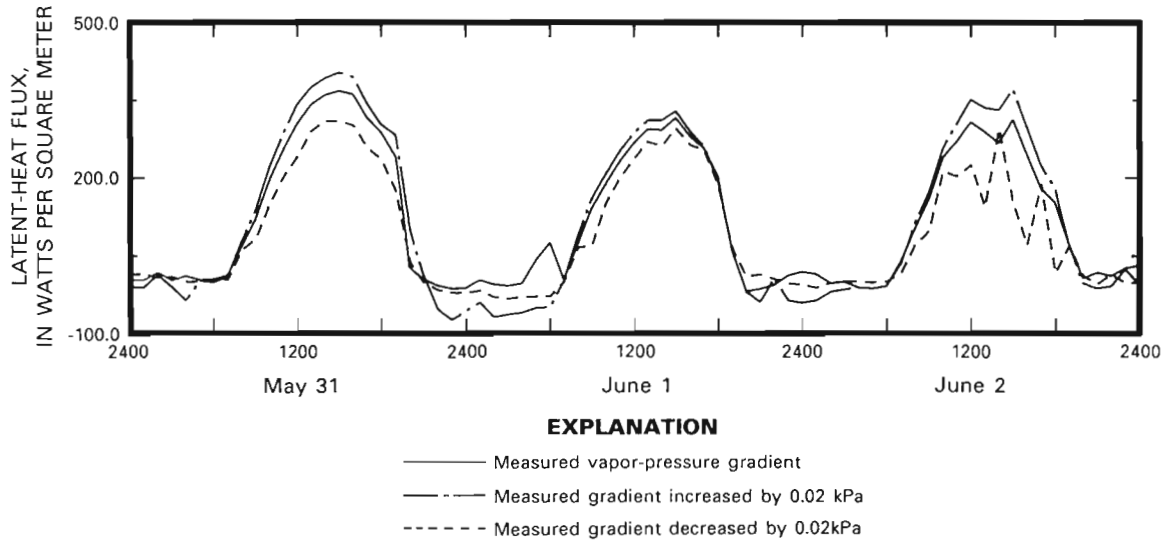

Figure 36. Effect of vapor-pressure gradient errors on hourly evapotranspiration estimates on May 31 through June 2, 1984, using the energy-budget method.

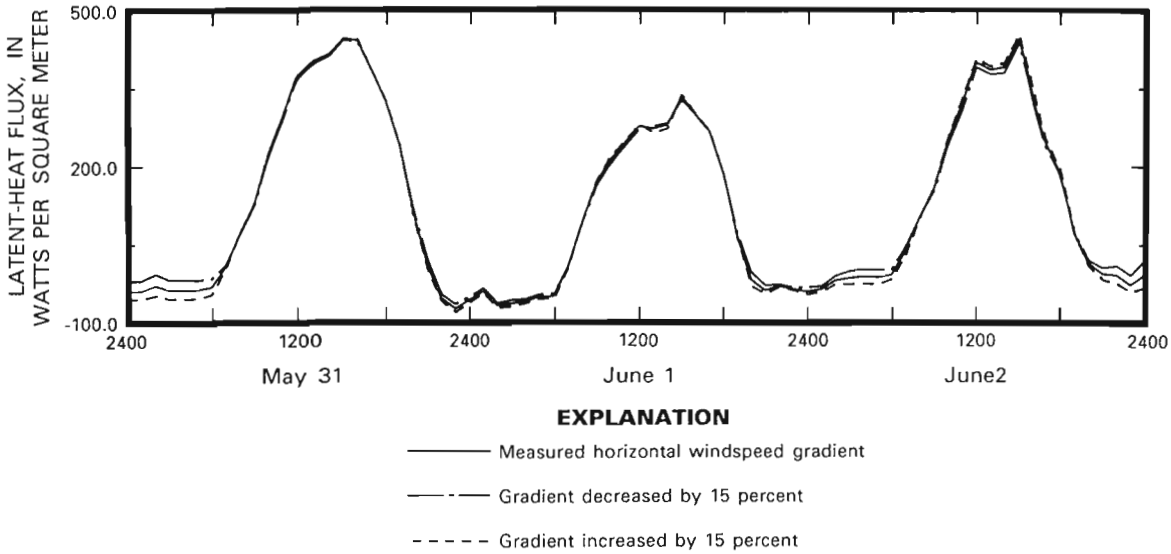

Figure 37. Effect of errors in horizontal windspeed gradient on hourly evapotranspiration estimates on May 31 through June 2, 1984, using the aerodynamic-profile method.

74 percent of potential evapotranspiration. Estimates calculated by the aerodynamic-profile and water-budget methods averaged 72 and 79 percent, respectively. There was no seasonal trend in the relation between actual and potential evapotranspiration rates.

Although the annual averages estimated by the different methods are quite close (within 6 percent), the reader is cautioned to keep in mind that there are inherent errors in all estimates. The good agreement among methods should be considered fortuitous, but under no circumstances should the range in different estimates be considered an indication of accuracy of any of the methods.

All three methods used to estimate evapotranspiration appear to be adequate for the environment of the Sheffield site. Each has some advantages and disadvantages compared to the others that should be weighed for use in future studies.

REFERENCES CITED

Anderson, E.R., 1954, Energy-budget studies, *in* Water-loss investigations: Lake Hefner studies, technical report: U.S. Geological Survey Professional Paper 269, p. 71–119.

Bellaire, F.R., and Anderson, L.J., 1951, A thermocouple psychrometer for field measurements: American Meteorological Society Bulletin, v. 32, no. 6, p. 217–220.

Blaney, H.F., and Criddle, W.D., 1962, Determining consumptive use and irrigation water requirements: U.S. Department of Agriculture Technical Bulletin 1275, 59 p.

Bowen, I.S., 1926, The ratio of heat losses by conduction and by evaporation from any water surface: Physical Review, v. 27, p. 779–787.

Brutsaert, W., 1982, Evapotranspiration into the atmosphere—theory, history, and applications: Boston, D. Reidel, 299 p.

Budyko, M.I., 1956, The heat balance of the Earth's surface: Leningrad, Hydrometeorological Publications [translated by N.A. Stepanova, 1958, U.S. Department of Commerce], 259 p.

Campbell, A.P., 1973, The effect of stability on evaporation rates measured by the energy balance method: Agricultural Meteorology, v. 11, p. 261–267.

Campbell, G.S., 1977, An introduction to environmental biophysics: New York, Springer-Verlag, 159 p.

Changnon, S.A., Jr., and Huff, F.A., 1980, Review of Illinois summer precipitation conditions: Illinois Institute of Natural Resources, State Water Survey Bulletin 64, 160 p.

Chemical Rubber Company, 1972, Handbook of chemistry and physics, 53d ed.: Chemical Rubber Company, Cleveland, Ohio.

Deacon, E.L., Priestley, C.H.B., and Swinbank, W.C., 1958, Evaporation and the water balance: Climatological Reviews of Research, UNESCO Arid Zone Research Service, v. 10, p. 9–34.

Denmead, O.T., and McIlroy, I.L., 1970, Measurement of nonpotential evaporation from wheat: Agricultural Meteorology, v. 7, p. 285–302.

Dyer, A.J., 1974, A review of flux-profile relationships: Boundary-layer Meteorology, v. 7, p. 363–372.

Fischer, J.N., 1983, Low-level radioactive-waste program of the U.S. Geological Survey—in transition, *in* Proceedings of the Fifth Annual Participants' Information Meeting, DOE Low-Level Waste Management Program, Denver, 1983: Idaho Falls, Idaho, U.S. Department of Energy, p. 52–61.

Foster, J.B., and Erickson, J.R., 1980, Preliminary report on the hydrogeology of a low-level radioactive-waste disposal site near Sheffield, Illinois: U.S. Geological Survey Open-File Report 79-1545, 87 p, 5 plates.

Foster, J.B., Erickson, J.R., and Healy, R.W., 1984, Hydrogeology of a low-level radioactive-waste disposal site near Sheffield, Illinois: U.S. Geological Survey Water-Resources Investigations Report 83-4125, 83 p.

Foster, J.B., Garklavs, G., and Mackey, G.W., 1984, Hydrogeologic setting east of a low-level radioactive-waste disposal site near Sheffield, Illinois: U.S. Geological Survey Water-Resources Investigations Report 84-4183, 20 p.

Fritschen, L.J., 1965, Accuracy of evapotranspiration determina-

tions by the Bowen ratio method, *in* Bulletin of the International Association of Scientific Hydrology, June, p. 38–48.

Fritschen, L.J., and Gay, L.W., 1979, Environmental instrumentation: New York, Springer-Verlag, 216 p.

Fuchs, M., and Tanner, C.B., 1970, Error analysis of Bowen ratios measured by differential psychrometry: Agricultural Meteorology, v. 7, p. 329–334.

Garklavs, G., and Healy, R.W., 1986, Hydrogeology, ground-water flow, and tritium movement at a low-level radioactive-waste disposal site near Sheffield, Illinois: U.S. Geological Survey Water-Resources Investigations Report 86-4153, 35 p.

Gee, G.W., and Kirkham, R.R., 1984, Transport assessment—arid: Measurement and prediction of water movement below the root zone, *in* Proceedings of the Sixth Annual Participants' Information Meeting, DOE Low-Level Waste Management Program, Denver, 1984: Idaho Falls, Idaho, U.S. Department of Energy, p. 503–519.

Geiger, R., 1961, Das klima der bodennahen luftschicht, Friedr, Vieweg & Sohn, Braunschweig (English transl.: Scripta Technica, Inc., 1965, The climate near the ground: Cambridge, Harvard University Press, 646 p).

Grant, D.R., 1975, Comparison of evaporation measurements using different methods: Quarterly Journal of the Royal Meteorological Society, v. 101, p. 543–550.

Gray, J.R., 1984, Runoff, sediment transport, and landform modifications near Sheffield, Illinois, *in* Proceedings of the Sixth Annual Participants' Information Meeting, DOE Low-Level Waste Management Program, Denver, 1984: Idaho Falls, Idaho, U.S. Department of Energy, p. 534–544.

Gray, J.R., and deVries, M.P., 1984, A system for measuring surface runoff and collecting sediment samples from small areas, *in* Meyer, E.L., ed., Selected Papers in the Hydrologic Sciences: U.S. Geological Survey Water-Supply Paper 2262, p. 7–11.

Healy, R.W., deVries, M.P., and Striegl, R.G., 1986, Concepts and data-collection techniques used in a study of the unsaturated zone at a low-level radioactive-waste disposal site near Sheffield, Illinois: U.S. Geological Survey Water-Resources Investigations Report 85-4228, 37 p.

Healy, R.W., Peters, C.A., deVries, M.P., Mills, P.C., and Moffett, D.L., 1984, Study of the unsaturated zone at a low-level radioactive waste disposal site, *in* Proceedings of Conference on Characterization and Monitoring of the Vadose Zone, Las Vegas, 1983: National Water Well Association, p. 820–830.

Huff, F.A., 1979, Spatial and temporal correlation of precipitation in Illinois: Illinois Institute of Natural Resources, State Water Survey Circular 141, 14 p.

Jensen, M.E., 1967, Evaluating irrigation efficiency: Journal of Irrigation and Drainage Division, Proceedings of American Society of Civil Engineers, v. 93, p. 83–98.

_____ ed., 1973, Consumptive use of water and irrigation water requirements: New York, American Society of Civil Engineers, 215 p.

Jones, D.M.A., 1966, Variability of evapotranspiration in Illinois: Illinois Institute of Natural Resources, State Water Survey Circular 89, 13 p.

McGuinness, J.L., and Bordine, E.F., 1972, A comparison of lysimeter-derived potential evapotranspiration with computed values: U.S. Department of Agriculture Technical Bulletin 1452, 71 p.

Monin, A.S., and Obukhov, A.M., 1954, Basic laws of turbulent mixing in the ground layer of the atmosphere: Tr. Geofiz. Instit. Akad. Nauk, S.S.S.R., no. 24(151), p. 163–187.

Monteith, J.L., 1973, Principles of environmental physics: New York, American Elsevier Publishing Company, 241 p.

Penman, H.L., 1948, Natural evaporation from open water, bare soil, and grass: Proceedings of the Royal Society of London, v. 193A, p. 120–146.

_____ 1956, Evaporation: An introductory survey: Netherlands Journal of Agricultural Science, v. 4, p. 9–29.

Penman, H.L., and Schofield, R.K., 1951, Some physical aspects of assimilation and transpiration: Symposium of the Society of Experimental Biology, v. 5, p. 115–129.

Revfeim, K.J.A., and Jordan, R.B., 1976, Precision of evaporation measurements using the Bowen ratio: Boundary-layer Meteorology, v. 10, p. 97–111.

Richardson, L.F., 1920, The supply of energy from and to atmospheric eddies: Proceedings of the Royal Society of London, v. A97, p. 354–373.

Robertson, J.B., 1981, Modeling in low-level radioactive waste management from the U.S. Geological Survey perspective, *in* Modeling and Low-Level Waste Management: An Interagency Workshop, Denver, 1980: Oak Ridge, Tennessee, Oak Ridge National Laboratory, p. 21–30.

Rouse, W.R., 1984, Microclimate at Arctic tree line, 1, radiation balance of tundra and forest: Water Resources Research, v. 20, no. 1, p. 57–66.

Schulz, R.K., 1984, Water management of humid area shallow land burial sites, *in* Proceedings of the Sixth Annual Participants' Information Meeting, DOE Low-Level Waste Management Program, Denver, 1984: Idaho Falls, Idaho, U.S. Department of Energy, p. 178–190.

Sellers, W.D., 1965, Physical climatology: Chicago, University of Chicago Press, 272 p.

Stricker, H., and Brutsaert, W., 1978, Actual evapotranspiration over a summer period in the "Hupsel Catchment": Journal of Hydrology, v. 39, p. 139–157.

Striegl, R.G., 1984, Methods for determining the transport of radioactive gases in the unsaturated zone, *in* Proceedings of the Sixth Annual Participants' Information Meeting, DOE Low-Level Waste Management Program, Denver, 1984: Idaho Falls, Idaho, U.S. Department of Energy, p. 579–587.

Sutton, O.B., 1953, Micrometeorology: New York, McGraw-Hill, 333 p.

Swinbank, W.L., and Dyer, A.J., 1967, An experimental study of micrometeorology: Quarterly Journal of the Royal Meteorological Society, v. 93, p. 494–500.

Tanner, C.B., and Pelton, W.L., 1960, Potential evapotranspiration estimates by the approximate energy balance method of Penman: Journal of Geophysical Research, v. 65, no. 10, p. 3391–3413.

Thom, A.S., and Oliver, H.R., 1977, On Penman's equation for estimating regional evaporation: Quarterly Journal of the Royal Meteorological Society, p. 345–357.

Thornthwaite, C.W., 1948, An approach toward a rational classification of climate: Geographical Review, v. 38, p. 55–94.

Thornthwaite, C.W., and Holzman, B., 1942, Measurement of evaporation from land and water surfaces: U.S. Department of Agriculture, Technical Bulletin 817, 75 p.

U.S. Department of Commerce, National Oceanic and Atmospheric

Administration, 1939–1984, Climatological data for Illinois, annual summary: Asheville, N.C., Environmental Data and Information Service, National Climatic Center.

U.S. Department of Energy, 1978, On the nature and distribution of solar radiation: HCP/T2552-01, UC-59, 62,63A, 256 p.

van Bavel, C.H.M., 1966, Potential evaporation: The combination concept and its experimental verification: Water Resources Research, v. 2, no. 3, p. 455-467.

van Bavel, C.H.M., and Ehrler, W.L., 1968, Water loss from a sorghum field and stomatal control: Agriculture Journal, v. 60, Jan.-Feb., p. 84–86.

van Hylckama, T.E.A., 1974, Water use by saltcedar as measured by the water budget method: U.S. Geological Survey Professional Paper 491-E, 30 p.

_____ 1980, Weather and evapotranspiration studies in a saltcedar thicket, Arizona: U.S. Geological Survey Professional Paper 491-F, 78 p.

Wallace, J.S., Batchelor, C.H., and Hodnett, M.G., 1981, Crop evaporation and surface conductance calculated using soil moisture data from central India: Agricultural Meteorology, v. 25, p. 83–96.

TABLE 6

Table 6. Daily estimates of evapotranspiration
[Dashes indicate no value. Values are in millimeters of water]

Date	Energy-budget method	Aero-dynamic-profile method	Poten-tial	Date	Energy-budget method	Aero-dynamic-profile method	Poten-tial
July 1, 1982	4.79	4.42	5.77	Aug. 21, 1982	--	--	3.68
July 2, 1982	1.21	1.07	1.59	Aug. 22, 1982	--	--	1.85
July 3, 1982	2.74	2.61	3.99	Aug. 23, 1982	--	--	2.20
July 4, 1982	5.74	5.53	5.32	Aug. 24, 1982	--	--	2.23
July 5, 1982	4.52	3.70	5.49	Aug. 25, 1982	--	--	4.13
July 6, 1982	2.70	2.67	3.70	Aug. 26, 1982	1.78	--	--
July 7, 1982	5.63	5.45	7.56	Aug. 27, 1982	2.78	--	2.48
July 9, 1982	4.57	--	--	Aug. 28, 1982	4.60	--	4.58
July 10, 1982	2.12	--	4.42	Aug. 29, 1982	2.68	--	3.76
July 11, 1982	3.88	4.21	6.60	Aug. 30, 1982	.46	--	.63
July 12, 1982	4.17	3.91	7.59	Aug. 31, 1982	.94	--	1.24
July 13, 1982	4.07	2.70	6.18	Sept. 1, 1982	1.38	1.72	2.61
July 14, 1982	2.78	--	3.83	Sept. 2, 1982	3.25	4.17	5.54
July 15, 1982	4.27	3.83	5.24	Sept. 3, 1982	3.49	--	--
July 16, 1982	2.80	1.99	3.64	Sept. 4, 1982	3.61	2.39	3.81
July 17, 1982	4.93	4.12	6.00	Sept. 5, 1982	2.91	2.69	3.60
July 18, 1982	2.34	2.21	3.44	Sept. 6, 1982	.61	.63	.64
July 19, 1982	2.87	--	3.86	Sept. 8, 1982	1.51	--	2.07
July 20, 1982	--	--	5.14	Sept. 9, 1982	2.60	1.75	3.11
July 21, 1982	3.52	2.56	4.31	Sept. 10, 1982	2.10	1.49	3.27
July 22, 1982	1.17	2.12	2.25	Sept. 11, 1982	--	--	3.42
July 23, 1982	--	--	5.05	Sept. 12, 1982	--	--	1.97
July 24, 1982	4.11	2.53	4.64	Sept. 13, 1982	2.58	2.52	2.21
July 25, 1982	3.79	3.36	4.68	Sept. 14, 1982	2.18	1.72	2.60
July 26, 1982	3.41	3.23	3.95	Sept. 15, 1982	1.85	1.99	2.77
July 27, 1982	2.30	2.35	3.09	Sept. 16, 1982	3.24	3.63	4.98
July 28, 1982	--	--	4.86	Sept. 17, 1982	.74	--	--
July 29, 1982	3.30	--	3.26	Sept. 18, 1982	2.25	--	--
July 30, 1982	3.40	4.96	5.09	Sept. 19, 1982	2.34	--	--
July 31, 1982	3.93	4.37	4.34	Sept. 20, 1982	1.15	--	--
Aug. 1, 1982	3.48	3.31	4.31	Sept. 21, 1982	2.57	--	--
Aug. 2, 1982	3.88	3.92	4.54	Sept. 22, 1982	3.05	3.09	2.89
Aug. 3, 1982	3.80	3.41	4.37	Sept. 23, 1982	2.19	--	2.17
Aug. 4, 1982	1.74	2.37	2.37	Sept. 24, 1982	.86	--	1.05
Aug. 5, 1982	1.78	1.94	1.89	Sept. 25, 1982	1.06	--	--
Aug. 6, 1982	.60	.54	.57	Sept. 26, 1982	.98	--	1.24
Aug. 7, 1982	1.15	.90	1.54	Sept. 27, 1982	2.02	--	2.65
Aug. 8, 1982	5.29	5.84	5.94	Sept. 28, 1982	2.13	--	--
Aug. 9, 1982	4.01	5.18	5.29	Sept. 29, 1982	--	--	2.49
Aug. 10, 1982	--	4.05	2.85	Sept. 30, 1982	1.76	--	2.93
Aug. 11, 1982	--	--	4.32	Oct. 1, 1982	1.62	.58	2.37
Aug. 12, 1982	4.46	3.72	4.73	Oct. 2, 1982	1.79	--	2.59
Aug. 13, 1982	4.27	3.03	4.80	Oct. 3, 1982	2.26	--	--
Aug. 14, 1982	3.75	2.31	4.43	Oct. 7, 1982	2.38	--	--
Aug. 15, 1982	2.59	2.40	2.61	Oct. 8, 1982	1.28	.49	1.92
Aug. 16, 1982	--	--	3.67	Oct. 9, 1982	1.17	1.14	1.43
Aug. 17, 1982	--	--	4.22	Oct. 10, 1982	1.25	--	1.68
Aug. 18, 1982	2.85	--	4.40	Oct. 11, 1982	.67	--	--
Aug. 19, 1982	2.40	2.49	4.67	Oct. 12, 1982	1.59	--	--
Aug. 20, 1982	--	--	3.60	Oct. 13, 1982	.43	.53	1.13

Table 6. Daily estimates of evapotranspiration—Continued

Date	Energy-budget method	Aero-dynamic-profile method	Poten-tial	Date	Energy-budget method	Aero-dynamic-profile method	Poten-tial
Oct. 14, 1982	1.00	--	2.69	Mar. 16, 1983	1.75	2.66	5.89
Oct. 15, 1982	--	--	2.68	Mar. 17, 1983	1.04	2.16	5.04
Oct. 16, 1982	--	1.52	2.64	Mar. 18, 1983	.00	.66	.62
Oct. 17, 1982	1.88	--	2.61	Mar. 19, 1983	.69	1.03	1.49
Oct. 18, 1982	1.94	--	--	Mar. 20, 1983	.00	-.53	--
Oct. 19, 1982	.00	--	--	Mar. 21, 1983	.00	--	--
Oct. 20, 1982	.94	--	.82	Mar. 22, 1983	.00	--	--
Oct. 21, 1982	.80	.92	1.30	Mar. 23, 1983	--	.03	--
Oct. 22, 1982	1.32	--	--	Mar. 24, 1983	.50	--	--
Oct. 23, 1982	1.67	--	1.93	Mar. 26, 1983	.26	.35	1.43
Oct. 24, 1982	1.78	--	2.02	Mar. 27, 1983	.46	.38	.40
Oct. 25, 1982	1.40	--	1.88	Mar. 28, 1983	1.98	1.49	1.35
Oct. 26, 1982	1.47	--	2.47	Mar. 29, 1983	1.13	1.96	--
Oct. 27, 1982	.72	--	--	Mar. 30, 1983	.90	.40	.51
Oct. 28, 1982	.79	--	--	Mar. 31, 1983	.67	.49	.58
Oct. 29, 1982	1.36	--	--	Apr. 1, 1983	.53	.87	.94
Nov. 1, 1982	.25	--	--	Apr. 2, 1983	-.02	-.27	-.06
Nov. 2, 1982	.30	--	--	Apr. 3, 1983	.81	.71	.40
Nov. 3, 1982	.90	--	--	Apr. 4, 1983	.86	1.21	1.00
Nov. 9, 1982	.80	--	--	Apr. 5, 1983	--	--	.45
Nov. 10, 1982	.00	--	--	Apr. 6, 1983	--	--	.65
Nov. 11, 1982	-.07	--	.47	Apr. 7, 1983	1.56	1.30	2.41
Nov. 15, 1982	--	--	.64	Apr. 9, 1983	--	--	.53
Nov. 16, 1982	.45	--	1.18	Apr. 11, 1983	--	1.46	1.67
Nov. 17, 1982	.74	--	1.19	Apr. 14, 1983	--	1.45	2.23
Nov. 18, 1982	.45	--	--	Apr. 15, 1983	--	2.00	3.44
Nov. 19, 1982	.00	--	-.05	Apr. 16, 1983	--	1.45	3.00
Nov. 20, 1982	.00	--	.51	Apr. 17, 1983	--	3.61	2.68
Nov. 21, 1982	--	--	1.12	Apr. 18, 1983	--	3.57	3.89
Nov. 22, 1982	.18	--	.48	Apr. 19, 1983	--	2.91	3.59
Nov. 23, 1982	.23	--	.59	Apr. 20, 1983	--	2.07	4.29
Nov. 26, 1982	.28	--	--	Apr. 21, 1983	3.65	2.38	4.87
Nov. 27, 1982	--	--	.58	Apr. 22, 1983	2.92	2.19	2.63
Nov. 28, 1982	.03	--	.21	Apr. 23, 1983	3.27	3.75	3.85
Nov. 29, 1982	.19	--	.22	Apr. 24, 1983	3.73	4.20	4.93
Nov. 30, 1982	.38	--	.25	Apr. 25, 1983	3.40	2.10	5.20
Mar. 1, 1983	--	.10	1.98	Apr. 26, 1983	2.85	2.80	6.13
Mar. 2, 1983	--	.08	2.50	Apr. 27, 1983	3.76	4.47	4.91
Mar. 3, 1983	--	.45	2.19	Apr. 28, 1983	3.52	3.52	3.27
Mar. 4, 1983	--	.44	1.12	Apr. 29, 1983	--	--	2.06
Mar. 5, 1983	--	.27	1.50	Apr. 30, 1983	--	--	3.36
Mar. 6, 1983	--	1.66	1.23	May 1, 1983	.49	--	1.44
Mar. 7, 1983	--	.49	.53	May 2, 1983	1.12	1.37	1.97
Mar. 8, 1983	--	.38	--	May 3, 1983	3.09	3.29	3.14
Mar. 10, 1983	--	1.05	--	May 4, 1983	4.89	4.68	6.70
Mar. 11, 1983	--	.94	--	May 5, 1983	2.78	2.15	3.53
Mar. 12, 1983	--	1.23	--	May 6, 1983	3.34	3.67	5.79
Mar. 13, 1983	.66	.26	2.15	May 7, 1983	1.08	.23	2.73
Mar. 14, 1983	.66	.58	1.42	May 8, 1983	5.19	5.40	5.36
Mar. 15, 1983	1.40	1.77	3.27	May 9, 1983	3.75	3.06	5.27

Table 6. Daily estimates of evapotranspiration—Continued

Date	Energy-budget method	Aero-dynamic-profile method	Poten-tial	Date	Energy-budget method	Aero-dynamic-profile method	Poten-tial
May 10, 1983	4.03	3.28	5.41	June 30, 1983	4.42	3.21	5.00
May 11, 1983	4.14	3.71	4.73	July 1, 1983	3.19	3.10	3.58
May 12, 1983	1.90	1.73	2.20	July 2, 1983	2.51	1.66	2.80
May 13, 1983	1.39	1.39	1.45	July 3, 1983	4.59	4.50	5.82
May 14, 1983	.94	.91	.89	July 4, 1983	4.51	4.79	6.69
May 15, 1983	--	--	4.69	July 5, 1983	--	--	4.23
May 16, 1983	3.40	2.28	4.12	July 6, 1983	--	--	4.70
May 17, 1983	1.92	1.73	2.35	July 7, 1983	--	--	5.30
May 18, 1983	1.79	1.99	2.43	July 8, 1983	4.69	4.74	5.47
May 19, 1983	1.85	2.05	3.85	July 10, 1983	4.58	2.18	5.28
May 20, 1983	4.44	4.56	5.50	July 11, 1983	5.21	5.19	5.80
May 21, 1983	2.17	1.58	2.40	July 12, 1983	--	--	4.92
May 22, 1983	3.72	3.87	5.09	July 13, 1983	3.41	1.70	4.29
May 23, 1983	--	5.51	7.68	July 14, 1983	3.25	2.77	3.60
May 24, 1983	--	4.90	7.68	July 15, 1983	2.53	.64	3.26
May 25, 1983	--	5.48	5.76	July 16, 1983	4.08	3.79	5.47
May 26, 1983	--	2.79	5.26	July 17, 1983	4.44	5.32	5.94
May 27, 1983	2.32	2.03	3.50	July 18, 1983	3.52	4.45	3.89
May 28, 1983	--	--	2.46	July 19, 1983	4.30	4.90	5.82
May 29, 1983	--	3.71	--	July 20, 1983	3.14	4.12	6.14
May 30, 1983	2.13	2.33	--	July 21, 1983	--	4.29	--
May 31, 1983	1.90	2.03	3.83	July 22, 1983	--	4.29	--
June 1, 1983	--	4.43	--	July 26, 1983	3.07	2.94	--
June 2, 1983	2.28	2.31	2.48	July 27, 1983	3.36	1.48	4.85
June 3, 1983	2.43	2.79	2.43	July 28, 1983	3.28	2.08	4.86
June 4, 1983	5.37	5.76	6.44	July 29, 1983	--	--	2.90
June 5, 1983	2.34	2.50	2.96	July 30, 1983	3.87	3.99	4.39
June 6, 1983	3.88	5.25	5.98	Aug. 1, 1983	--	5.11	5.06
June 7, 1983	--	5.03	--	Aug. 2, 1983	4.28	--	5.03
June 8, 1983	4.50	3.57	6.49	Aug. 3, 1983	4.34	3.42	5.13
June 9, 1983	--	3.58	--	Aug. 4, 1983	3.21	--	3.93
June 10, 1983	3.83	2.98	4.59	Aug. 6, 1983	4.18	--	3.88
June 11, 1983	--	3.43	4.46	Aug. 7, 1983	4.96	--	4.43
June 12, 1983	--	3.41	4.82	Aug. 8, 1983	4.75	--	4.68
June 13, 1983	--	3.17	4.14	Aug. 9, 1983	--	--	4.23
June 14, 1983	--	.99	1.70	Aug. 10, 1983	3.84	--	5.37
June 15, 1983	4.64	3.58	5.78	Aug. 11, 1983	3.88	--	3.53
June 16, 1983	--	--	3.19	Aug. 13, 1983	4.10	--	3.99
June 17, 1983	--	--	2.82	Aug. 14, 1983	2.55	--	2.34
June 18, 1983	--	--	5.14	Aug. 15, 1983	3.38	--	3.54
June 19, 1983	--	--	4.01	Aug. 16, 1983	3.77	--	4.45
June 20, 1983	3.00	--	3.89	Aug. 17, 1983	3.29	--	3.98
June 21, 1983	3.33	--	4.73	Aug. 18, 1983	--	--	3.03
June 22, 1983	4.41	--	6.08	Aug. 19, 1983	4.23	--	4.28
June 23, 1983	3.93	--	4.50	Aug. 20, 1983	3.79	--	3.54
June 24, 1983	4.50	3.08	5.27	Aug. 21, 1983	3.45	--	4.55
June 25, 1983	4.12	--	5.44	Aug. 22, 1983	--	--	1.62
June 26, 1983	3.19	--	4.77	Aug. 23, 1983	--	--	2.03
June 27, 1983	2.06	--	2.71	Aug. 24, 1983	2.18	--	2.36
June 28, 1983	--	--	2.75	Aug. 25, 1983	2.70	--	2.42

Table 6. Daily estimates of evapotranspiration—Continued

Date	Energy-budget method	Aero-dynamic-profile method	Poten-tial	Date	Energy-budget method	Aero-dynamic-profile method	Poten-tial
Aug. 26, 1983	3.11	--	--	Oct. 19, 1983	0.44	0.69	1.07
Aug. 29, 1983	3.66	--	--	Oct. 20, 1983	.60	.83	1.01
Aug. 30, 1983	1.73	--	--	Oct. 21, 1983	.32	.44	.85
Aug. 31, 1983	3.97	--	--	Oct. 22, 1983	.10	-.01	.61
Sept. 2, 1983	3.72	--	--	Oct. 23, 1983	.73	.69	1.15
Sept. 3, 1983	3.16	--	--	Oct. 24, 1983	.51	.67	.60
Sept. 4, 1983	2.83	--	--	Oct. 25, 1983	1.95	1.81	2.33
Sept. 5, 1983	1.45	--	--	Oct. 26, 1983	2.11	1.76	3.37
Sept. 6, 1983	2.95	--	--	Oct. 27, 1983	1.38	.74	3.52
Sept. 7, 1983	4.05	--	--	Oct. 28, 1983	1.33	.71	3.69
Sept. 8, 1983	3.30	--	--	Oct. 29, 1983	.96	--	1.25
Sept. 10, 1983	3.15	--	4.09	Oct. 30, 1983	.63	.73	1.16
Sept. 11, 1983	2.79	--	2.38	Oct. 31, 1983	1.31	.55	1.22
Sept. 12, 1983	3.16	--	2.66	Nov. 1, 1983	.76	.75	1.12
Sept. 13, 1983	3.73	--	3.30	Nov. 2, 1983	.36	.45	.39
Sept. 14, 1983	3.42	--	2.87	Nov. 3, 1983	.58	1.09	2.48
Sept. 15, 1983	.80	--	--	Nov. 4, 1983	.82	1.65	1.30
Sept. 16, 1983	2.68	2.60	3.95	Nov. 5, 1983	.92	.53	1.49
Sept. 17, 1983	2.64	1.61	3.19	Nov. 6, 1983	.42	.43	.93
Sept. 18, 1983	2.43	2.23	3.04	Nov. 7, 1983	.37	.50	.36
Sept. 19, 1983	2.66	2.39	3.03	Nov. 8, 1983	.99	.25	1.39
Sept. 20, 1983	.27	1.17	1.37	Nov. 9, 1983	.59	.67	.89
Sept. 21, 1983	2.01	2.17	--	Nov. 10, 1983	.53	.66	.86
Sept. 22, 1983	1.58	1.67	--	Nov. 11, 1983	--	1.68	1.96
Sept. 23, 1983	2.57	1.64	5.04	Nov. 12, 1983	--	.61	--
Sept. 24, 1983	2.47	1.88	4.39	Nov. 13, 1983	--	.89	1.20
Sept. 25, 1983	.38	.48	.97	Nov. 14, 1983	.39	.45	.94
Sept. 26, 1983	1.54	--	2.32	Nov. 15, 1983	.00	.00	.41
Sept. 27, 1983	2.18	--	2.59	Nov. 16, 1983	.95	1.01	1.31
Sept. 28, 1983	2.25	1.49	2.53	Nov. 17, 1983	.68	.38	.72
Sept. 29, 1983	2.04	--	--	Nov. 18, 1983	.49	-.41	.87
Sept. 30, 1983	2.76	1.80	3.52	Nov. 19, 1983	.19	.35	.75
Oct. 1, 1983	2.24	1.28	2.90	Nov. 20, 1983	.50	.34	1.00
Oct. 2, 1983	2.35	2.11	3.74	Nov. 21, 1983	1.03	.46	1.04
Oct. 3, 1983	2.05	1.84	3.02	Nov. 22, 1983	.00	.10	.79
Oct. 4, 1983	1.91	1.55	2.58	Nov. 23, 1983	.21	--	.55
Oct. 5, 1983	2.31	2.15	2.76	Nov. 24, 1983	--	.66	--
Oct. 6, 1983	1.97	--	--	Nov. 25, 1983	--	1.08	--
Oct. 7, 1983	1.97	1.84	4.36	Nov. 26, 1983	.28	.55	.86
Oct. 8, 1983	.88	.77	1.49	Nov. 27, 1983	.12	--	.87
Oct. 9, 1983	1.89	1.19	2.51	Mar. 1, 1984	--	1.08	--
Oct. 10, 1983	1.81	.99	2.31	Mar. 2, 1984	--	2.46	--
Oct. 11, 1983	1.48	1.58	2.44	Mar. 13, 1984	--	.27	--
Oct. 12, 1983	1.90	2.32	2.35	Mar. 14, 1984	--	.52	--
Oct. 13, 1983	.86	1.13	1.83	Mar. 15, 1984	1.56	1.65	.95
Oct. 14, 1983	1.87	1.16	2.54	Mar. 16, 1984	.38	1.20	1.13
Oct. 15, 1983	1.73	1.53	2.94	Mar. 17, 1984	--	.38	--
Oct. 16, 1983	1.03	1.00	2.37	Mar. 18, 1984	--	-.16	--
Oct. 17, 1983	1.81	.98	2.59	Mar. 19, 1984	--	.22	--
Oct. 18, 1983	1.95	1.87	2.13	Mar. 20, 1984	.73	--	--

Table 6. Daily estimates of evapotranspiration—Continued

Date	Energy-budget method	Aero-dynamic-profile method	Poten-tial	Date	Energy-budget method	Aero-dynamic-profile method	Poten-tial
Mar. 21, 1984	0.10	0.27	0.07	May 13, 1984	5.86	6.27	8.15
Mar. 22, 1984	2.10	2.41	1.45	May 14, 1984	4.43	4.74	4.79
Mar. 23, 1984	2.03	2.82	2.00	May 15, 1984	5.09	5.24	6.34
Mar. 24, 1984	.90	.94	--	May 16, 1984	--	3.69	--
Mar. 25, 1984	.81	.71	2.19	May 17, 1984	4.99	4.74	6.43
Mar. 26, 1984	1.45	1.48	2.17	May 18, 1984	5.53	5.09	6.83
Mar. 27, 1984	.46	.45	--	May 19, 1984	2.34	2.38	2.77
Mar. 28, 1984	1.24	--	--	May 20, 1984	4.12	4.49	4.46
Mar. 30, 1984	1.25	1.42	2.03	May 21, 1984	1.44	.71	1.48
Mar. 31, 1984	2.51	2.67	2.89	May 22, 1984	.32	.58	.64
Apr. 1, 1984	1.61	1.17	3.45	May 23, 1984	5.47	5.60	8.02
Apr. 2, 1984	.71	1.35	1.91	May 24, 1984	5.33	5.13	6.62
Apr. 3, 1984	.60	.75	1.36	May 25, 1984	1.14	1.56	2.09
Apr. 4, 1984	.30	.06	.11	May 26, 1984	3.82	3.94	5.37
Apr. 5, 1984	3.45	3.70	4.43	May 27, 1984	2.76	2.89	5.16
Apr. 6, 1984	3.26	3.81	4.36	May 28, 1984	.84	.74	1.66
Apr. 7, 1984	2.02	1.35	3.97	May 29, 1984	4.60	4.47	6.69
Apr. 8, 1984	1.43	1.74	1.77	May 30, 1984	3.75	3.92	7.00
Apr. 9, 1984	1.14	1.23	2.73	May 31, 1984	5.13	5.07	6.44
Apr. 10, 1984	2.90	2.89	5.38	June 1, 1984	3.84	3.24	4.55
Apr. 11, 1984	1.87	1.79	4.19	June 2, 1984	4.02	4.42	5.80
Apr. 12, 1984	1.01	1.64	2.50	June 3, 1984	4.59	3.75	5.78
Apr. 13, 1984	.96	.89	1.36	June 4, 1984	3.35	3.85	4.04
Apr. 14, 1984	.70	1.09	.98	June 5, 1984	4.78	4.93	5.40
Apr. 15, 1984	.49	.63	.51	June 6, 1984	2.64	3.49	3.55
Apr. 16, 1984	.63	.63	.97	June 7, 1984	2.46	4.06	4.25
Apr. 17, 1984	2.35	2.56	--	June 8, 1984	3.91	4.44	4.51
Apr. 18, 1984	.62	--	1.78	June 9, 1984	2.47	3.18	--
Apr. 19, 1984	--	3.26	--	June 10, 1984	5.30	--	5.69
Apr. 20, 1984	3.11	3.97	5.07	June 11, 1984	5.28	--	4.98
Apr. 21, 1984	--	1.45	--	June 12, 1984	5.99	6.10	5.81
Apr. 22, 1984	.40	.27	.47	June 15, 1984	1.45	1.68	1.91
Apr. 23, 1984	.47	.89	.38	June 16, 1984	3.23	2.91	3.61
Apr. 24, 1984	3.27	3.65	3.12	June 17, 1984	5.42	5.45	5.47
Apr. 25, 1984	3.51	2.78	4.94	June 18, 1984	4.27	4.68	4.70
Apr. 26, 1984	3.56	2.97	4.61	June 19, 1984	4.14	4.18	3.45
Apr. 27, 1984	--	2.29	--	June 20, 1984	5.21	5.09	6.16
Apr. 28, 1984	--	3.70	5.23	June 21, 1984	2.77	2.28	3.87
Apr. 29, 1984	--	.85	.58	June 22, 1984	3.76	3.53	4.13
May 2, 1984	3.71	4.45	7.31	June 23, 1984	5.18	5.18	5.98
May 3, 1984	.17	.58	--	June 24, 1984	5.83	6.38	7.70
May 4, 1984	2.24	3.25	2.64	June 25, 1984	5.19	6.31	5.94
May 5, 1984	3.39	3.06	3.92	June 26, 1984	4.94	5.90	5.64
May 6, 1984	3.04	2.98	3.45	June 27, 1984	6.15	6.31	7.98
May 7, 1984	2.51	2.92	5.14	June 28, 1984	3.86	4.16	4.34
May 8, 1984	.93	4.16	--	June 29, 1984	3.80	--	4.71
May 9, 1984	--	4.80	--	June 30, 1984	3.09	1.91	3.64
May 10, 1984	1.86	1.51	2.52				
May 11, 1984	2.37	1.78	1.92				
May 12, 1984	4.94	4.25	6.63				